ISSN 0038-3872

SOUTHERN CALIFORNIA ACADEMY OF SCIENCES

BULLETIN

Volume 118 **Number 1**

118(1) 1-78 (2019) **April 2019**

Southern California Academy of Sciences

Founded 6 November 1891, incorporated 17 May 1907

Membership is open to scholars in the fields of natural and social sciences, and to any person interested in the advancement of science. Dues for membership, changes of address, and requests for missing numbers lost in shipment should be addressed to: Southern California Academy of Sciences, the Natural History Museum of Los Angeles County, Exposition Park, Los Angeles, California 90007-4000.

Professional Members $80.00
Student Members $50.00
Memberships in other categories are available on request.

Fellows: Elected by the Board of Directors for meritorious services.

The Bulletin is published three times each year by the Academy. Submissions of manuscripts for publication and associated guidelines is at SCASBULLETIN.ORG. All other communications should be addressed to the Southern California Academy of Sciences in care of the Natural History Museum of Los Angeles County, Exposition Park, Los Angeles, California 90007-4000.

Date of this issue 10 April 2019

♾ This paper meets the requirements of ANSI/NISO Z39.48-1992 (Permanence of Paper).

Bull. Southern California Acad. Sci.
118(1), 2019, pp. 1–20

Range Expansion or Range Shift? Population Genetics and Historic Range Data Analyses of the Predatory Benthic Sea Slug *Phidiana hiltoni* (Mollusca, Gastropoda, Nudibranchia)

Clara Jo King,[1] Ryan A. Ellingson,[2] Jeffrey H.R. Goddard,[3] Rebecca F. Johnson,[4] and Ángel Valdés[1]*

[1]*Department of Biological Sciences, California State Polytechnic University, 3801 West Temple Avenue, Pomona, CA 91768*
[2]*Department of Ecology and Evolutionary Biology, University of California, Los Angeles, CA 90095*
[3]*Marine Science Institute, University of California, Santa Barbara, CA 93106*
[4]*Department of Invertebrate Zoology and Geology, California Academy of Sciences, 55 Music Concourse Drive, San Francisco, CA 94118*

Abstract.—Phidiana hiltoni is a conspicuous nudibranch sea slug native to the northeastern Pacific Ocean. Over the past thirty years the range of *P. hiltoni* has expanded about 200 km northward, but the mechanism that facilitated this expansion is poorly understood. In this study, we use mtDNA and microsatellite data to investigate the population structure of *P. hiltoni* in its historical range as well as in recently colonized localities. Microsatellite analyses reveal little to no genetic structure and thus high gene flow throughout the range of *P. hiltoni*. This is consistent with mtDNA analysis results, which revealed shared haplotypes between Southern, Central and Northern populations. However, AMOVA of mtDNA data did recover some genetic structure among geographic regions. This, along with same group memberships in the microsatellite data of individuals from sites like Cave Landing, suggest a certain degree of local recruitment and reduced vagility. Recently established populations in Northern California contain two unique mtDNA haplotypes that are not present elsewhere, but microsatellite data do not differentiate these from other populations. The mismatch between mtDNA and microsatellite data could be explained by the mating system of this aggressive, hermaphroditic species as well as the sporadic nature of the northward dispersal. Analyses of historical abundance data of *P. hiltoni* suggest a population decline in Southern California. Together, these results suggest a northward population shift, rather than a range expansion, possibly related to ongoing changes in nearshore oceanographic conditions in the region.

Rising ocean temperatures driven by global climate change are having dramatic impacts on coastal ecosystems around the world (McGowan et al. 1998; Sorte et al. 2011). One of the most noticeable effects is the poleward range expansion of certain species (Dawson et al. 2010; Sorte et al. 2011; Sunday et al. 2012; Canning-Clode and Carlton 2017). Particularly problematic are range expansions of predatory species, which can have significant impacts on the trophic structure of newly colonized ecosystems (Zeidberg and Robinson 2007; Gallardo et al. 2016). However, not all of these range expansions are permanent;

* Corresponding author: aavaldes@cpp.edu

some result from regular oscillations in ocean temperatures (e.g., El Niño events). In these cases, populations often return to their original range following ephemeral warming events, making it difficult to attribute in the short term any particular range shift to longer term climate change (Schultz et al. 2011). Poleward range expansions can also be accompanied by extirpation at lower latitudes, resulting in shifts at both ends of species ranges (Parmesan et al. 1999; Bates et al. 2014). Range shifts may constitute a more pervasive indication of permanent changes in the ecological structure of biotas as they can be more difficult to reverse (Parmesan et al. 1999; Schultz et al. 2011). However, range shifts are difficult to detect and precisely quantify, particularly in marine species with low abundance and/or population densities (Bates et al. 2015).

Phidiana hiltoni is a relatively large and conspicuous aeolid nudibranch native to the northeastern Pacific Ocean. Like most nudibranchs, *P. hiltoni* is a simultaneous hermaphrodite, but the mating behavior of this species is poorly understood. The diet of *P. hiltoni* consists mostly of hydroids and other cnidarians; however, individuals of this species are known to attack and consume other sea slugs, particularly small, soft-bodied aeolids and dendronotaceans, including conspecifics (Goddard et al. 2011). *Phidiana hiltoni* has relatively large eggs and lecithotrophic larval development (Goddard 2004); its larvae do not need to feed in the water column and are capable of settlement and metamorphosis within a day or two of hatching. Thus, compared to planktotrophic species, dispersal by the larvae of *P. hiltoni* is greatly reduced. Historically, *P. hiltoni* was found as far south as Isla Cedros off the coast of Baja California, Mexico and as far north as Pacific Grove, California (Goddard et al. 2011). In 1977, *Phidiana hiltoni* was discovered north of Monterey Bay (Goddard et al. 2011). Once across Monterey Bay, *P. hiltoni* rapidly made its way up the coast; it was found just north of San Francisco Bay (Duxbury Reef, Marin County) in 1992 and now is present as far north as Bodega Bay, California, representing a 200-km northward range expansion in 40 years (Goddard et al. 2011; Goddard et al. 2018). At Duxbury Reef, *P. hiltoni* quickly became the dominant sea slug, with apparent negative impacts on other nudibranch species, likely through a combination of direct predation and competition for shared hydroid prey (Goddard et al. 2011).

The mechanism behind the range expansion of *P. hiltoni* is not well understood, but has been potentially linked to warming coastal waters and shifts in ocean currents along the California coast (Schultz et al. 2011). Changes in ocean circulation, which drives larval transport, can potentially increase the risk of species introductions and/or dispersals (Harley et al. 2006; Sorte et al. 2011; Wilson et al. 2016). Whereas the dispersal potential of species with planktonic feeding larvae is relatively well understood (Scheltema 1986), less is known about how species with lecithotrophic development may respond to oceanographic changes. A majority of lecithotrophic sea slug species are found in warmer, nutrient-poor waters, where having a short-lived, non-feeding larval stage can lead to reductions in larval mortality at the cost of reduced fecundity and vagility (Goddard 2004; Goddard and Hermosillo 2008). *Phidiana hiltoni* is one of the few lecithotrophically developing nudibranchs found in temperate waters in the Northeast Pacific Ocean (Goddard 2004), and its recent range expansion may reflect long-term changes in regional nearshore circulation regimes and productivity (Rebstock 2003). These factors make *P. hiltoni* a particularly interesting system for studying the complex interactions between climate change, range shifts, and marine invasion biology.

If the dispersal of *P. hiltoni* has been facilitated by changes of oceanographic regimes and warming waters at the northern edge of its range, the most likely source for the new populations north of Monterey Bay are Central California populations. However, it is also

possible that individuals from father south were introduced into northern California either by larval dispersal or human activities. The lecithotrophic larval development of *P. hiltoni* makes it an ideal candidate for ballast water dispersal, and less likely to disperse long distances naturally in response to environmental changes. Two of the busiest commercial ports in North America are located in California, with the Los Angeles-Long Beach Harbor well within the historic range of *P. hiltoni*, and the Oakland-San Francisco Harbor (San Francisco Bay) in the center of the extended portion of the range. However, the absence of *P. hiltoni* from San Francisco Bay along with its prevalence in open-coast rocky reefs (Goddard et al. 2011) contradicts the ballast water introduction hypothesis. Another possible vector for the spread of *P. hiltoni* could be small vessel traffic between regional ports and harbors (Wasson et al. 2001), but the mobile hunting behavior of this species makes it an unlikely fouling organism. Regardless of the mechanism of dispersal, Schultz et al. (2011) noted that *P. hiltoni* has persisted at higher latitudes despite ocean temperature fluctuations from El Niño/La Niña cycles, suggesting this species may be an indicator of faunal range shifts due to climate change.

Although the range expansion and some of the associated ecological effects of *P. hiltoni* are well documented (Goddard et al. 2011), many questions remain. No genetic studies have been conducted on *P. hiltoni*, thus the population structure of the species is unknown, hampering our ability to understand the mechanisms of dispersal. Also, very little attention has been paid to the southern range limit of *P. hiltoni*, leaving unanswered the question as to whether recent observations indicate a northern range expansion or overall range shift. In the present study, we examine population structure in *P. hiltoni*, explore the genetic signature of its range expansion, and hypothesize possible dispersal mechanisms into Northern California. Additionally, we reviewed historical collection data near the southern range of *P. hiltoni* in order to document population density changes that may help to understand the population dynamics of this species.

Materials and Methods

Whole specimens and tissue samples of *Phidiana hiltoni* (Table S1) were obtained from different sources and various locations along the California coast (Fig. 1). Some individuals were collected at the shoreline during low tide, other specimens and tissue samples were provided by colleagues or obtained from collections of the Natural History Museum of Los Angeles County (LACM), the Santa Barbara Museum of Natural History (SBMNH) and the California Academy of Sciences (CASIZ). Fieldwork was conducted under the California Department of Fish and Wildlife permit #13256. Specimens collected in the field were preserved in 95% ethanol and deposited at the California State Polytechnic University Invertebrate Collection (CPIC).

DNA was extracted from sixty specimens (Table 1) using a DNeasy Blood and Tissue Kit (Qiagen, Valencia, CA) using standard protocols provided by the manufacturer. A fragment of the cytochrome c oxidase subunit I (COI) mitochondrial gene was amplified and sequenced using universal primers (LCO1490 5′-GGTCAACAAATCATAAAGATATTGG-3′, HCO2198 5′-TAAACTTCAGGGTGACCAAAAAATCA-3′) (Folmer et al. 1994). PCR reaction conditions were as follows: denaturation at 95°C for 3 min, followed by 35 cycles of 94°C for 45 sec, 50°C for 45 sec, and 72°C for 2 min with final elongation at 72°C for 10 min. Successful DNA amplification was confirmed using an agarose gel electrophoresis and ethidium bromide. The PCR products were purified with a

Table 1. Number and collection sites of specimens for which the COI sequence data (mtDNA) and microsatellite fragment genotype data (nDNA) were analyzed. For the isolates, a plus sign (+) indicates only the COI gene was analyzed, asterisk (*) indicates only microsatellite data were analyzed.

	Sampling site	mtDNA	nDNA	Collection years	Isolates
Northern California	Pillar Point	16	15	2015	CK60+, CK61, CK62, CK63, CK64, CK65, CK66, CK67, CK68, CK69, CK70, CK71, CK73, CK74, CK75, CK76
	Scott Creek	0	1	2015	CK114*
Central California	Carmel Point	2	3	2011, 2016	CK111*, CK117, CK118
	Cayucos	2	0	2017	CK130+, CK131+
	Cave Landing	18	26	2016	CK29, CK30, CK31, CK32, CK33, CK34+, CK77, CK78, CK79, CK80*, CK81, CK82, CK83, CK84*, CK86, CK87, CK88, CK89, CK90*, CK91*, CK92*, CK93, CK94, CK95*, CK96*, CK97*, CK98
	Jalama Beach	8	8	2009	CK46, CK47, CK48, CK49, CK50, CK51, CK52, CK53
Southern California	Naples	1	1	2009	CK34+, CK36*
	San Clemente Is.	1	1	1961	CK11

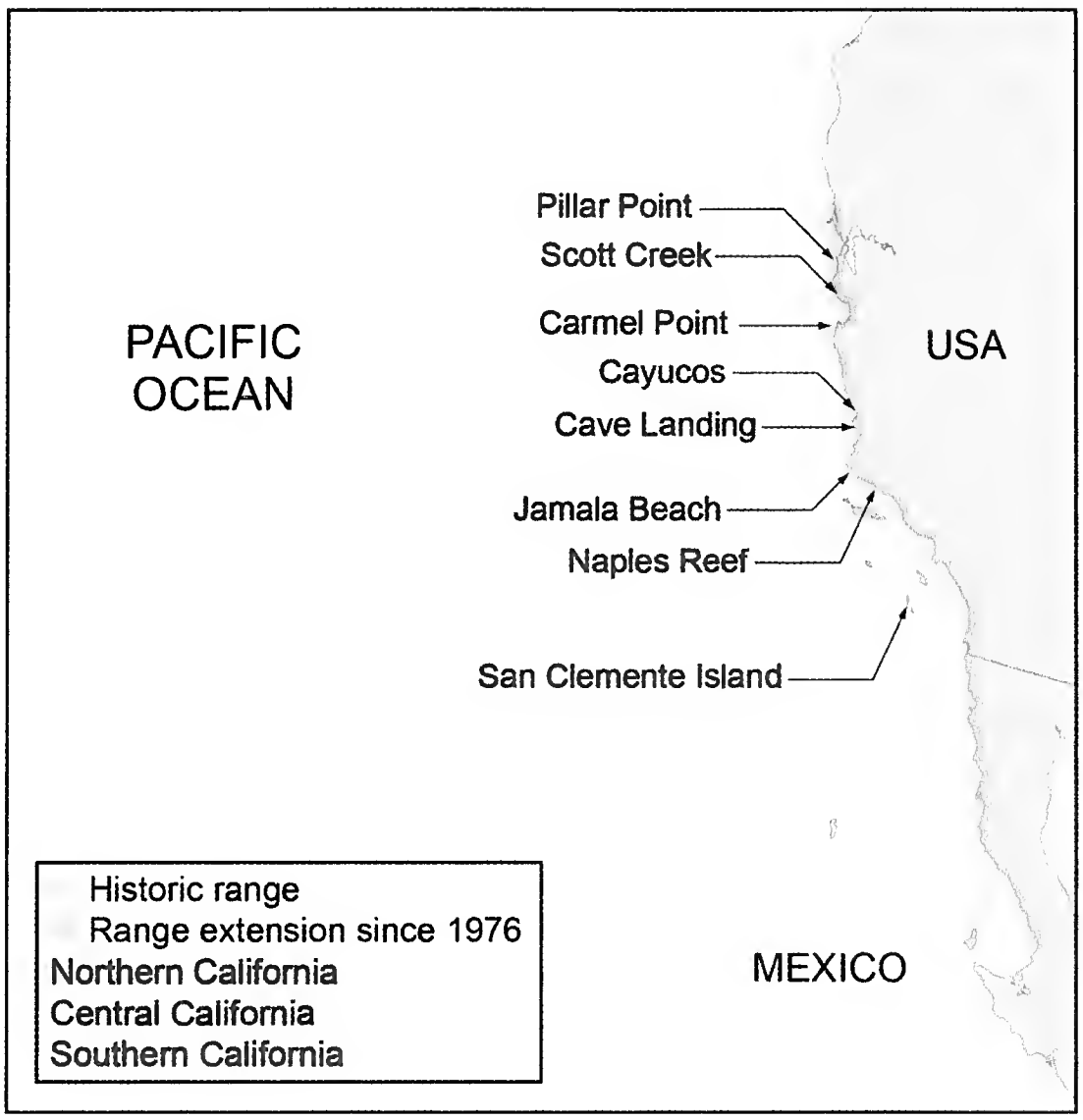

Fig. 1. Map of the historic and expanded range of *Phidiana hiltoni* along the western coast of North America. Sampling localities are indicated by arrows and coded with different grey tones by geographic regions.

GeneJET PCR Purification Kit (Fermentas, Waltham, MA) using standard protocols and were sent for sequencing to Source Bioscience Inc. (Santa Fe Springs, CA).

Sequences were assembled and aligned using Geneious v8.1.8 (Kearse et al. 2012). The geographic distribution of mtDNA haplotypes was visualized by producing a haplotype network using the program PopArt v1.7 (Leigh and Bryant 2015) using the TCS option. Haplotypes were pattern-coded by locality. Genetic structure within and among populations and among groups was examined using analysis of molecular variance (AMOVA) as implemented in Arlequin v3.5 (Excoffier and Lischer 2010). Three different AMOVA analyses were run to test for the effects of arranging populations into different groups based on the distribution of genetic variation. In the first AMOVA test, populations established after 1977 were included in the Northern California group while historic range populations were divided into two groups: Central California (populations north of Point Conception) and Southern California (populations south of Point Conception); this is the hypothesized biogeographic structure if Point Conception acts as a biogeographic barrier (Blanchette et al. 2008). To examine possible genetic similarities between newly formed populations in Northern California and those from southern Monterey Bay, two additional AMOVAs were run with different group arrangements, to examine whether this resulted in different distributions of genetic diversity among groups and among populations within groups. In the second AMOVA, the groups were kept the same except central California populations were split into two groups, Northern Central California (southern Monterey Bay) and Southern Central California (populations further south), see Blanchette et al. (2008). In the third AMOVA populations from southern Monterey Bay were pooled with Northern

California. Significance of the AMOVAs was tested using 16,000 permutations of individuals between groups. Arlequin v3.5 was also used to calculate pairwise Φ_{ST} between populations (1,000 permutations). Because the Southern California populations (Naples and San Clemente) were represented by one sequence each, populations were pooled together.

Microsatellite loci were identified through sequencing by synthesis with a MiSeq platform (Illumina, Inc., San Diego, CA). DNA was extracted from a single specimen collected from Pillar Point, California (CASIZ 190249), tagged with a unique barcode during library preparation, and pooled with other samples for Illumina sequencing. Sequencing was conducted at the UCLA Genotyping and Sequencing Core facility. Automated screening of sequences for tetranucleotide repeats and primer design were performed simultaneously in MSATCOMMANDER v1.0.8 (Faircloth 2008). Twenty-two primer pairs were purchased from Eurofins (Louisville, KY) with a M13 tail added to the 3′ end of each forward primer sequence.

Five of the twenty-two primer pairs were tested with ten specimens that consistently amplified for mtDNA to determine the PCR protocol. PCR protocol settings for the primers were optimized from a standard protocol by adjusting the annealing temperatures and elongation times until amplification was achieved. The PCR Master Mix for each locus in these tests included the forward primer with a M13 tail, reverse primer, and BSA (bovine serum albumin) and used Thermo Fisher Platinum Hot Start PCR Master Mix. The final PCR reaction conditions were as follows: denaturation at 95°C for 15 min, followed by 30 cycles of 94°C for 30 sec, 60–65°C for 30 sec, and 68°C for 30 sec with final elongation at 60°C for 10 min. All twenty-two primer pairs were tested with ten specimens that consistently amplified for mtDNA using the above conditions. Of the twenty-two primer pairs tested, ten polymorphic loci amplified reliably. Using the ten reliable primer pairs (Table S2) and the above amplification conditions, PCR was carried out with fifty-seven specimens. The PCR Master Mix for each locus in this final round now included a fluorescent M13 tag (5′-[6-FAM] AGGGTTTTCCCAGTCACGACGTT-3′) along with the original components. Genotyping was outsourced to Laragen Incorporated (Culver City, CA). Genotypes were scored using the Microsatellite Analysis External Plugin v1.4.4 implemented in Geneious v8.1.8 using the Two Surrounding Peaks setting (Kearse et al. 2012).

In total, fifty-five individual specimens were genotyped for all 10 microsatellite loci. This is a small sample size for this type of study, but specimens were difficult to obtain in the field. Collecting sea slugs is serendipitous in nature and after two years of fieldwork only a small number of specimens was obtained. Additionally, most museum specimens examined were unsuitable for molecular work. Population subdivision in the nuclear genome was inferred using STRUCTURE v2.3.4 (Pritchard et al. 2000) with the default parameters; 5 replicates for each value of K were run for 1,000,000 MCMC iterations following a burn-in period of 100,000. To detect the true number of clusters (K) using the Evanno Method (Evanno et al. 2005) the result file from STRUCTURE was processed with STRUCTURE Harvester v0.6.9.84 (Earl and vonHoldt 2012). Using the selected K value (3) the resulting files were processed with CLUMPP v1.1.2 (Rosenberg et al. 2002) and Distruct v1.1 (Rosenberg, 2004) to generate a graphic display of the population structure. AMOVA and F_{ST} pairwise genetic differentiation comparisons between populations were conducted following the same methodology as in the mtDNA analyses. Microsatellite data were also analyzed via Discriminant Analysis of Principal Components (DAPC) using the *adegent* package in R (Jombart et al. 2010).

To determine whether the abundance of *P. hiltoni* in Southern California has changed since the mid-20th century, counts of nudibranchs by James R. Lance dating from 1953

to 2001[1] at six rocky intertidal sites in San Diego County (Point Loma, Hill Street, False Point, Bird Rock, Windansea, and South Casa Reef) were examined and analyzed. The data for *P. hiltoni* were extracted and grouped by site, decade, and before and after 1963, the year when, excepting one brief trip to Bird Rock in 1956, Lance started sampling outer coast sites in San Diego County other than Point Loma. Counts made on consecutive or near-consecutive dates at any given site were excluded from analysis in order to reduce autocorrelation in the data; the count retained was the one with the highest number of *P. hiltoni*. Twenty-one additional counts conducted by either JG or CK from 2000 to 2016 at 4 of the same sites (Point Loma, Hill Street, Bird Rock, and South Casa Reef) were also included in the analysis. A Wilcoxon sign-rank test was implemented in JMP v13, SAS Institute Inc. (Cary, NC) and used to compare the number of *P. hiltoni* found at Point Loma before and after 1963. Additional information on the recent occurrence of *P. hiltoni* in San Diego County was obtained from the website iNaturalist (https://www.inaturalist.org/taxa/48724-Phidiana-hiltoni) and the species database on Divebums, a San Diego dive website (http://species.divebums.com/index.php?l=sciname&n=Phidiana%20hiltoni), and confirmed by the authors.

Results

The haplotype network of the mitochondrial COI gene recovered five distinct haplotypes (Fig. 2). Thirty-three individuals spanning all seven populations share the most common haplotype. Three haplotypes diverge from the most common haplotype by only two nucleotides. The most common of these three haplotypes was found exclusively in fourteen individuals from Pillar Point, Northern California. The other two haplotypes are only found in specimens originating from Cayucos and Cave Landing, Central California. An additional specimen from Cave Landing possessed a haplotype diverging from the most common haplotype by three nucleotides.

In the first AMOVA test (Northern California: Pillar Point; Central California: Cave Landing, Jalama Beach, Cayucos, and Carmel Point) most of the genetic variation is recovered among groups (70.05%) and within populations (30.59%), with virtually no variation among populations within groups (-0.63%) (Table 2). In the second AMOVA test (Northern California: Pillar Point; Northern Central California: Carmel Point; Southern Central California: Jalama Beach, Cave Landing, Cayucos) most of the genetic variation is again among groups (65.94%) and within populations (32.82%) and very little variation among populations within groups (1.24%) (Table 2). In the third AMOVA test (Northern California: Pillar Point, Carmel Point; Central California: Jalama Beach, Cave Landing, Cayucos) most of the genetic variation is found again among groups (50.47%) and within populations (33.5%) however genetic variation is found among populations within groups (16.04%) (Table 2).

A pairwise Φ_{ST} test was run on all populations and resulted in relatively high values between Pillar Point and all other populations and also between Carmel Point and Cayucos. The only significant difference in genetic variation found was between Pillar Point, Northern California and each of the four Central California populations: Jalama Beach, Cave

[1] Goddard, J.H.R. 2013. Opisthobranch gastropods observed on the outer coast of San Diego County, California by James R. Lance, 1953–2001. knb.298.2. [online] California Academy of Sciences. Available https://knb.ecoinformatics.org/knb/metacat/knb.298.2/knb [2017 Jun 15].

Table 2. AMOVA test results for mitochondrial haplotype data of three separate population groupings obtained with Arlequin v3.5, significant values ($p \leq 0.05$) in bold. **Grouping 1**: Northern California (Pillar Point), Central California (Jalama Beach, Cave Landing, Cayucos, Carmel Point), and Southern California (San Clemente, Naples). **Grouping 2**: Northern California (Pillar Point), Northern Central California (Carmel Point), Southern Central California (Jalama Beach, Cave Landing, Cayucos) and Southern California (San Clemente, Naples). **Grouping 3**: Northern California (Pillar Point, Carmel Point), Central California (Jalama Beach, Cave Landing, Cayucos), and Southern California (San Clemente, Naples).

Source of variation	d.f.	Sum of squares	Variance components	% of variation	Fixation indices	*p* value
Grouping 1						
Among Groups	2	8.258	0.33629	70.05	-0.02112	**0.01019**
Among Populations within Groups	4	0.533	-0.00304	-0.63	0.69413	**0**
Within Populations	41	6.021	0.14685	30.59	0.70046	**0.02775**
Total	47	14.812	0.48011			
Grouping 2						
Among Groups	3	8.268	0.29502	65.94	0.03642	0.20297
Among Populations within Groups	3	0.524	0.00555	1.24	0.67179	**0**
Within Populations	41	6.021	0.14685	32.82	0.65938	0.09205
Total	47	14.812	0.44742			
Grouping 3						
Among Groups	2	6.900	0.22123	50.47	0.32374	**0.01969**
Among Populations within Groups	4	1.892	0.0703	16.04	0.66502	**0**
Within Populations	41	6.021	0.14685	33.5	0.50466	0.11511
Total	47	14.812	0.43838			

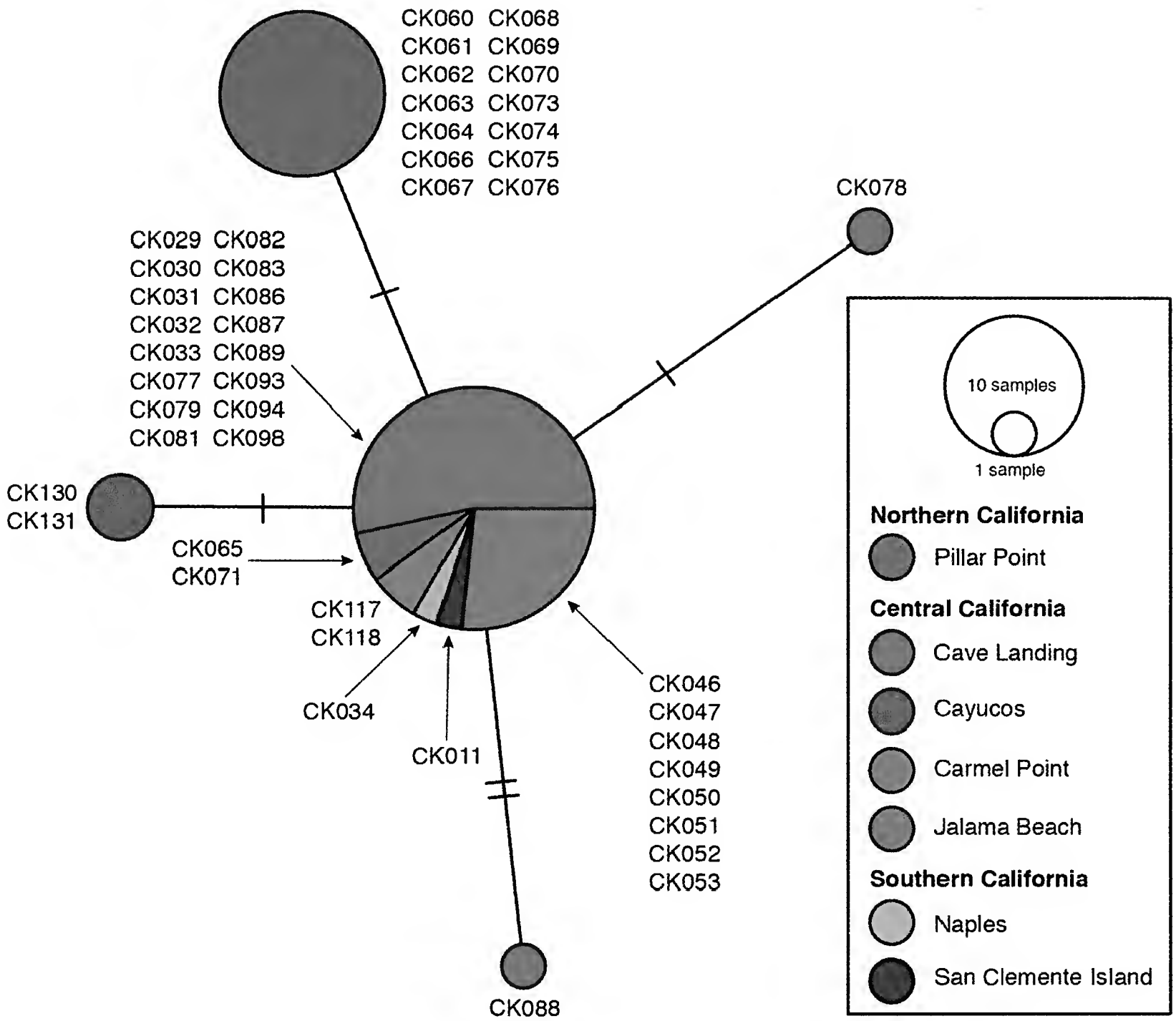

Fig. 2. Haplotype network of COI mitochondrial sequences generated with PopArt v1.7. Each circle represents a unique haplotype and its area is proportional to the number of specimens sequenced with that haplotype. Each pattern represents the geographic origin of the individual specimens, as indicated in the legend. Isolate codes are indicated next to each haplotype.

Landing, Cayucos and Carmel Point ($\Phi_{ST} = 0.69$, $p = 0.03$; $\Phi_{ST} = 0.75$, $p = 0.00$; $\Phi_{ST} = 0.69$, $p = 0.00$; $\Phi_{ST} = 0.67$, $p = 0.04$ respectively) (Table 3). This suggests genetic differentiation between Pillar Point and the other populations. However, this result, as well as the lack of significant differentiation among other pairwise comparisons, must be interpreted with caution due to the limited number of samples from all collection sites except for Pillar Point and Cave Landing.

Analysis of microsatellite data with Structure Harvester using Evanno's method (Evanno et al. 2005), a maximum value of the rate of change (ΔK) in the log probability of data was obtained at $K = 3$ (Fig. 3B). These three recovered clusters are unevenly distributed among geographic regions with no obvious geographic subdivision (cluster 1: red, cluster 2: blue, cluster 3: yellow, Fig. 3A). Moreover, all individuals exhibit a non-zero probability of belonging to any one of the three clusters.

All AMOVA tests with different groupings produced very similar results; the overwhelming majority of the genetic variation was recovered within populations (92.32–93.61%) and some among populations within groups (6.51–9.98%), with virtually no variation among groups (-3.59–1.17%) (Table 4). Pairwise F_{ST} comparisons produced very low values

Table 3. Φ_{ST} pairwise comparison values for mitochondrial haplotype data obtained with Arlequin v3.5 (lower triangular) and associated p values (upper triangular). Significant values ($p \leq 0.05$) in bold.

	Pillar Point	Carmel Point	Cayucos	Cave Landing	Jalama Beach	Naples	San Clemente
Pillar Point	–	**0.03062**	**0.00019**	**0.0000**	**0.03537**	0.09994	0.99994
Carmel Point	0.69490	–	0.21358	0.32000	0.99994	0.99994	0.99994
Cayucos	0.75345	0.62791	–	0.99994	0.99994	0.99994	0.99994
Cave Landing	0.68730	0.29687	-0.05381	–	0.99994	0.99994	0.99994
Jalama Beach	0.66771	0.0000	0.0000	-0.33043	–	0.99994	0.99994
Naples	0.61778	0.0000	0.0000	0.0000	0.0000	–	0.99994
San Clemente	0.61778	0.0000	0.0000	0.0000	0.0000	0.0000	–

across the entire range suggesting little to no genetic differentiation between populations (Table 5). DAPC, which attempts to group individuals using a k-means clustering algorithm, suggests that the entire metapopulation of *P. hiltoni* cannot be divided into more than one group based on microsatellite data (Fig. 4).

From 1953 to 1962, Jim Lance sampled for nudibranchs on the outer coast of San Diego County only at Point Loma, where he found at least one *Phidiana hiltoni* during half of his 28 trips during that period (Fig. 5A). In 1964 he began to sample additional outer coast sites. Since then, only two more *P. hiltoni* were found at Point Loma (Figure 5A & B), one by Lance in July 1968 and one by JG in June 2001. Similarly, *P. hiltoni* was observed on only about 10% of the trips to each of the other five outer coast sites (Fig. 5A), and was found in lower numbers per trip than had been seen in the earlier period at Point Loma (Fig. 5B). Significantly fewer *P. hiltoni* were found at Point Loma after 1963 than before (Wilcoxon rank sum test, P = 0.002) (Figs. 5B, C). Except for the 1990s, when only 10 total trips were made to two sites, *P. hiltoni* has been found in San Diego County in low numbers in each of the decades since the 1960s (Fig. 5C). Finally, *P. hiltoni* has been photographed subtidally in San Diego County at least 10 times since 2005 (http://species.divebums.com/index.php?l = sciname&n = Phidiana%20hiltoni; https://www.inaturalist.org/taxa/48724-Phidiana-hiltoni).

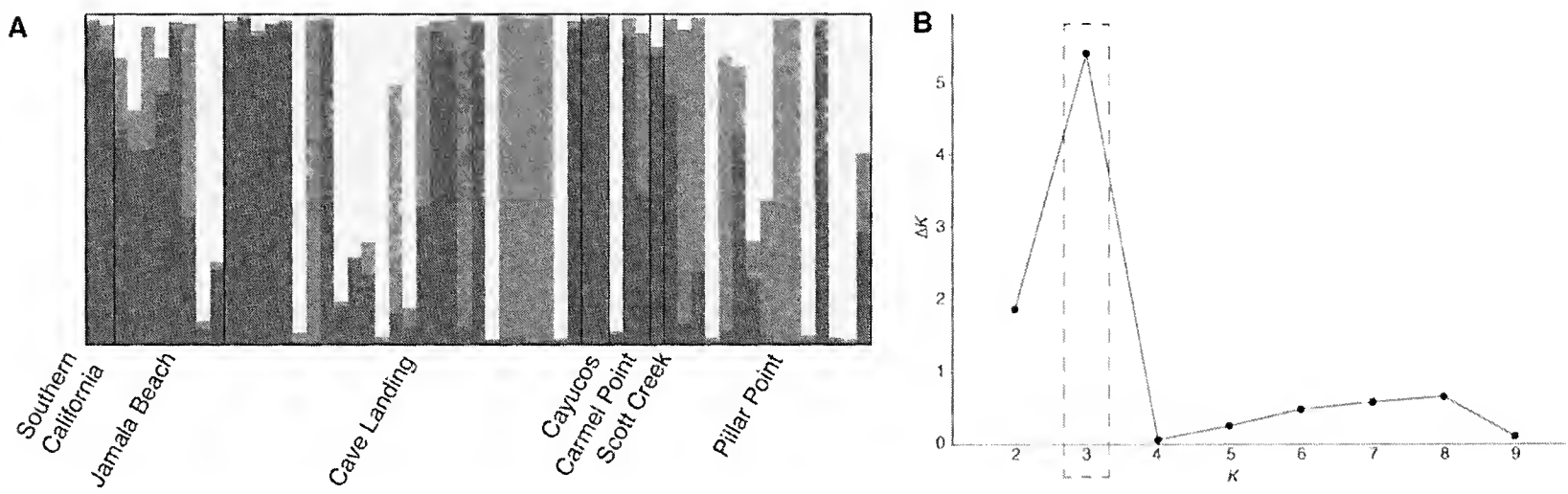

Fig. 3. Genetic clustering analysis for the entire data set of 57 individuals and 10 microsatellite regions as estimated by STRUCTURE v2.3.4. **A.** Genetic clustering plot for $K = 3$ clusters, generated with CLUMPP v1.1.2. Each grey tone represents a different genetic cluster. Bar graphs show average posterior probability of membership (y-axis) of each individual. Populations are delimited by dark vertical lines. **B.** Graph of ΔK = mean ($|L''(K)|$) / sd($L(K)$) as a function of K (potential number of genetic clusters) generated by STRUCTURE Harvester v0.6.9.84. The most likely number of clusters is indicated by the modal value, in this case $K = 3$.

Table 4. AMOVA test results for microsatellite genotype data with three separate population groupings obtained with Arlequin v3.5, significant values ($p \leq 0.05$) in bold. **Grouping 1**: Northern California (Pillar Point), Central California (Jalama Beach, Cave Landing, Cayucos, Carmel Point), and Southern California (San Clemente, Naples). **Grouping 2**: Northern California (Pillar Point), Northern Central California (Carmel Point), Southern Central California (Jalama Beach, Cave Landing, Cayucos) and Southern California (San Clemente, Naples). **Grouping 3**: Northern California (Pillar Point, Carmel Point), Central California (Jalama Beach, Cave Landing, Cayucos), and Southern California (San Clemente, Naples).

Source of variation	d.f.	Sum of squares	Variance components	% of variation	Fixation indices	*p* value
Grouping 1						
Among Groups	2	16.091	-0.15376	-3.59	0.06387	**0.01075**
Among Populations within Groups	3	27.962	0.42745	9.98	0.09630	**0.00719**
Within Populations	104	417.174	4.01129	93.61	-0.03588	0.49775
Total	109	461.227	4.28498			
Grouping 2						
Among Groups	3	28.051	0.05088	1.17	0.07679	**0.01106**
Among Populations within Groups	3	16.002	0.28276	6.51	0.06585	0.27272
Within Populations	104	417.174	4.01129	92.32	0.01171	0.15679
Total	109	461.227	4.34492			
Grouping 3						
Among Groups	2	17.137	-0.09775	-2.27	0.06886	**0.01106**
Among Populations within Groups	3	26.916	0.3944	9.16	0.08952	**0.0245**
Within Populations	104	417.174	4.01129	93.11	-0.02269	0.37895
Total	109	461.227	4.30793			

Table 5. F_{ST} pairwise comparison values for microsatellite genotype data, obtained with Arlequin v3.5 (lower triangular) and associated p values (upper triangular), significant values ($p \leq 0.05$) in bold. The two southern California populations of Naples and San Clemente were combined into one due to low sampling numbers.

	Pillar Point	Scott Creek	Carmel Point	Cave Landing	Jalama Beach	S. California
Pillar Point	–	0.93776	**0.01968**	0.64388	0.39049	0.35181
Scott Creek	0.13279	–	0.99994	0.99994	0.99994	0.99994
Carmel Point	0.14426	0.35183	–	**0.00306**	**0.00444**	0.10229
Cave Landing	0.01779	0.17272	0.15117	–	0.06255	0.05986
Jalama Beach	0.04219	0.23112	0.19336	0.05260	–	0.19821
S. California	0.12656	0.36283	0.30272	0.15087	0.15965	–

Discussion

The California coast is a prime example of a region where climate change is impacting native marine ecosystems through changes in ocean temperatures, seawater chemistry, and coastal current regimes (Barry et al. 1995; Sagarin et al. 1999; Harley et al. 2006). With ocean temperatures increasing, species are predicted to shift their ranges poleward, a trend that has already been observed across a wide range of taxonomic groups, mostly at temperate latitudes (Dawson et al. 2010; VanDerWal et al. 2012). It is difficult to predict how environmental change, including biotic exchanges resulting from species range shifts and introductions, will affect ecological systems. Hellman et al. (2008) emphasized that

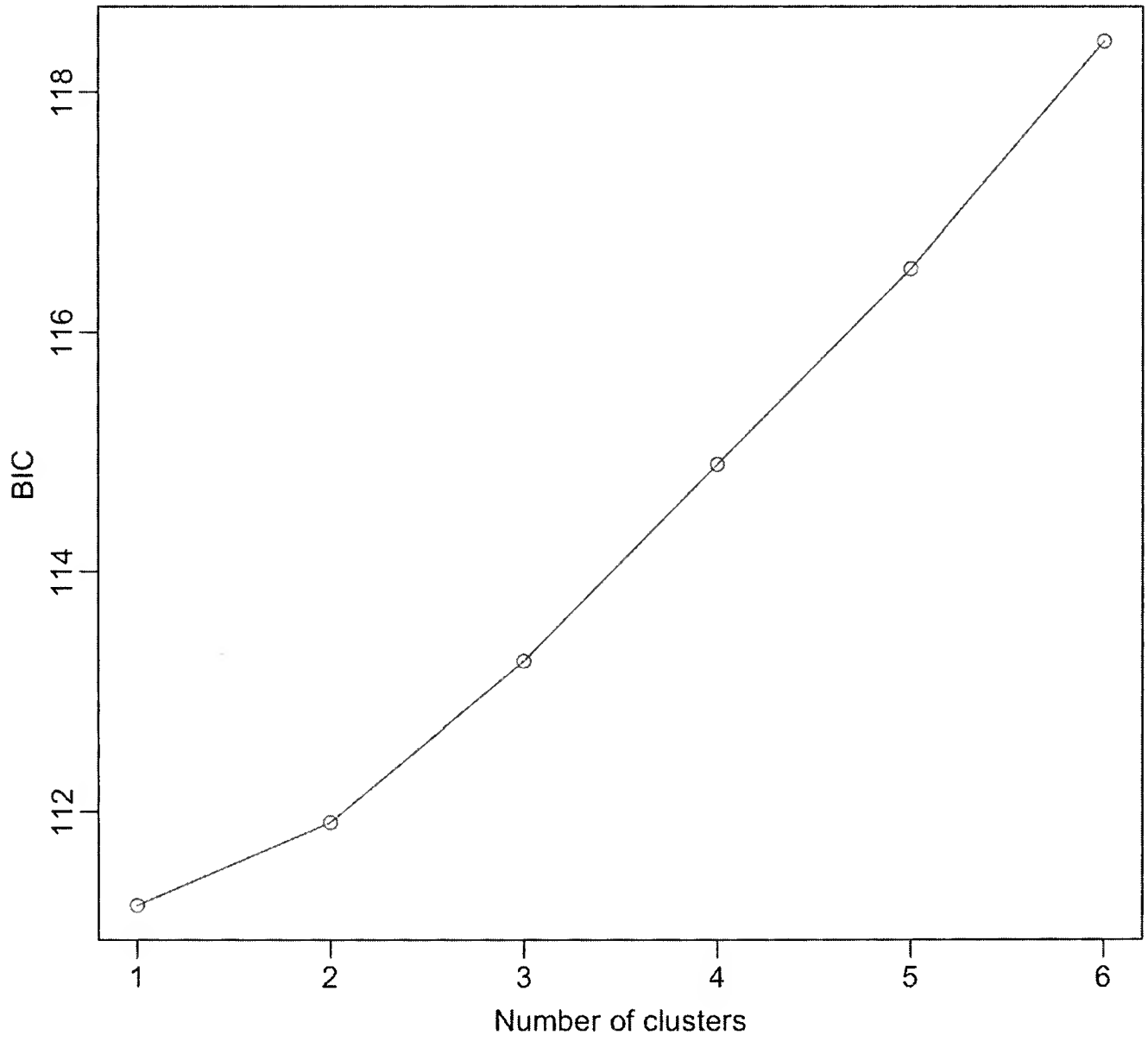

Fig. 4. Results of the DAPC analysis indicating that the data, when analyzed as principal components, cannot be divided into more than one group.

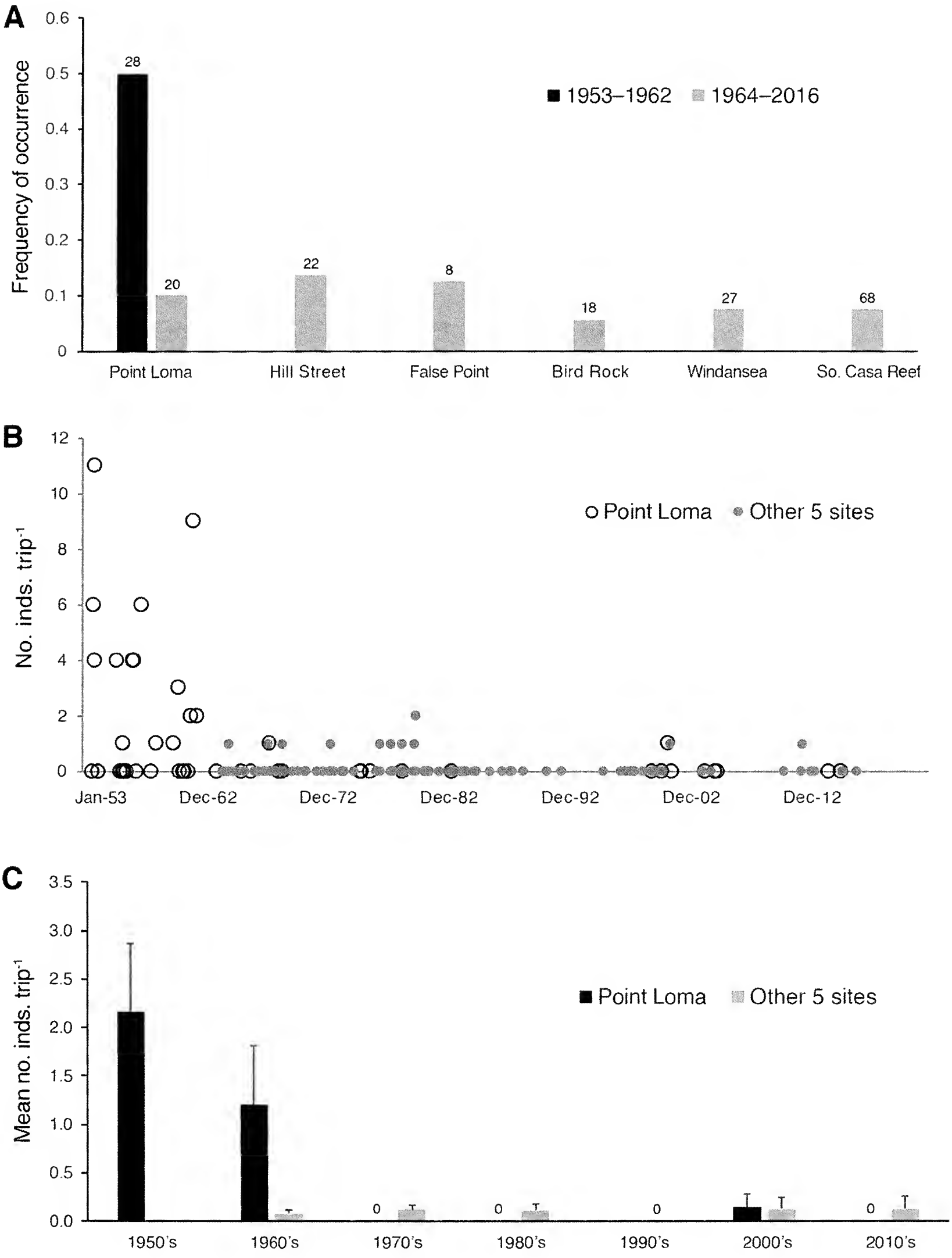

Fig. 5. Occurrence of *Phidiana hiltoni* at six rocky intertidal sites in San Diego County, 1953–2016. **A**. Frequency of occurrence by site, 1953–1962 and 1964–2016. Number of trips to each site shown above bars. **B**. Number of *P. hiltoni* found on each trip, 1953–2016. **C**. Mean number (± SE) of *P. hiltoni* found per trip at Point Loma and other sites combined, by decade.

global climate change compounds this difficulty because it transforms transport and introduction mechanisms, impacts the distribution of existing invasive species, and alters the effectiveness of control strategies. Efforts to manage and conserve marine ecosystems in the face of climate change will require improvements to the existing predictive framework to aid in preventing future introductions (Harley et al. 2006). In this context, understanding the mechanisms behind range expansions (or shifts) of individual species will contribute to a larger body of evidence, critically important for predicting the biological effects of climate change.

The data presented in this paper provide insight into the processes underlying the range expansion in *P. hiltoni*. The analysis of mitochondrial DNA (mtDNA) sequence data of *Plidiana hiltoni* across both its historical range and extended range in Northern California revealed limited genetic structure. The COI haplotype network shows very little polymorphism with only five haplotypes in total being recovered (Fig. 2). The most common of these haplotypes is shared among individuals from all seven populations, including the newly formed populations in Northern California. However, there are a few haplotypes only detected in certain populations. For example, one of the two haplotypes found at Pillar Point, north of Monterey Bay, was found nowhere else. Because populations north of Monterey Bay did not exist prior to 1977 (Goddard et al. 2011), it is likely that this unique haplotype is also present south of Monterey Bay but at such low frequency that it has not been yet detected, and may have become more common in the recently colonized populations due to founder effects. To better understand the geographic structure of *P. hiltoni* based on mtDNA, three AMOVA analyses were run, each with different population groupings. In each of the three groupings, the highest percent variation was consistently found among groups (Table 2). However, there is a decrease in this percent variation as the groupings structure are altered (70.05%, 65.94%, 50.47% respectively), suggesting that the first grouping arrangement (in which the Northern California group includes only populations found in the extended range) best represents population genetic structure according to mtDNA data. Pairwise Φ_{ST} comparisons agree with the geographic structure recovered in the AMOVAs (Table 3). Relatively high Φ_{ST} values indicating genetic differentiation were found between Pillar Point and the Central and Southern California populations, and between Carmel Point and the two populations of Cayucos and Cave Landing. This is consistent with the haplotype network results, showing that Pillar Point, Cayucos and Cave Landing possess divergent haplotypes from the most common haplotype found across the range of *P. hiltoni*.

While analyses of mtDNA sequences suggest population structure and genetic differentiation among groups, no genetic pattern corresponding to geography was detected using microsatellite data. Across the range of *P. hiltoni*, Structure analyses showed several individuals have nearly identical probabilities of cluster membership, a pattern that is particularly apparent at Cave Landing. This genetic uniformity could be an indication of self-recruitment at Cave Landing, where the concavity in the coastline (accentuated by the 750-meter long rock jetty on Point San Luis) may encourage larval retention. Goddard et al. (2011) suggested that population structure in *P. hiltoni* should be affected by upwelling shadows, resulting in local retention of short-lived larvae, particularly at the northern end of bights along the coastline (Graham and Largier 1997; Roughan et al. 2005). AMOVAs on microsatellite data included the same three distinct groupings as mitochondrial analyses except for the addition of Scott Creek to the Northern California group and the removal of Cayucos (where microsatellite data were not successfully recovered). In all AMOVA tests, most genetic variance was found within populations (93.61%, 92.32% and

93. 11%, respectively) (Table 4). Consistently low variation among groups is indicative of high levels of gene flow across the range, as seen in the mtDNA data. Pairwise comparisons of F_{ST} values from microsatellite data are also consistent with high gene flow across the range, with generally low F_{ST} values between populations (Table 5). The slightly higher F_{ST} values found between Scott Creek and Carmel Point, as well as between Carmel Point and Southern California are unreliable due to the low sample sizes from Scott Creek and Southern California.

AMOVA and pairwise Φ_{ST} comparisons using mtDNA data suggest Northern California populations are genetically distinct, and consequently the origin of the recently founded populations remains unclear. On the contrary, microsatellite data indicate very high levels of gene flow in *P. hiltoni,* with Northern California populations genetically indistinguishable from those in Central California. This discrepancy of results from mtDNA vs. nuclear data might be explained by the reproductive behavior of *P. hiltoni.* Rutowksi (1983) found that species with high rates of cannibalism require several couplings, usually with different mates, in order for all the eggs in the egg mass to be fertilized. It is very likely that *P. hiltoni* (considering the pugnacious and cannibalistic nature of this species) exhibits abbreviated coupling times, requiring several mates to fully fertilize egg masses. Additionally, *P. hiltoni* exhibits locally high population densities in Central California, potentially facilitating promiscuity and thus intense sperm competition. The main consequence of this mating system would be that egg masses produced by a single individual (functional female) will be sired by multiple partners, generating offspring with genetically identical mitochondria but different nuclear alleles. If recently established populations in Northern California are the result of sporadic events involving dispersal of larvae (or rafting of egg masses) produced by a small number of females, it is likely that founder effects facilitated retention of these rare mitochondrial haplotypes. While the diversity of nuclear alleles should also decrease due to drift and founder effects, the polyandrous mating system of *P. hiltoni* has the potential to mitigate these effects. Under this scenario, Northern California populations could harbor mitochondrial haplotypes that were previously very rare in the historic range, while nuclear alleles from the source population are more broadly represented. If this hypothesis is correct, additional sampling from Central California should detect all or most Northern California haplotypes. An alternative explanation is that the lack of genetic structure in microsatellite data is an artifact of the limited sample size. If this is the case, additional sampling across the range of *P. hiltoni* would improve the reliability of the results of this study.

Another outstanding question is what mechanism(s) allowed *P. hiltoni* to cross Monterey Bay starting in the late 1970s, or what physical or biological barriers restricted the prior range of this species. If recently established populations in Northern California are indeed the result of sporadic dispersal by a limited number of individuals, this would suggest that this dispersal was not triggered by a gradual process, such as increasing ocean temperatures, but instead by the temporary or intermittent opening of a corridor. One distinct possibility is that a weakening of the upwelling shadow in Monterey Bay (Graham and Largier 1997) due to climate change may have facilitated this process. Pennington et al. (2000) documented decadal-scale changes in the oceanographic conditions near the center of Monterey Bay region consistent with those described for the 1976–77 climate shift in the North Pacific Ocean. These include increased stratification of surface waters, warmer, less productive waters during non-upwelling seasons and a later onset of upwelling. These changes may have reduced larval retention in northern Monterey Bay, allowing *P. hiltoni* to disperse into Northern California.

Few studies have examined the population genetics of other marine invertebrate taxa that have experienced recent range expansions or range shifts. In California, a similar study by Dawson et al. (2010) examined three hypotheses/scenarios that explain the causes of range limits of species, and concluded that in the volcano barnacle, *Tetraclita rubescens*, the northern range boundary is maintained by migration load arising from flow of maladapted alleles into peripheral locations. Dawson et al. (2010) proposed that in this species (with planktonic-dispersing larvae), environmental amelioration, likely due to climate change, resulted in a reduction of the strength of selection against immigrant phenotypes in the northern range boundary, allowing the species to expand northward. The case of *P. hiltoni* is very different in several respects, but the main difference is that whereas *T. rubescens* was declining near its northern range limit, *P. hiltoni* has been and remains common. Framing of our data in the three scenarios/hypotheses proposed by Dawson et al. (2010) suggest physical barriers to dispersal is the most likely mechanism that historically restricted migration in *P. hiltoni*.

This study included a sample of 57 individual specimens collected across the range of *P. hiltoni*, but the sample size from Southern California, south of Point Conception, is small. Only two individuals were collected despite a substantial collecting effort by the senior author in this region during two consecutive years. This suggests that *P. hiltoni* could have become rare in the southern portion of its range. However, this assumption should be interpreted with caution. Bates et al. (2015) shown that abundance-related species detectability, particularly important in uncommon, difficult-to-detect marine species such as *P. hiltoni*, has the potential to confound our understanding of the true location of range edges. Bates et al. (2015) emphasized the importance of simulation and modeling, but also long-term monitoring with consistent sampling effort through time. In this case, we analyzed high-quality, long-term observational data collected at fairly regular intervals from the same region. These data suggest that the historical abundance of *P. hiltoni* in San Diego County, especially Point Loma (the type locality of *P. pugnax* Lance 1961 [= *P. hiltoni*]) has declined (Figs. 4A–C). Reasons for this decline remain unknown and warrant further investigation, although rising ocean temperatures appears to be a viable hypothesis. Notably, the abundance of another species of sea slug, *Felimare californiensis*, was once-common in Southern California, but became extinct there in the 1980's (Goddard et al. 2013). Although individuals of *F. californiensis* reappeared in 2003 and the species has since been found in a few isolated localities in Southern California (Goddard et al. 2013; Hoover 2015), its populations have not completely recovered. It is unclear whether there is a link between the decline of these two ecologically distinct species, but if there is, it may be a symptom of larger and more pervasive environmental change. The apparent decline of *P. hiltoni* in Southern California along with its dispersal northward needs to be substantiated with further monitoring and additional data analyses (Bates et al. 2015), but if confirmed, would suggest this is a true poleward range expansion rather than a temporary shift (Parmesan et al. 1999). Understanding the process by which *P. hiltoni* migrated northward may provide insight as to how other benthic organisms will respond to rising ocean temperatures and changes in ocean current systems (McGowan et al. 1998).

Acknowledgements

This project was funded by graduate student research awards from Conchologists of America and the Department of Biological Sciences, California State Polytechnic University to CJK. Specimen loans were facilitated by Lindsey Groves (LACM) and Daniel

Geiger (SBMNH). Jayson Smith read an early version of the manuscript and helped with the statistical analyses of the historical data. Donna Pomeroy provided support in the field at Pillar Point.

Literature Cited

Barry, J.P., C.H. Baxter, R.D. Sagarin, and S.E. Gilman. 1995. Climate-related, long-term faunal changes in a California rocky intertidal community. Science, 267:672–675.

Bates, A.E., T.J. Bird, R.D. Stuart-Smith, T. Wernberg, J.M. Sunday, N.S. Barrett, G.J. Edgar, S. Frusher, A.J. Hobday, G.T. Pecl, and D.A. Smale. 2015. Distinguishing geographical range shifts from artefacts of detectability and sampling effort. Divers. Distrib., 21:13–22.

—, G.T. Pecl, S. Frusher, A.J. Hobday, T. Wernberg, D.A. Smale, J.M. Sunday, N. Hill, N.K. Dulvy, R.K. Colwell, N.J. Holbrook, E.A. Fulton, D. Slawinski, M. Feng, G.J. Edgar, B.T. Radford, P.A. Thompson, and R.A. Watson. 2014. Defining and observing stages of climate-mediated range shifts in marine systems. Glob. Environ. Change, 26:27–38.

Blanchette, C.A., C. Melissa Miner, P.T. Raimondi, D. Lohse, K.E. Heady, and B.R. Broitman. 2008. Biogeographical patterns of rocky intertidal communities along the Pacific coast of North America. J. Biogeogr., 35:1593–1607.

Canning-Clode, J. and J.T. Carlton. 2017. Refining and expanding global climate change scenarios in the sea: Poleward creep complexities, range termini, and setbacks and surges. Divers. Distrib., 23: 463–473.

Dawson, M.N., R.K. Grosberg, Y.E. Stuart, and E. Sanford. 2010. Population genetic analysis of a recent range expansion: mechanisms regulating the poleward range limit in the volcano barnacle *Tetraclita rubescens*. Mol. Ecol., 19:1585–1605.

Earl, D.A., and B.M. vonHoldt. 2012. Structure Harvester: A website and program for visualizing STRUCTURE output and implementing the Evanno method. Conserv. Genet. Resour., 4:359–361.

Evanno, G., S. Regnaut, and J. Goudet. 2005. Detecting the number of clusters of individuals using the software Structure: A simulation study. Mol. Ecol., 14:2611–2620.

Excoffier, L., and H. E. Lischer. 2010. Arlequin suite ver 3.5: A new series of programs to perform population genetics analyses under Linux and Windows. Mol. Ecol. Resour., 10:564–567.

Faircloth, B.C. 2008. MSATCOMMANDER: Detection of microsatellite repeat arrays and automated, locus-specific primer design. Mol. Ecol. Resour., 8:92–94.

Folmer, O., M. Black, W. Hoeh, R. Lutz, and R. Vrijenhoek. 1994. DNA primers for amplification of mitochondrial cytochrome c oxidase subunit I from diverse metazoan invertebrates. Mol. Mar. Biol. Biotechnol., 3:294–299.

Gallardo, B., M. Clavero, M.I. Sánchez, and M. Vilà. 2016. Global ecological impacts of invasive species in aquatic ecosystems. Glob. Change. Biol., 22:151–163.

Goddard, J.H.R. 2004. Developmental mode in benthic opisthobranch molluscs from the Northeast Pacific Ocean: Feeding in a sea of plenty. Can. J. Zool., 82:1954–1968.

—, and A. Hermosillo. 2008. Developmental mode in opisthobranch molluscs from the tropical Eastern Pacific Ocean. Veliger, 50:83–96.

—, T.M. Gosliner, J.S. Pearse. 2011. Impacts associated with the recent range shift of the aeolid nudibranch *Phidiana hiltoni* (Mollusca, Opisthobranchia) in California. Mar. Biol., 158:1095–1109.

—, M.C. Schaefer, C. Hoover, A. Valdés. 2013. Regional extinction of a conspicuous dorid nudibranch (Mollusca: Gastropoda) in California. Mar. Biol., 160:1497–1510.

—, N. Treneman, T. Prestholdt, C. Hoover, B. Green, W.E. Pence, D.E. Mason, P. Dobry, J.L. Sones, E. Sanford, R. Agarwal, G.R. McDonald, R.F. Johnson, and T.M. Gosliner. 2018. Heterobranch sea slug range shifts in the northeast Pacific Ocean associated with the 2015-16 El Niño. Proc. Calif. Acad. Sci., 65(3):107–131.

Graham, W.M., and J.L. Largier. 1997. Upwelling shadows as nearshore retention sites: The example of northern Monterey Bay. Cont. Shelf Resour., 17:509–532.

Harley, C.D.G., et al. 2006. The impacts of climate change in coastal marine systems. Ecol. Lett., 9:228–241.

Hellmann, J.J., J.E. Byers, B.G. Bierwagen, and J.S. Dukes. 2008. Five potential consequences of climate change for invasive species. Conserv. Biol., 22:534–543.

Hoover, C. 2015. Phylogenetics and population genetics of *Felimare californiensis*. M.S. dissertation, California State Polytechnic University, Pomona.

Jombart, T., S. Devillard, and F. Balloux. 2010. Discriminant analysis of principal components: a new method for the analysis of genetically structured populations. BMC Genetics, 11:94.

Kearse, M., R. Moir, A. Wilson, S. Stones-Havas, M. Cheung, S. Sturrock, S. Buxton, A. Cooper, S. Markowitz, C. Duran, and T. Thierer. 2012. Geneious Basic: An integrated and extendable desktop software platform for the organization and analysis of sequence data. Bioinform., 28:1647–1649.

Leigh, J.W., and D. Bryant. 2015. PopArt: Full-feature software for haplotype network construction. Methods Ecol. Evol., 6:1110–1116.

McGowan, J.A. 1998. Climate-ocean variability and ecosystem response in the Northeast Pacific. Science, 281:210–217.

Parmesan, C., N. Ryrholm, C. Stefanescu, and J.K. Hill. 1999. Poleward shifts in geographical ranges of butterfly species associated with regional warming. Nature, 399:579–583.

Pennington, J.T., and F.P. Chavez. 2000. Seasonal fluctuations of temperature, salinity, nitrate, chlorophyll and primary production at station H3/M1 over 1989–1996 in Monterey Bay, California. Deep-Sea Res. II Trop. Stud. Oceanogr., 47:947–973.

Pritchard, J.K., P. Stephens, and P. Donnelly. 2000. Inference of population structure using multilocus genotype data. Genetics, 155:31–45.

Rebstock, G.A. 2003. Long-term change and stability in the California Current System: lessons from CalCOFI and other long-term data sets. Deep-Sea Res. II Trop. Stud. Oceanogr., 50:2583–2594.

Rosenberg, N. 2004. Distruct: A program for the graphical display of population structure. Mol. Ecol. Notes, 4:137–138.

—, J.K. Pritchard, J.L. Weber, H.M. Cann, K.K. Kidd, L.A. Zhivotovsky, and M.W. Feldman. 2002. Genetic structure of human populations. Science, 298:2981–2985.

Roughan, M., A.J. Mace, J.L. Largier, S.G. Morgan, J.L. Fisher, and M.L. Carter. 2005. Subsurface recirculation and larval retention in the lee of a small headland: A variation on the upwelling shadow theme. Geophysics 110:10027.

Rutowksi, R.L. 1983. Mating and egg mass production in the aeolid nudibranch *Hermissenda crassicornis* (Gastropoda; Opisthobranchia). Biol. Bull., 165:276–283.

Sagarin, R.D., J.P. Barry, S.E. Gilman, and C.H. Baxter. 1999. Climate-related change in an intertidal community over short and long time scales. Ecol. Monogr., 69:465–490.

Scheltema, R.S. 1986. On dispersal and planktonic larvae of benthic invertebrates: an eclectic overview and summary of problems. Bull. Mar. Sci., 39:290–322.

Schultz, S.T., J.H.R. Goddard, T.M. Gosliner, D.E. Mason, W.E. Pence, G.R. McDonald, V.B. Pearse, and J.S. Pearse. 2011. Climate-index response profiling indicates larval transport is driving population fluctuations in nudibranch gastropods from the northeast Pacific Ocean. Limnol. Oceanogr., 56:749–763.

Sorte, C.J. B., S.L. Williams, and J.T. Carlton. 2010. Marine range shifts and species introductions: Comparative spread rates and community impacts. Glob. Ecol. Biogeogr. 19:303–316.

Sunday, J.M., A.E. Bates, and N.K. Dulvy. 2012. Thermal tolerance and the global redistribution of animals. Nature Clim. Chang. 2:686–690.

VanDerWal, J., H.T. Murphy, A.S. Kutt, G.C. Perkins, B.L. Bateman, J.J. Perry, and A.E. Reside. 2012. Focus on poleward shifts in species' distribution underestimates the fingerprint of climate change. Nature Clim. Chang., 3:239–243.

Wasson, K., C.J. Zabin, L. Bedinger, M.C. Diaz, and J.S. Pearse. 2001. Biological invasions of estuaries without international shipping: the importance of intraregional transport. Biol. Conserv., 102:143–153.

Wilson, L.J., C.J. Fulton, A.M. Hogg, K.E. Joyce, B. Radford, and C.I. Fraser. 2016. Climate-driven changes to ocean circulation and their inferred impacts on marine dispersal patterns. Glob. Ecol. Biogeogr., 25:923–939.

Zeidberg, L.D., and B.H. Robison. 2007. Invasive range expansion by the Humboldt Squid, *Dosidicus gigas*, in the Eastern North Pacific. PNAS, 104:12948–12950.

Appendix

Table S1. Complete list of specimens sequenced for this study, including isolate number, locality, collection date, and GenBank accession numbers.

Isolate	Locality	Collection date	GenBank accession #
CK11	San Clemente Island, CA	1961	MK333330
CK29	Cave Landing, CA	10/8/2014	MK333291
CK30	Cave Landing, CA	10/8/2014	MK333292
CK31	Cave Landing, CA	10/8/2014	MK333293
CK32	Cave Landing, CA	10/8/2014	MK333294
CK33	Cave Landing, CA	10/8/2014	MK333295
CK34	Naples, CA	12/2009	MK333313
CK46	Tarantula Reef, Jalama Beach, CA	12/15/2009	MK333331
CK47	Tarantula Reef, Jalama Beach, CA	12/15/2009	MK333332
CK48	Tarantula Reef, Jalama Beach, CA	12/15/2009	MK333333
CK49	Tarantula Reef, Jalama Beach, CA	12/15/2009	MK333334
CK50	Tarantula Reef, Jalama Beach, CA	12/15/2009	MK333335
CK51	Tarantula Reef, Jalama Beach, CA	12/15/2009	MK333336
CK52	Tarantula Reef, Jalama Beach, CA	12/15/2009	MK333337
CK53	Tarantula Reef, Jalama Beach, CA	12/15/2009	MK333338
CK60	Pillar Point, CA	6/18/2015	MK333314
CK61	Pillar Point, CA	6/18/2015	MK333315
CK62	Pillar Point, CA	6/18/2015	MK333316
CK63	Pillar Point, CA	6/18/2015	MK333317
CK64	Pillar Point, CA	6/22/2015	MK333318
CK65	Pillar Point, CA	6/22/2015	MK333319
CK66	Pillar Point, CA	6/22/2015	MK333320
CK67	Pillar Point, CA	6/22/2015	MK333321
CK68	Pillar Point, CA	6/22/2015	MK333322
CK69	Pillar Point, CA	6/22/2015	MK333323
CK70	Pillar Point, CA	6/22/2015	MK333324
CK71	Pillar Point, CA	6/22/2015	MK333325
CK73	Pillar Point, CA	6/22/2015	MK333326
CK74	Pillar Point, CA	6/22/2015	MK333327
CK75	Pillar Point, CA	6/22/2015	MK333328
CK76	Pillar Point, CA	6/22/2015	MK333329
CK77	Cave Landing, CA	1/16/2016	MK333296
CK78	Cave Landing, CA	1/16/2016	MK333297
CK79	Cave Landing, CA	1/16/2016	MK333298
CK80	Cave Landing, CA	1/16/2016	MK333299
CK81	Cave Landing, CA	1/16/2016	MK333300
CK82	Cave Landing, CA	1/16/2016	MK333301
CK83	Cave Landing, CA	1/16/2016	MK333302
CK84	Cave Landing, CA	1/16/2016	MK333303
CK86	Cave Landing, CA	1/16/2016	MK333304
CK87	Cave Landing, CA	1/16/2016	MK333305
CK88	Cave Landing, CA	1/16/2016	MK333306
CK89	Cave Landing, CA	2/5/2016	MK333307
CK93	Cave Landing, CA	2/5/2016	MK333308
CK94	Cave Landing, CA	2/5/2016	MK333309
CK98	Cave Landing, CA	2/5/2016	MK333310
CK117	Carmel Pt, Monterey Bay CA	–	MK333289
CK118	Carmel Pt, Monterey Bay CA	–	MK333290
CK130	Cayucos, CA	–	MK333311
CK131	Cayucos, CA	–	MK333312

Table S2. List of primer pairs (and their sequences) used to amplify polymorphic microsatellite loci in *P. hiltoni*. Bolded portion of forward primers indicate M13 tail.

Primer	Sequence
Phil760625F	**AGGGTTTTCCCAGTCACGACGTT**AACGTCGTCATGGAATTCACAG
Phil760625R	GTTTATTAATGGCGGCGATGTGAC
Phil792112F	**AGGGTTTTCCCAGTCACGACGTT**AACCAATCGACGACAAGCTAAC
Phil792112R	GTTTGTCTCCGTGTTAAGTGTTGC
Phil820905F	**AGGGTTTTCCCAGTCACGACGTT**ACATTACTCCACTCGACTCAGG
Phil820905R	GTTTAGTCTCGGTCCATGAATCAGG
Phil928092F	**AGGGTTTTCCCAGTCACGACGTT**GATTCTATGCCACACACCTTGG
Phil928092R	GTTTAATGTATCTGCTTCATCCGTGC
Phil98151F	**AGGGTTTTCCCAGTCACGACGTT**AGAGGAATAGTCGCGGAACTAC
Phil98151R	GTTTCATCATTGCGTCAGATGTCC
Phil109255F	**AGGGTTTTCCCAGTCACGACGTT**CACACGTTCATACACTCACCTG
Phil109255R	GTTTAACACCGAGACAAGACATGC
Phil585958F	**AGGGTTTTCCCAGTCACGACGTT**ACTCTCTCACACCTGTCAAGTC
Phil585958R	GTTTCACCTCAGTACAGTCTCGTG
Phil918696F	**AGGGTTTTCCCAGTCACGACGTT**ACTCTCTCACACCTGTCAAGTC
Phil918696R	GTTTCACCTCAGTACAGTCTCGTG
Phil121774F	**AGGGTTTTCCCAGTCACGACGTT**GTCAAGTGAATAAGACGGCGAG
Phil121774R	GTTTCTGCCTGCTATACATCCATCC
Phil315595F	**AGGGTTTTCCCAGTCACGACGTT**GTAACACAGTGTCCGTATGTGG
Phil315595R	GTTTATCATTCTACGTGCATGCTGTC

Bull. Southern California Acad. Sci.
118(1), 2019, pp. 21–41

Status of the Endangered Indian Knob Mountainbalm *Eriodictyon altissimum* (Namaceae) in Central Coastal California

Christopher P. Kofron,[1]* Connie Rutherford,[1] Lisa E. Andreano,[2]
Michael J. Walgren,[2] and Heather Schneider[3]

[1] *U.S. Fish and Wildlife Service, 2493 Portola Road, Suite B, Ventura, CA 93003*
[2] *California Department of Parks and Recreation, 750 Hearst Castle Road, San Simeon, CA 93452*
[3] *Santa Barbara Botanic Garden, 1212 Mission Canyon Road, Santa Barbara, CA 93105*

Abstract.—Indian Knob Mountainbalm *Eriodictyon altissimum* (Namaceae) is a shrub endemic to western San Luis Obispo County in central coastal California, and little has been published regarding it. The species was listed as endangered under the California Endangered Species Act in 1979 and the U.S. Endangered Species Act in 1995. At Federal listing in 1995, Indian Knob mountainbalm was known from six occurrences, two of which were in protected areas, with a total population estimate of <600 individuals. As of 2019, Indian Knob mountainbalm is known from seven occurrences, six of which are in protected areas and one (the largest) mostly in a protected area, with a total population count of 6,489+ individuals in 2016. Two occurrences are likely extirpated. Indian Knob mountainbalm is considered a fire-adapted chaparral plant. Reproduction is reported to be primarily vegetative by underground rhizomes, and it is specialized for substrates with physical disturbances, including: steep rocky slopes, cliff faces, fallen rock debris, sand dunes (shifting sand), roadsides, old graded substrates such as dirt/rock roads, the talus of graded substrates, and trails. We report the species grows up to 5.5 m tall and at 98 to 263 m elevation. In consideration of the life history traits used by Anacker et al. (2013) for rare plants in California, Indian Knob mountainbalm would be considered highly vulnerable to climate change. Using the international standards of IUCN, Indian Knob mountainbalm meets the criteria for classification as endangered including the following: geographic range, fragmented; extent of occurrence, 34 km^2 (<100 km^2); area of occupancy, <2.3 km^2 (<10 km^2); and quality of habitat, continuing to decline (dense vegetation, lack of recent fire). Coordinated conservation and research are needed to further understand the species, and to restore and maintain the five extant occurrences.

Indian Knob mountainbalm *Eriodictyon altissimum* (Namaceae, Luebert et al. 2016; Fig. 1) is a shrub endemic to western San Luis Obispo County in central coastal California (Fig. 2). The species was listed as endangered under the California Endangered Species Act in 1979 (CDFW 2016) and the U.S. Endangered Species Act in 1995 (USFWS 1994). It is recognized also as a 1B.1 rare plant (seriously threatened) by the California

* Corresponding author: chris_kofron@fws.gov

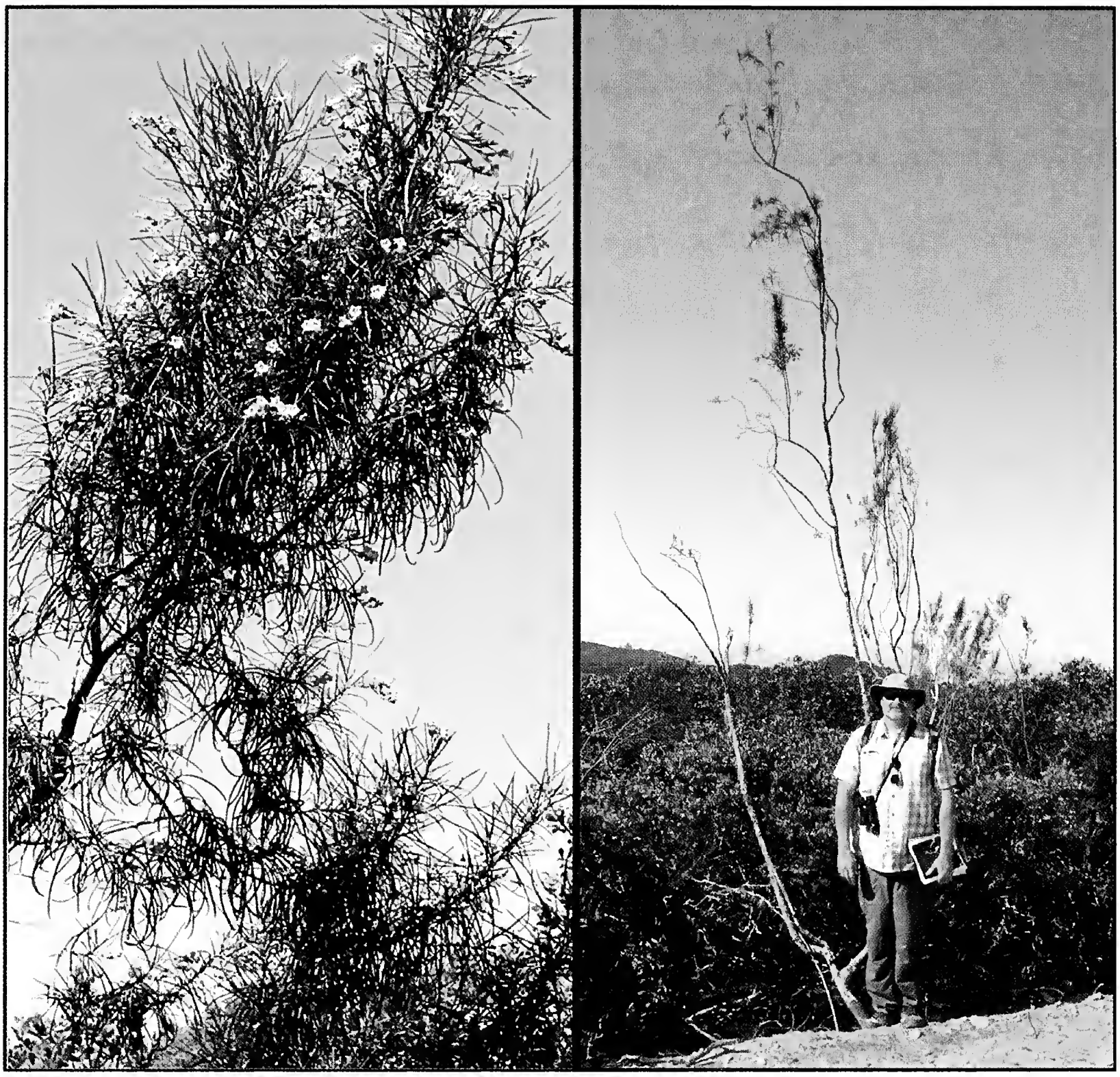

Fig. 1. Left: A tall individual of Indian Knob mountainbalm *Eriodictyon altissimum* with flowers in Morro Dunes Ecological Reserve East in Los Osos, San Luis Obispo County, California (occurrence 6), 20 April 2016. Right: An extraordinarily tall individual of Indian Knob mountainbalm rising above the mature chaparral comprised predominantly of Santa Margarita manzanita *Arctostaphylos pilosula* at Baron Canyon Ranch Estates (previously occurrence 7, now part of occurrence 5), San Luis Obispo County, California, 27 July 2016. The foreground is recently cleared and graded. Brandon Sanderson of California Department of Fish and Wildlife is 1.88 m tall.By extrapolation, the individual of Indian Knob mountainbalm is determined to be ~5.5 m tall.

Native Plant Society[1]. At Federal listing in 1995, Indian Knob mountainbalm was known from six occurrences, two of which were in protected areas, with a total population estimate of <600 individuals (USFWS 1994). Five of the occurrences were small and reported to each comprise <50 individuals, and the largest occurrence on the private Guidetti Ranch was reported to comprise <350 individuals (USFWS 1994). Three of these occurrences were on private properties, two were on land owned by the State of California

[1] California Native Plant Society. 2018. *Eriodictyon altissimum*. *In*: Inventory of rare and endangered plants of California. Available (July 2018): http://www.rareplants.cnps.org/detail/623.html.

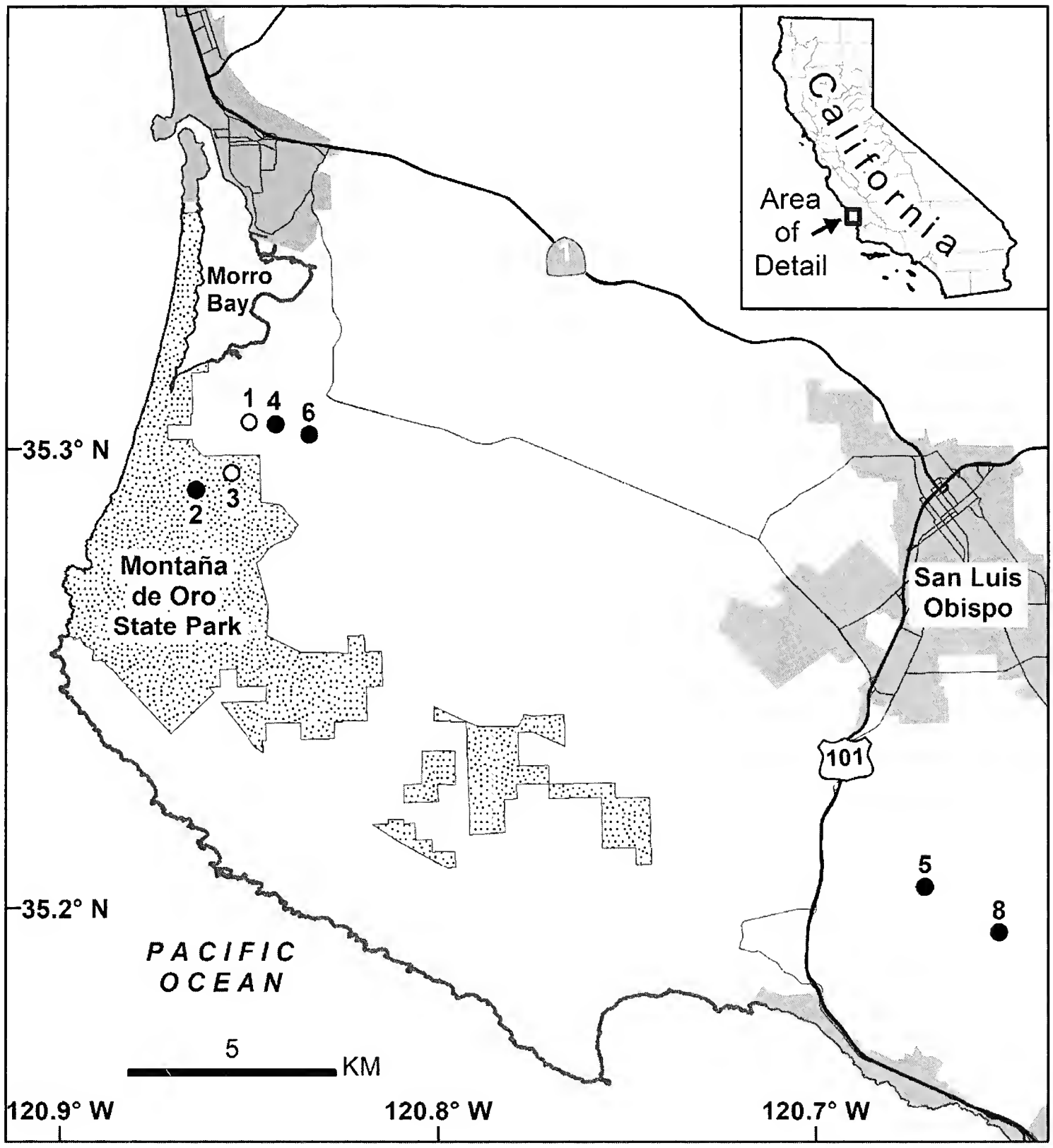

Fig. 2. The known geographic distribution of Indian Knob mountainbalm *Eriodictyon altissimum* in western San Luis Obispo County in central coastal California. Each occurrence is indicated by a black dot (extant) or black circle (likely extirpated) with the number assigned by the California Natural Diversity Database. Occurrence 8 is new.

(Montaña de Oro State Park), and one was on land owned by the County of San Luis Obispo and used for wastewater treatment. The primary threat at the time of listing was habitat loss as a result of potential development (USFWS 1994), specifically potential surface mining at the largest occurrence on Indian Knob mountain, and potential residential development at two small occurrences in Los Osos. Our purpose is to review and enhance the knowledge of Indian Knob mountainbalm, in particular its distribution, ecology, abundance, threats, management and conservation status in 2019. Herein we present the first comprehensive survey and census of the species throughout its geographic range.

Materials and Methods

Little has been published regarding Indian Knob mountainbalm (but see Wells 1962; Carlquist et al. 1983; Hannan 2012). We use our newly-collected data, along with the sparse

published literature, information in the California Natural Diversity Database (CDFG 2006; CDFW 2017), unpublished reports and other documents in files of the USFWS to provide a status review of the species. We searched for Indian Knob mountainbalm, and censused and mapped the known occurrences in 2016, 2017 and 2018. Our searches included nearby and potential habitat, and we state the specific dates of our searches in Appendix 1. In accordance with IUCN (2014) recommended guidelines for colonial and modular organisms, we counted the numbers of stems (including ramets) of Indian Knob mountainbalm as we walked along the trails and through the open areas at each known occurrence. In addition, at previous occurrence 7 (Baron Canyon Ranch Estates, now part of occurrence 5), we used binoculars to count the number of stems in the distance rising above the vegetation canopy, and we also counted the number of stems along the primary ridge road (Balm Ridge Way) as we drove slowly on it (due to time limitation). In order to determine potential pollinators, we opportunistically collected insects inside the corolla tubes of flowers of Indian Knob mountainbalm during April and May 2016. We measured the stem height and basal diameter of several extraordinarily large individuals that were accessible to us. Using all available information, we summarize the body of knowledge of Indian Knob mountainbalm, including its distribution, known occurrences, ecology, abundance, threats, management and conservation status in 2019. We considered a location with the species as a separate occurrence if it was >0.4 km from the nearest occurrence (CDFG 2011). Latitude, longitude and elevation were determined with a global positioning system (GPS) device in the field, or they were determined using Google Earth aerial imagery. Common and Latin names of plants follow Baldwin et al. (2012). Stated areas (ha) of properties are from records of the County of San Luis Obispo. In Appendix 1, we discuss each occurrence in sequence according to its assigned number in the California Natural Diversity Database (CDFG 2006; CDFW 2017). Thus, there may be no numerical sequence for neighboring occurrences. Our stated numbers of plants are the numbers that we recorded but they should be considered best approximates due to the counting methods and difficult landscapes, and in this context we refer to plants, individuals and stems interchangeably. The findings and conclusions in this article are those of the authors and do not necessarily represent the views of the USFWS.

Results and Discussion

Review of Indian Knob Mountainbalm.—Indian Knob mountainbalm is one of 11 species (plus additional subspecies and varieties) in the genus *Eriodictyon* that occurs in southwest United States and Mexico (Hannan 2012). It is a diffusely-branched, evergreen shrub with a main stem, long narrow leaves (5 to 9 cm by 2 to 4 mm), and lavender bell-shaped flowers (11 to 16 mm long; USFWS 1998; Hannan 2012; Fig. 3). The species possesses underground rhizomes and aboveground stems. Although reported heights of stems are up to 4 m and basal stem diameters up to 12 cm (Wells 1962; CDFG 2005; Hannan 2012), we observed one individual that was ~5.5 m tall (Fig. 1) and another individual with basal stem diameter of ~20 cm. Individuals just several centimeters tall are capable of producing flowers (Fig. 3). We collected a total of 56 insects inside the corolla tubes of flowers of Indian Knob mountainbalm, with ants (43%) and beetles (23%) comprising 66% of the sample. The insect species were diverse and included 24 ants (individuals), 13 beetles, 8 bumblebees, 6 flies (5 bee flies + 1 other fly), 4 butterflies, and 1 aphid. These data indicate that Indian Knob mountainbalm receives many floral visitors but it is unknown which are effective pollinators.

Fig. 3. Upper: Flowers of Indian Knob mountainbalm *Eriodictyon altissimum* on a tall individual, southwest Guidetti Ranch, San Luis Obispo County, California (occurrence 5), 4 May 2016. Lower: An individual of Indian Knob mountainbalm that is only several centimeters tall and with flowers at southwest Guidetti Ranch (occurrence 5), San Luis Obispo County, California, 5 May 2016.

Wells (1962) described Indian Knob mountainbalm as rapidly growing and short lived, although USFWS (1998) considered the species long lived in light of the slow growing lichens on some individuals. We and Dr. Jon Keeley (U.S. Geological Survey) examined the growth rings in the dead stems of several large individuals. Despite wood rot destruction, one individual had >50 visible growth rings. Although we do not know if one growth ring equates to 1 yr, J. Keeley (pers. comm. 2018) speculated the stems were >50 yr of age. Carlquist and Eckhart (1984) reported that the underground rhizomes of *Eriodictyon* are the more permanent parts of the plant, and they may be older than the aboveground stems.

Indian Knob mountainbalm is a pioneer, early successional or edge species in chaparral communities. At Indian Knob, Wells (1962) referred to it as a pioneer species that is "aggressive on roadsides with numerous young plants invading such disturbed sites." CDFW (2017) summarized the habitat as ridges in open disturbed areas within chaparral on sandstone and shale, and openings in chaparral on stabilized sand dunes. Specifically, we observed the species on sandstone and sand, including steep rocky slopes, cliff faces, fallen rock debris, sand dunes, roadsides, old graded substrates such as dirt/rock roads, the talus of graded substrates, and trails. In particular, we did not observe the species on shale at any occurrence.

Although Indian Knob mountainbalm is considered to be fire-adapted (Wells 1962; USFWS 1994, 1998, 2013b; CDFG 2005), there is no direct evidence because of the absence of recent fire at the known occurrences. However, in general, establishment of seedlings of chaparral plants is abundant after fire but uncommon under mature chaparral (Keeley 1984). Reproduction of Indian Knob mountainbalm is believed to be primarily vegetative by underground rhizomes (USFWS 1994, 1998, 2013b; CDFG 2005; Fig. 4), although there is no direct evidence to support this. Because little is published about Indian Knob mountainbalm, information is frequently extrapolated from what is known about other species in the genus, such as Lompoc yerba santa *E. capitatum* and California yerba santa *E. californicum*. Lompoc yerba santa, which occurs in Santa Barbara County, is self-incompatible, meaning that pollen from genetically different plants is needed to produce seeds (Elam 1994). This species exhibits low seed production, which is attributed to the combined effects of self-incompatibility and some single-clone populations (Elam 1994). Likewise, Indian Knob mountainbalm is expected to be self-incompatible[2]. California yerba santa is a fire-following species. Seeds stored in the soil for decades germinate readily during the first spring after a fire, and new stems sprout from underground rhizomes following disturbances such as fire (Immel 2006). Further, in the absence of fire to cue seed germination, *Eriodictyon* species most often reproduce vegetatively by rhizomes (USFWS 2013b). Carlquist et al. (1983) described species in the genus *Eriodictyon* as resistant to fire and drought because of their morphology composed of underground rhizomes and aboveground stems. They reported Indian Knob mountainbalm to be adapted to dry habitats, with the underground rhizomes functioning as succulent water-storage and stem innovation organs.

Wells (1962) suspected that the rhizomes of Indian Knob mountainbalm serve for reproduction when the aboveground structures are destroyed by fire, which seems likely. In addition based upon our observations, the rhizomes appear to be the primary source of reproduction where the substrate is physically disturbed, such as by a rock slide or

[2] Knapp, D. 2016. 2015 annual report to U.S. Fish and Wildlife Service. Santa Barbara Bot. Garden, Calif., 16 pp.

Fig. 4. Upper: Ramets (the vertical stems) produced from underground rhizomes (indicated by black arrows) of Indian Knob mountainbalm *Eriodictyon altissimum* at southwest Guidetti Ranch, San Luis Obispo County, California (occurrence 5), 5 May 2016. Lower: A collapsed individual of Indian Knob mountainbalm growing in an open area along the old graded dirt/rock road on the main ridge of Indian Knob mountain, southwest Guidetti Ranch, San Luis Obispo County, California (occurrence 5), 5 May 2016. New vertical stems have sprouted from the primary stem, which is now horizontal on the ground.

grading, and where there is an absence of recent fire. When the stem is removed or destroyed, a new stem may be produced from the underground rhizome if present. We observed that the stems of Indian Knob mountainbalm initially stand erect. However, because the stems and branches are pliable, taller plants bend outward when not supported by adjacent vegetation (Fig. 5). This results in some stems and branches touching the ground, and eventually collapsing to become horizontal on the ground (Fig. 5). This presents an ideal situation for horizontal stems on the ground to be covered by falling rocks or shifting sand and to become contact points for layering (subsequent rooting and sprouting of shoots). We observed many stems in this horizontal position and with new vertical stems arising from the horizontal stems (Fig. 4), although we did not specifically see or search for new roots. Thus, Indian Knob mountainbalm appears well-adapted for substrates with physical disturbances, including: steep rocky slopes (Fig. 6), cliff faces, fallen rock debris (Fig. 6), sand dunes (shifting sand; Fig. 5), roadsides (Fig. 7), old graded substrates such as dirt/rock roads, the talus of graded substrates, and trails.

Indian Knob mountainbalm can reproduce also by seeds, which are minute (~0.4 mm length, mean 0.2 mg mass; Wells 1962). Wells (1962) observed a large production of seeds in individuals at the largest occurrence at Indian Knob mountain. However, John Chesnut (Los Osos, Calif., pers. comm. to Diane Steeck, USFWS, 1997) observed a low ratio of seeds/ovules (structures that develop into seeds when fertilized; 10% or less) in the western occurrences in the Los Osos area and also a low number of seeds per ramet. Some occurrences may have low genetic diversity due to rhizomatous reproduction[2] and could consist of only a single clone (USFWS 1998, 2013a). Although the role of fire in reproduction is not known, it obviously reduces dense mature vegetation and removes debris litter, and it may be needed to somehow revitalize mature stands of Indian Knob mountainbalm[2,3] (USFWS 1998) or to cue seed production or germination (USFWS 2013b). USFWS (2013b) discussed the potential roles of fire in the species' ecology in a status report.

As of 2019, Indian Knob mountainbalm is known from seven occurrences, with a total population count of 6,489+ individuals in 2016 (Table 1). The seven occurrences comprise a geographic range of 34 km^2, which spans a distance of 23 km from southeast of Indian Knob (5.1 km south of the city of San Luis Obispo), northwest to Hazard Canyon (400 m south of Los Osos) in Montaña de Oro State Park (Fig. 2). This area has a Mediterranean climate (warm dry summers, cool wet winters). The dry season is May to August, with most rain falling from December to March. Mean annual temperature and rainfall are ~15.1 °C and ~536 mm, respectively (Ryan 1994). We document the occurrences at 98 to 263 m elevation. The known occurrences are at the two ends of the geographic range, and the Irish Hills comprise most of the intervening area. We suspect the species occurs at additional locations in the intervening area, however, access is difficult because of distance from roads, lack of trails, steep terrain and/or private ownership.

Six occurrences (1, 2, 3, 4, 6, 8) of Indian Knob mountainbalm are in protected areas (Table 2), and one occurrence (5) is mostly in a protected area. Two occurrences (1, 3) are likely extirpated, one occurrence (5) contains a large number of plants (6,346+ stems in 2016), and four occurrences (2, 4, 6, 8) contain low numbers of plants ($\leq$80 stems in 2016) of which two (occurrences 2, 4) are in decline. The likely extirpations and declines may be linked to the altered fire regime, specifically the lack of recent fire (fire suppression) in the

[3] Bittman, R. 1985. Element preservation plan for *Eriodictyon altissimum* (Indian Knob mountain balm). Nature Conserv., San Francisco, Calif., 5 pp.

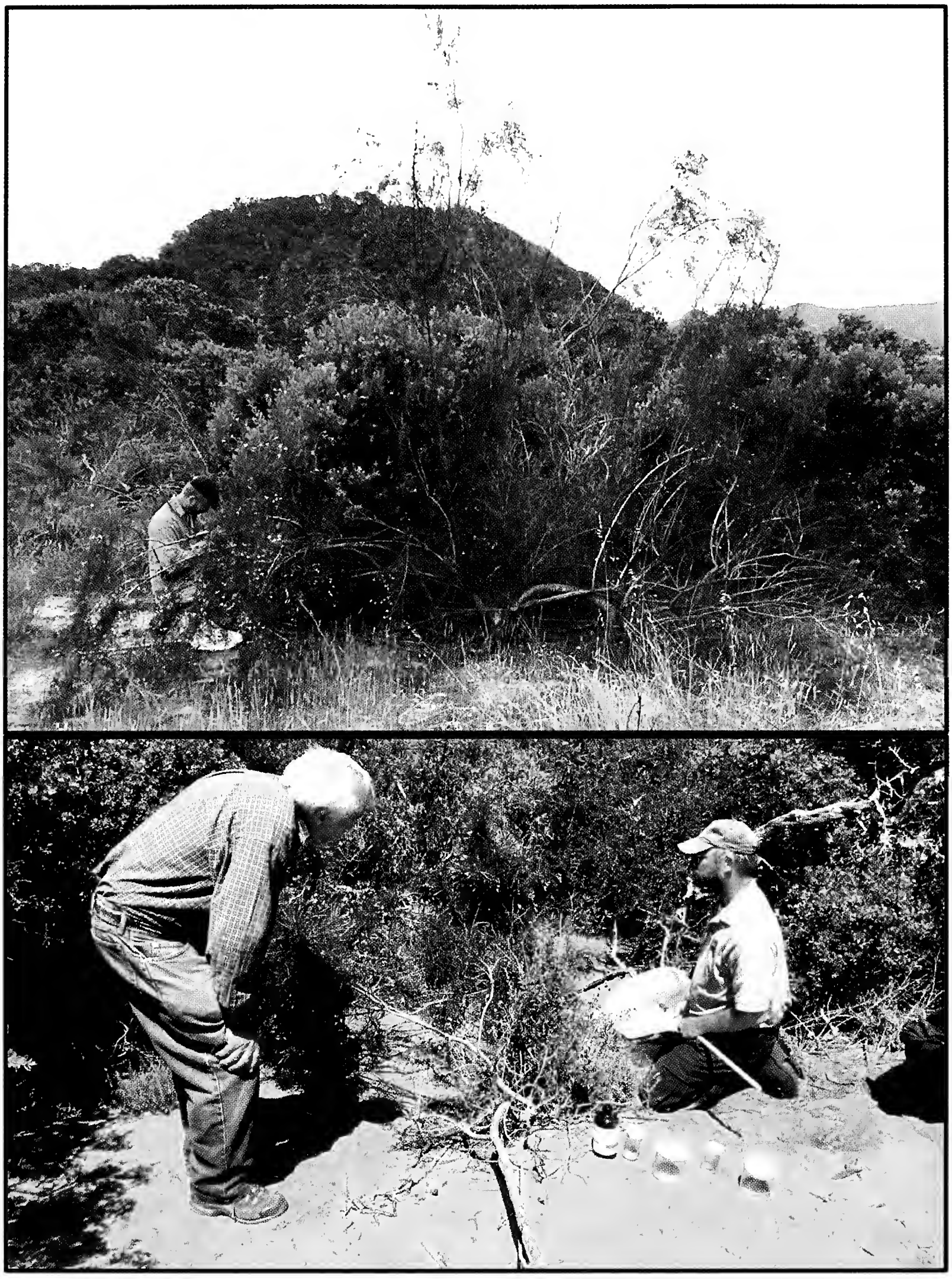

Fig. 5. Upper: An individual of Indian Knob mountainbalm *Eriodictyon altissimum* growing in an open area on the main ridge of Indian Knob mountain, southwest Guidetti Ranch, San Luis Obispo County, California (occurrence 5), 4 May 2016. This tall plant (3 to 4 m height) is supported behind by the adjacent vegetation, however, it is collapsing in front where there is no support. Lower: A collapsed individual of Indian Knob mountainbalm on a sand dune in Morro Dunes Ecological Reserve East, Los Osos, San Luis Obispo County, California (occurrence 6), 20 April 2016. This previously tall plant (3 to 4 m) is now horizontal on the ground and growing in an open area along the trail. Michael J. Walgren of California Department of Parks and Recreation is collecting insects while David Chipping of California Polytechnic State University observes.

Fig. 6. Upper: A colony of Indian Knob mountainbalm *Eriodictyon altissimum* growing on an old rockslide on a steep slope of Indian Knob mountain, southwest Guidetti Ranch, San Luis Obispo County, California (occurrence 5), 5 May 2016. Lower. A colony of Indian Knob mountainbalm growing in fallen rock debris of a crumbling cliff face on Indian Knob mountain, southwest Guidetti Ranch, San Luis Obispo County, California (occurrence 5), 4 May 2016.

Table 1. Reported numbers of Indian Knob mountainbalm *Eriodictyon altissimum* in the seven known occurrences in western San Luis Obispo County, California. Occurrence 7 was combined into occurrence 5 in 2018. Occurrence 8 is new. X = species observed. Italics indicate the words as used by the footnoted references. *(Continued on next page).*

	Occurrence							
	1	2	3	4	5		6	8
Year					5 before 2018	7 before 2018		
2018	0[A]			X[AA]				
2017	not found[A]		0[A]	X[A]			X[A]	
2016	not found[A]	20[A]	not found[A]	23[A]	5,720+[A]	626+[A]	20[A]	80[A]
2015					200[L]		X[U]	
2012	not found[J]	X[E]		not found[J]	*somewhat common*[Y]		15[J T]	
2011		X[M]						
2010		X[M]				X[F]	10[V]	
2009	not found[J]	37[A]	not found[A]	not found[J]			11[A]	
							20-25[J]	
2008	not found[J]	28[P]						
2006	not found[J]			not found[J]				
2005		37[A]						
1999						X[G]		
1998		40[N]						
1991					350[S]	>500[Q]		
1988				25[K]				
1986				X[I]				
1985	*might have washed away*[Z]	62-150[D]	7[D]	30[D]	>100[D]		11-50[D]	
	not found[D]	51-100[H]						
1982				X[I]				
1981			7[B]					
1979	*about 30*[C]	*slightly larger than 30*[C]		6[B]	12[C]			
					grows abundantly[W]			
1974	X[Z]	24[B]		X[B]				
1972		*frequent in rocky places along road*[O]						

Table 1. Continued.

Year	Occurrence							
	1	2	3	4	5		6	8
					5 before 2018	7 before 2018		
1966					*locally plentiful*[R]			
1960					*large population*[X]			

[A] pers. obs.
[B] McLeod 1981 in CDFW 2017.
[C] CDFG 1979.
[D] McLeod 1985 in CDFW 2017.
[E] Sayer in USFWS 2013b.
[F] Langle 2010 in CDFW 2017.
[G] Althouse and Meade. 1999. April 1999 botanical survey parcel map CO 90-080, parcel 2 per mitigation agreement for parcel 2, COAL 89-374 doc. no.: 1997-071413, San Luis Obispo County. Paso Robles, Calif., 19 pp.
[H] Holland 1985 in CDFW 2017.
[I] Consortium of California Herbaria. 2017. UC/JEPS: Consortium search results for *Eriodictyon altissimum*. Available (Nov. 2017): http://ucjeps.berkeley.edu/consortium, 2 pp.
[J] USFWS 2013b.
[K] Gambs and Holland 1988.
[L] Knapp, D. 2016. 2015 annual report to U.S. Fish and Wildlife Service. Santa Barbara Bot. Garden, Calif., 16 pp.
[M] David Chipping (Calif. Polytech. St. Univ., San Luis Obispo, pers. comm. 2016).
[N] Hickson and Hillyard in CDFW 2017.
[O] Anderson 1972.
[P] Sayers 2008 in CDFW 2017.
[Q] LynneDee Althouse (Paso Robles, Calif., pers. comm. 2017).
[R] CDFW 2017.
[S] USFWS 1994.
[T] Winchell, C. 2012. Photo of *Eriodictyon altissimum* Indian Knob mountainbalm, with information, 12 June 2012. Available (Nov. 2017): https://calphotos.berkeley.edu/cgi/img_query?seq_num = 414939&one = T, 1 pp.
[U] Chesnut, J. 2015. *Eriodictyon altissimum* Indian Knob mountainbalm, 8 Mar.2015. Available (Nov. 2017): https://calphotos.berkeley.edu/cgi/img_query?seq_num = 637393&one = T, 1 p.
[V] Butterworth 2010 in CDFW 2017.
[W] Vanderwier 1987.
[X] Wells 1962.
[Y] Harms, M. 2012. *Eriodictyon altissimum*, Indian Knob mountain balm, Guidetti Ranch, Indian Knob. Available (Nov. 2017): https://www.flickr.com/photos/marlinharms/7213654930/in/photostream/, 1 p.
[Z] McLeod 1986 in CDFW 2017.
[AA] Melissa Mooney (Calif. Native Plant Soc., San Luis Obispo, pers. comm. 2018).

Table 2. Conservation status of the seven known occurrences of Indian Knob mountainbalm *Eriodictyon altissimum* in western San Luis Obispo County, California. Occurrences 8 is new.

Occurrence	Location	Landowner	Protected Area	Status	Immediate threats
1	Broderson site in Los Osos	County of San Luis Obispo	Y	likely extirpated	dense vegetation, altered fire regime/fire suppression
2	Montaña de Oro State Park	California Department of Parks and Recreation	Y	20 stems in 2016, in decline	low number of plants, dense vegetation at one colony, altered fire regime/fire suppression
3	Montaña de Oro State Park	California Department of Parks and Recreation	Y	likely extirpated	dense vegetation, altered fire regime/fire suppression
4	Morro Dunes Ecological Reserve East	California Department of Fish and Wildlife	Y	23 stems in 2016, in decline	low number of plants, altered fire regime/fire suppression
5	southwest Guidetti Ranch	private w/conservation easement to City of San Luis Obispo	Y	6,346+ stems in 2016	dense vegetation, altered fire regime/fire suppression, unauthorized clearing of vegetation
	Baron Canyon Ranch Estates	multiple private	N		
	adjacent land south	private Pacific Gas and Electric Company	N		
6	Morro Dunes Ecological Reserve East	California Department of Fish and Wildlife	Y	20 stems in 2016	low number of plants, dense vegetation, hikers trampling plants, unauthorized trimming of vegetation, altered fire regime/fire suppression
8	south central Guidetti Ranch	private w/conservation easement to City of San Luis Obispo	Y	80 stems in 2016	low number of plants, vehicles running over plants, road maintenance

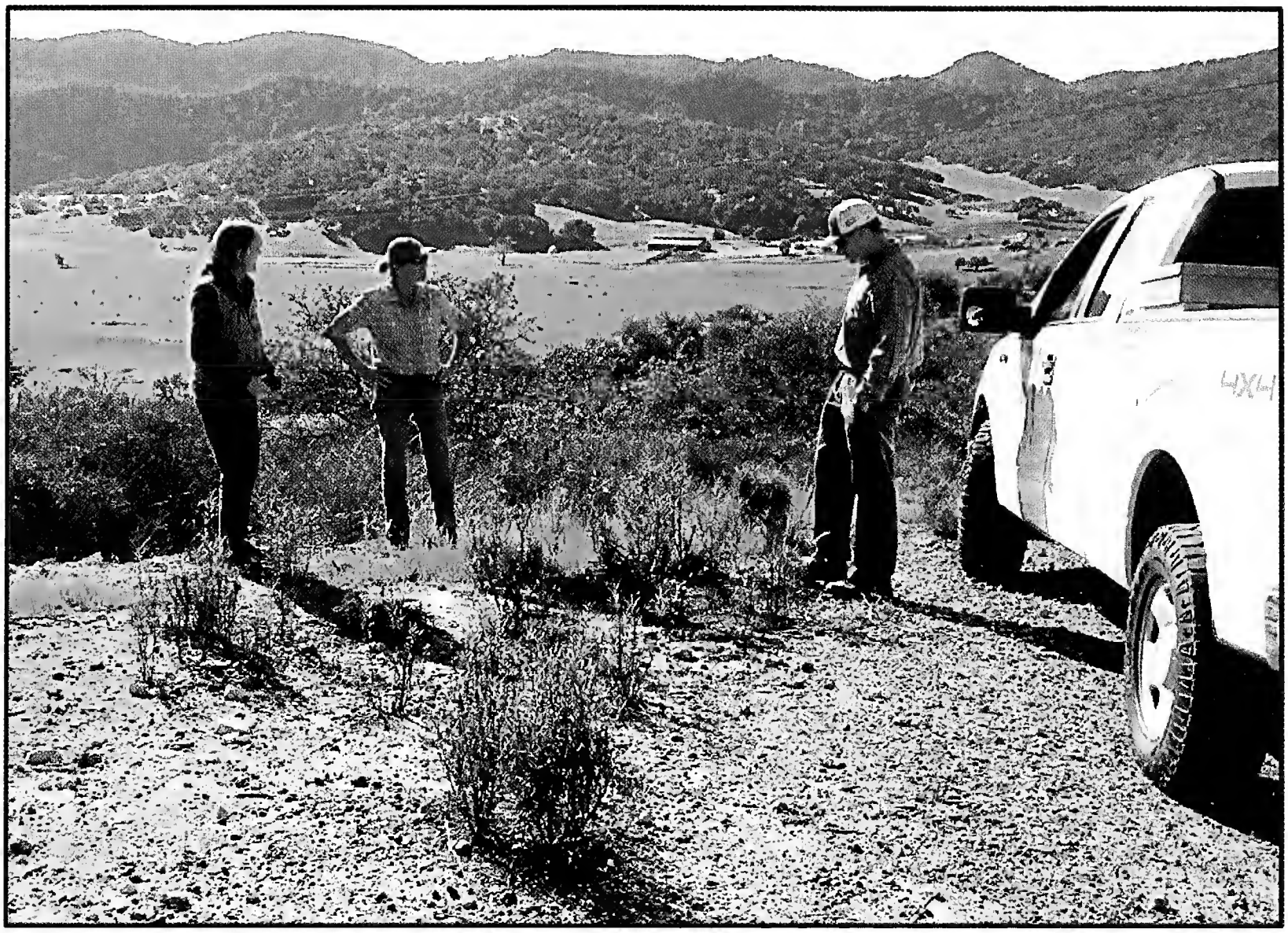

Fig. 7. A colony of Indian Knob mountainbalm *Eriodictyon altissimum* beside the dirt/rock road in south central Guidetti Ranch, San Luis Obispo County, California (new occurrence 8), 1 December 2016. The colony is 1.14 km southeast of the nearest colony of occurrence 5 on southwest Guidetti Ranch (below Indian Knob). The stretch of road at occurrence 8 was covered with soil/rock from below Indian Knob. It seems likely the plants at occurrence 8 originated from individuals that were transported with soil/rock extracted from occurrence 5.

habitat (Gambs and Holland 1988; USFWS 2013b). Regarding occurrence 5 that is mostly in a protected area, 53% (32 ha) is on the private Guidetti Ranch with a conservation easement to the City of San Luis Obispo, 40% (24 ha) is on multiple private properties in Baron Canyon Ranch Estates, and 8% (5 ha) is on private property of Pacific Gas and Electric Company.

The primary threat to the species identified in 1994 has been eliminated: habitat loss as a result of potential development (USFWS 1994), specifically potential surface mining at the largest occurrence on Indian Knob mountain, and potential residential development at two small occurrences in Los Osos. At the private Guidetti Ranch (occurrence 5; Tables 1, 2) that includes much of Indian Knob mountain and where the bulk of the largest population exists, the City of San Luis Obispo purchased a conservation easement in 1996 that allows continued operation of the ranch for livestock grazing while protecting Indian Knob mountainbalm and its habitat, and it also allows limited access for natural resource conservation and public education. At listing in 1995, occurrences 4 and 6 were on two private properties (83 ha) in Los Osos owned by a development corporation that intended to build houses. These two properties were purchased by the State of California in 2001, and they now comprise CDFW's Morro Dunes Ecological Reserve East. In 2019, dense vegetation is a threat at all occurrences except occurrence 8 (see details for each occurrence in Appendix 1). Also in 2019, four of the five extant occurrences of Indian Knob

mountainbalm are threatened by stochastic events because small numbers of individuals comprise them (each $\leq$80 plants), and also because of their isolation (distance) from other extant occurrences. These threats were recognized previously by USFWS (1994).

In addition to the immediate threats (Table 2), climate change could be a long-term threat to Indian Knob mountainbalm because California is becoming hotter and drier. The summers of 2017 and 2016 were each the warmest in California since record keeping began in the late 1800's[4]. Considering data up to 2015, most of the warming occurred in the past 35 years with 15 of the 16 warmest years occurring since 2001[5]. The 3-yr period from 2012 to 2014 was the hottest and driest in California in the 100-yr time frame considered by Mann and Gleick (2015), and it was the most severe drought in California in the past 1,200 yrs (Griffin and Anchukaitis 2014). In consideration of the life history traits used to assess climate change vulnerability for rare plants in California (Anacker et al. 2013), Indian Knob mountainbalm would be considered highly vulnerable to climate change. These traits include low dispersal ability, an apparent narrow historical climate exposure, dependence on particular disturbance regimes, habitat specialization, and likely low genetic diversity.

Based upon our field observations, the several statements by USFWS[6][7][8] (2013a) that invasive nonnative grasses, particularly perennial veldt grass *Ehrharta calycina*, pose the strongest threat to Indian Knob mountainbalm are not correct. To the contrary, no occurrence of Indian Knob mountainbalm is immediately threatened by non-native grasses. Although perennial veldt grass exists in the surrounding landscapes, we observed it only at occurrence 5 with just a few clumps at one location. Although perennial veldt grass could become a threat in the future by invading an occurrence after fire (USFWS 2013a), it is more abundant in coastal sage scrub and ruderal and disturbed plant communities than in chaparral.

Using our information and international standards (IUCN 2012, 2014), Indian Knob mountainbalm in 2019 meets the IUCN criteria for endangered including the following: geographic range, fragmented; extent of occurrence, 34 km^2 (<100 km^2); area of occupancy, <2.3 km^2 (<10 km^2); and quality of habitat, continuing to decline (dense vegetation, lack of recent fire). Considering these attributes, Indian Knob mountainbalm faces an extremely high risk of extirpation at four of the five extant occurrences. Four of the five extant occurrences are small with $\leq$80 individuals each, and two other occurrences are likely extirpated. One occurrence is large with >6,000 individuals, and it is mostly in a protected area.

---

[4] NOAA National Centers for Environmental Information. 2018. Climate at a glance: U.S. time series, average temperature. Available (Feb. 2018): https/www.ncdc.noaa.gov/cag/time-series/us.

[5] Brown, D., M. Cabbage, and L. McCarthy. 2016. NASA, NOAA analyses reveal record-shattering global warm temperatures in 2015. Press release available (Jan. 2016): http://www.nasa.gov/press-release/nasa-noaa-analyses-reveal-record-shattering-global-warm-temperatures-in-2015.

[6] U.S. Fish and Wildlife Service. 2011. Indian Knob mountainbalm. Photo with information, 21 May 2011. Available (Nov. 2017): https://www.flickr.com/photos/usfws_pacificsw/11177193066/in/photolist-i2G36h-HraCuj-i2ER6H-c91K3d-i2E28B-HtxhRz-HtxgkD-GPHFev, 1 p.

[7] U.S. Fish and Wildlife Service. 2011. Indian Knob mountainbalm. Photo with information, 31 May 2011. Available (Nov. 2017): https://www.flickr.com/photos/usfws_pacificsw/11176960975/in/photostream/, 1 p.

[8] U.S. Fish and Wildlife Service. 2012. Indian Knob mountainbalm and habitat. Photo with information, 12 May 2012. Available (Nov. 2017): https://www.flickr.com/photos/usfws_pacificsw/11176799613/, 1 p.

Recommendations.—Despite increased attention in recent years, little is known about the biology and ecology of the endangered Indian Knob mountainbalm in 2019. Therefore, coordinated conservation and research are needed to further understand the species, and to restore and maintain the five extant occurrences. These efforts should include management actions to benefit the occurrences, searches for additional locations, studies of genetic diversity and reproductive biology, introduction of Indian Knob mountainbalm into living collections at botanic gardens, investigations of potential barriers to recruitment, and investigations of the species' relationship with fire. Specifically, we intend to make a conservation seed collection for seed banking in the near future, and a subset of these seeds will be used to investigate germination requirements, including cues associated with fire-following species. In addition, cuttings will be collected and cultivated along with seeds to develop protocols for propagation of the species. Finally, a study of population genetics is planned to investigate genetic diversity within and among the occurrences.

Acknowledgements

We thank the following persons for assistance in the field: C. M. Guilliams of Santa Barbara Botanic Garden; J. Chesnut, D. Chipping and M. Mooney of California Native Plant Society (San Luis Obispo); K. O'Brien and S. Krenn of Pacific Gas and Electric Company; and R. Hill of the City of San Luis Obispo. The following persons engaged in valuable discussion: V. Cicero of California Department of Parks and Recreation; R. Stafford of California Department of Fish and Wildlife; K. Ballantyne of County of San Luis Obispo; and C. Darst, S. Henry, R. Root and J. Vanderwier of U.S. Fish and Wildlife Service. R. S. Taylor and M. Metevier produced the map. C. Darst also read and commented on the draft manuscript. K. Gross and K. Lazar of the California Department of Fish and Wildlife provided information from the California Natural Diversity Database. Finally, we thank T. Guidetti for permission to access the largest population of Indian Knob mountainbalm on his private ranch, and also for his advice, discussion and assistance.

Literature Cited

Anacker B.L., M. Gogol-Prokurat, K. Leidholm, and S. Schoenig. 2013. Climate change vulnerability assessment of rare plants in California. Madroño, 60:193–210.

Anderson, B.H. 1972. A contribution to the flora of Montaña de Oro State Park, California. M.S. thesis, Calif. Polytech. St. Univ., San Luis Obispo, 133 pp.

Baldwin, B.G., D.H. Goldman, D.J. Keil, R. Patterson, T.J. Rosatti, and D.H. Wilken (eds.). 2012. The Jepson Manual: Vascular Plants of California (2nd ed.). Univ. Calif. Press, 1,600 pp.

California Department of Fish and Game [CDFG]. 1979. California State Endangered Plant Program, scientific name: *Eriodictyon altissimum* Wells. Sacramento, Calif., 3 pp.

———. 2005. The status of rare, threatened, and endangered plants and animals of California 2000—2004. Sacramento, Calif., 549 pp.

———. 2006. Element occurrence reports for *Eriodictyon altissimum*. *In*: California Natural Diversity Database. Cumulative data current from 3 June 2006 to 3 December 2006. Sacramento, Calif., 6 pp.

———. 2011. Special vascular plants, bryophytes, and lichens list. Sacramento, Calif., 71 pp.

California Department of Fish and Wildlife [CDFW]. 2016. State and federally listed endangered, threatened, and rare plants of California. Sacramento, Calif., 7 pp.

———. 2017. Element occurrence reports for *Eriodictyon altissimum*. In: California Natural Diversity Database. Cumulative data current from 1 Oct. 2017 to 1 Apr. 2018. Sacramento, Calif., 6 pp.

Carlquist, S. and V.M. Eckhart. 1984. Wood anatomy of Hydrophyllaceae. II. Genera other than *Eriodictyon*, with comments on parenchyma bands containing vessels with large pits. Aliso, 10:527–546.

———, ———, and D.C. Michener. 1983. Wood anatomy of Hydrophyllaceae. I. Eriodictyon. Aliso 10: 397–412.

Carpenter, E.J. and R.E. Storie. 1928. Soil survey of the San Luis Obispo area, California.Bur. Chem. and Soils, U.S. Dept. Agric., Washington, D.C., 60 pp.

Elam, D.R. 1994. Genetic variation and reproductive output in plant populations: effects of population size and incompatibility. Ph.D. thesis, Univ. Calif. Riverside, 194 pp.

Gambs, R.D. and V.L. Holland. 1988. Ecology of the Morro Bay kangaroo rat (*Dipodomys heermanni morroensis*). Final Report. Contract No. 14-16-0001-85154 NR. U.S. Fish Wildl. Serv., Sacramento, Calif., 140 pp.

Griffin, D. and K.J. Anchukaitis. 2014. How unusual is the 2012–2014 California drought? Geophys. Res. Lett. 41:9017–9023.

Hannan, G.L. 2012. *Eriodictyon* yerba santa. Pp. 471–473 in The Jepson manual: vascular plants of California (2nd ed.). (Baldwin, B.G., D.H. Goldman, D.J. Keil, R. Patterson, T.J. Rosatti, and D.H. Wilken, eds.) Univ. Calif. Press, 1,600 pp.

Immel, D.L. 2006. Plant guide: California yerba santa *Eriodictyon californicum* (Hook. & Arn.) Torr. U.S. Dept. Agric., Nat. Res. Conserv. Serv., Natl. Plant Data Center, Davis, Calif., 3 pp.

IUCN. 2012. IUCN Red List categories and criteria: Version 3.1. 2nd ed. IUCN, Gland, Switzerland, 32 pp.

———. 2014. Guidelines for using the IUCN Red List categories and criteria: version 11 (February 2014). IUCN, Gland, Switzerland, 87 pp.

Keeley, J.E. 1984. Factors affecting germination of chaparral seeds. BSCAS, 83:113–120.

Luebert, F., L. Cecchi, M.W. Frohlich, M. Gottschling, C.M. Guilliams, K.E. Hasenstab-Lehman, H.H. Hilger, J.S. Miller, M. Mittelbach, M. Nazaire, M. Nepi, D. Nocentini, D. Ober, R.G. Olmstead, F. Selvi, M.G. Simpson, K. Sutorý, B. Valdés, G.K. Walden, and M. Weigend. 2016. Familial classification of the Boraginales. Taxon, 65:502–522.

Mann, M.E. and P.H. Gleick. 2015. Climate change and California drought in the 21st century. PNAS, 112:3858–3859.

Ryan, G. 1994. Climate of San Luis Obispo, California. NOAA Techinical Memorandum NWS WR-223, 54 pp.

U.S. Fish and Wildlife Service [USFWS]. 1994. Endangered and threatened wildlife and plants; endangered or threatened status for five plants and the Morro shoulderband snail from western San Luis Obispo County, California. Fed. Register 59:64613–64623.

———. 1998. Recovery plan for the Morro shoulderband snail and four plants from western San Luis Obispo County, California. Portland, Oregon, 75 pp.

———. 2013a. Endangered and threatened wildlife and plants; 12-month finding on a petition to reclassify *Eriodictyon altissimum* as threatened. Fed. Register, 78:75313–75321.

———. 2013b. Final species report: *Eriodictyon altissimum* (Indian Knob mountainbalm). Ventura, Calif, 34 pp.

Vanderwier, J. 1987. A study of the vegetation of the Indian Knob area, San Luis Obispo County, California. M.S. thesis, Calif. Polytech. St. Univ., San Luis Obispo, 122 pp.

Wells, P.V. 1962. A subarborescent new *Eriodictyon* (Hydrophyllaceae) from San Luis Obispo County, California. Madroño, 16:184–186.

Wiegers, M.O. 2009. Geologic map of the Morro Bay south 7.5' quadrangle, San Luis Obispo County, California: a digital database (version 1.0) [online]. Calif. Geol. Surv., Sacramento. Available (Jun. 2018): ftp://ftp.consrv.ca.gov/pub/dmg/rgmp/Prelim_geo_pdf/MorroBaySouth24k_prelim.pdf, 1p.

Appendix 1

The seven known occurrences of Indian Knob mountainbalm *Eriodictyon altissimum* in western San Luis Obispo County in central coastal California.

Occurrence 1. ~35.303567, −120.846864; 119 m elevation. The coordinates that we give are in a former gully ~119 m E of the intersection of Travis Drive and Houston Drive in Los Osos. The location is on the Broderson site (32 ha), which is owned by the County of San Luis Obispo and used as a leach field (3 ha) for recycled water from the Los Osos wastewater treatment plant. The occurrence is in the area (29 ha) protected by deed restriction executed in 2017, and managed per a habitat management plan approved by the California Coastal Commission in 2017 (Kate Ballantyne, Co. of San Luis Obispo, Calif., pers. comm. 2017). It is on Baywood Fine Sand comprising ancient stabilized sand dunes of windblown origin during the late to middle Pleistocene Epoch (Carpenter and Storie 1928; CDFG 2005; Wiegers 2009). We searched on 22 June 2018, 10 April 2017 and 20 April 2016, and we found no Indian Knob mountainbalm. There is confusion

regarding this occurrence. The only records are CDFG (1979) and McLeod (1986 in CDFW 2017). CDFG (1979) states the following: "Three populations. The Indian Knob population consists of 12 individuals, the Broderson Road site includes about 30, and the Hazard Canyon population is slightly larger. Development activities following existing high volume recreational uses have caused significant decline in the Roderson [sic] Road population." The maps of CDFG (1979) and McLeod (1986 in CDFW 2017) both depict a circle immediately E of the bend of Travis Drive, which is part of Cabrillo Estates (~250 homes). McLeod (1986 in CDFW 2017) stated the following: "Population 1 was originally discovered by Dirk [Walters] in the early '70s. He and I tramped over the whole area last year and couldn't locate it. Dirk said recently that it might have been washed away as it was along a gully. I'm sorry we couldn't find it as that was the population with which you would probably be most concerned." This occurrence and occurrence 4 are on properties that in the 1980's were proposed for the community sewage system[9]. Gambs and Holland (1988) conducted a vegetation survey of the properties with occurrences 1 and 4. Although Gambs and Holland (1988) discussed occurrence 4, they did not mention occurrence 1. Using Google Earth aerial imagery (dated 27 May 1994), we observed that a gully previously existed in the mapped area for occurrence 1 (CDFG 1979; McLeod 1986 in CDFW 2017) and parallel to Travis Drive, but which is not obvious in 2017 because of dense vegetation. Unconfirmed word of mouth is that the Indian Knob mountainbalm were located ~100 m northeast of the intersection of Travis Drive and Houston Drive, which is in the mapped areas of CDFG (1979) and McLeod (1986 in CDFW 2017), and also in the former gully reported by McLeod (1986 in CDFW 2017). Because of multiple unsuccessful attempts to locate occurrence 1, USFWS (2013a, b) considered occurrence 1 to be extirpated. In contrast, CDFW considered occurrence 1, which is west of Broderson Avenue extended, to be a mis-smapping of occurrence 4, which is in the same landscape but east of Broderson Avenue extended. Consequently, CDFW combined occurrences 1 and 4 in 2013. However, instead of removing occurrence 1 from the California Natural Diversity Database, CDFW removed occurrence 4 while retaining occurrence 1 but with coordinates for occurrence 4 (K. Gross, pers. comm. 2017). Although no herbarium specimens document occurrence 1, it appears to be valid as indicated by CDFG (1979) and McLeod (1986 in CDFW 2017).

Occurrence 2. 35.290381, −120.859230; 35.290216, −120.859599; 35.290156, −120.859721; 35.291068, −120.864935; 154 to 210 m elevation. The coordinates that we give are from our GPS device next to the plants. Also, Sayers 2008 (in CDFW 2017; Lazar 2018 pers. comm.) reported two additional colonies at the following two locations that are along or near the same trail: 35.290202, −120.860118; 35.290336, −120.860566; 208 to 212 m. We surveyed and censused this occurrence on 21 April 2016. It comprises six disjunct colonies (we refer to them as A, B, C, D, E and F, from east to west) along the old Manzanita Trail on a south-facing ridge on the south side of Hazard Canyon in Montaña de Oro State Park, ~384 m south of Los Osos. The trail is an old dirt/rock road between the east section of the Hazard Peak Trail and the Bloody Nose Trail that was graded likely in the 1940's or 1950's when the land was private property. The trail is closed to the public. The location of this occurrence as mapped by McLeod (1981 in CDFW 2017) is off by >500 m. The greatest number of recorded individuals for this occurrence was 62 to 150 plants by McLeod (1985 in CDFW 2017), and the recorded numbers have declined since then: 40 plants in 1998 (Hickson and Hillyard 1998 in CDFW 2017), 37 plants in 2005 (pers. obs.), 28 plants in 2008 (Sayers 2008 in CDFW 2017), 37 plants in 2009 (pers. obs.), and 20 plants in 2016 (pers. obs.). In 2016 this occurrence comprised 20 plants (15 big individuals with woody stems, 5 small leafy sprouts) in four colonies (A, B, C, F), while two colonies (D, E) reported by Sayers (2008 in CDFW 2017) were not observed. The six colonies are separated by 38 m, 10 m, 33 m, 44 m and 402 m, respectively, spanning a straight-line distance of 530 m with a total area of 11,121 m^2. Colony A is two big plants at the top of a cliff face (road cut). Sayers (2008 in CDFW 2017), likewise, reported two plants here in 2008. Colony B (six large stems, one little stem) and colony C (three large stems) are in the fallen rock debris of a collapsed cliff face (road cut) that fell in 2011, and the bulk of the two colonies were covered. Additional plants previously grew on the downslope adjacent to the trail and were covered by the fallen rock debris. The rock is very old cemented dune sand (D. Chipping, pers. comm. 2016), and it is friable and relatively soft (Wiegers 2009). Colony F comprised seven plants (three big individuals with woody stems, four small leafy sprouts) in an area of 38 m^2 in 2016. Four small stems were growing in the sandstone road (shale according to McLeod 1985 in CDFW 2017 is incorrect) and three big plants in the rock talus pushed down the slope. Sayers (2008 in CDFW 2017) reported

---

[9] Gambs, R.D. 1986. Biological assessment: the effects of a proposed wastewater system in the communities of Los Osos and Baywood Park, California on the endangered Morro Bay kangaroo rat (*Dipodomys heermanni morroensis*). Report to Morro Group, Inc., San Luis Obispo, Calif., 26 p.

17 stems here in 2008, and McLeod (1985 in CDFW 2017) reported 51-100 stems in 1985. With only seven stems in 2016, this colony is in decline and near extirpation. As an urgent recovery action for this colony, we recommend that the vegetation within a radius of 8 m be thinned and that the potential for a controlled miniburn be evaluated. We attribute herbarium specimen CDA17581, which was collected "ca. 2 mi E of Pecho Road along S leg of East Hazard Canyon loop trail," to this occurrence[10]. The overland distance from Pecho Valley Road to occurrence 2 is ~3.2 km when using Hazard Canyon Road and the ascending Manzanita Trail.

Occurrence 3. ~35.294023, −120.850953; 239 m elevation. The coordinates that we give are from our GPS device in the field. This occurrence is on the north side of Hazard Canyon in Montaña de Oro State Park in southwest Los Osos. McLeod (1981 and 1985 in CDFW 2017) reported seven plants at this occurrence in 1981 and 1985, but no one has reported on this occurrence since. Although McLeod (1981 in CDFW 2017) provided a map, the precise location has remained unknown. We searched for this occurrence on 25 April 2017, and we are confident that we found the general location. However, we saw no plants. The soil at the general location is Baywood Fine Sand on a ridge top. The vegetation is now dense, predominantly chamise and manzanita, and with some open areas. We suspect that in the 1980's the vegetation was less dense, and in the ensuing decades the vegetation has become denser and crowded out the Indian Knob mountainbalm, which is now likely extirpated at occurrence 3. We searched also along Cable Trail from Pecho Valley Road to the ridge with occurrence 3. We found no plants, although conditions appeared suitable in several places. In addition, we identified a nearby area (405 m west of occurrence 3) with collapsed cliff faces that appeared to be habitat. We tried but without success to access the fallen rock debris from Cable Trail above and from Hazard Canyon Road below. Using binoculars we saw no Indian Knob mountainbalm. In brief, unknown colonies of Indian Knob mountainbalm may exist along the north side of Hazard Canyon.

Occurrence 4. 35.305865, −120.837545; 35.304063, −120.838908; 35.302020, −120.836210 (M. Mooney, pers. comm. 2018); 98 to 118 m elevation. The coordinates that we give are from GPS devices next to the plants in three colonies. This occurrence is in southwest Los Osos in CDFW's Morro Dunes Ecological Reserve East, and it is on Baywood Fine Sand. D. Walters identified this occurrence in 1974 (McLeod 1981 in CDFW 2017). Recorded numbers of plants were six individuals in 1979 (McLeod 1981 in CDFW 2017), 30 in 1985 (McLeod 1985 in CDFW 2017), 25 in 1988 (Gambs and Holland 1988), and 23 in 2016 (pers. obs.). There is confusion regarding this occurrence, whose specific location became "lost" after 1988. McLeod (1981 in CDFW 2017) mapped the location of occurrence 4 at 73 to 85 m elevation between the sand extensions of Palisades Avenue and Ravenna Avenue, but closer to the former. McLeod (1985 in CDFW 2017) described the location as "south of the end of Palisade St Los Osos 100 yds W of stand of Bishop pine [*Pinus muricata*]" at 91 m elevation but marking 79 to 85 m elevation on his map. Gambs and Holland (1988) mapped the location of Bishop pine in the landscape, showing two stands near Palisades Avenue sand extension and the most relevant one at 98 m elevation (35.304162, −120.837298). Gambs and Holland (1988) described the location of occurrence 4 as two groups: one group of 25 individuals ~100 m west of the sand extension of Palisades Avenue at ~76 m elevation, and "an isolated individual discovered by Dirk Walters in the early 1970's south of the end of Ravenna Avenue" that they could not find. CDFG (2006) recognized occurrence 4 with coordinates 35.30563, −120.83734 at 83 m elevation. We are not able to reconcile the previously stated elevations and maps for occurrence 4 with our own observations. Because of the multiple unsuccessful attempts to find this occurrence, USFWS (2013a, b) considered occurrence 4 to be extirpated. Also in 2013, CDFW combined occurrence 4 with occurrence 1 because they believed that occurrence 1 (35.30467, −120.84598; CDFG 2006) was a mapping error. CDFW removed occurrence 4 from the California Natural Diversity Database and retained occurrence 1 but with the new coordinates 35.30556, −120.83771 at 79 m elevation, which is 35 m southwest of the former occurrence 4 (CDFG 2006). However, we affirm that our occurrence 4 is separate and distinct from our occurrence 1. J. Chesnut of the California Native Plant Society (San Luis Obispo) led us to occurrence 4 on 20 April 2016. We observed 23 individuals in two colonies separated by 40 m: colony A with 21 plants (10 big individuals with woody stems, 11 small sprouts; 14 m^2) in a clearing, and a more western colony B with two big individuals with woody stems (3 m^2) at the edge of California live oak woodland *Quercus agrifolia* with ceanothus *Ceanothus*, manzanita *Manzanita* and chamise *Adenostoma fasciculatum*. J. Chesnut (pers. comm. 2016) had observed the two colonies previously during field work in 1986, and he recalled there were other individuals on the

[10] Consortium of California Herbaria. 2017. UC/JEPS: Consortium search results for *Eriodictyon altissimum*. Available (Nov. 2017): http://ucjeps.berkeley.edu/consortium, 2 p.

sand ridge extending north. We subsequently searched the sand ridge on 10 April 2017 but saw no other plants. We observed colony B again on 10 April 2017, and one plant was dead and the other dying. The coordinates that we give for colony A are 139 m west of the stand of Bishop pine at 98 m elevation near the end of the sand extension of Palisades Avenue (Gambs and Holland 1988), which is likely the location referred to by McLeod (1981 and 1985 in CDFW 2017) and Gambs and Holland (1988). Colony B is at the edge of dense vegetation, and it is 40 m west of colony A and even closer to the sand extension of Ravenna Avenue. In August 2018, M. Mooney (pers. comm. 2018) observed one individual ~30 cm height at a new location (colony C), 330 m southeast of colony A and in chaparral. Five herbarium specimens document occurrence 4: CHSC69826 and HSC77146 collected in 1982; and RSA522505, SBBG95658 and UC1583847 collected in 1986[10]. The total area is 0.62 ha.

Occurrence 5. Based upon the information for occurrences 5 and 7 in a draft of this paper that was reviewed by CDFW, in 2018 they officially combined occurrence 7 into occurrence 5 because the two occurrences were no longer separated by >0.4 km (K. Lazar, pers. comm. 2018). However, because of the different land ownerships and different management, we present the separate information for occurrences 5 and 7 prior to 2018 (see also Table 1). The total known occupied area is ~60 ha: Guidetti Ranch, 32 ha; Baron Canyon Ranch Estates, 24 ha; and Pacific Gas and Electric Company, 5 ha. The approximate center of occurrence 5 is now 35.200234, −120.669741. The total count in 2016 was 6,346+ stems. USFWS (1994) reported 350 stems in 1991.

Occurrence 5 before 2018. 35.200538, −120.669342 to 35.198472, −120.657299; and 35.201136, −120.662712 to 35.196987, −120.662644; 197 to 263 m elevation. The coordinates that we give are from our field observations and Google Earth aerial imagery. The approximate center of the occurrence is at 35.199150, −120.663379. This occurrence is narrowly situated on Indian Knob mountain and the nearby ridges and upper slopes, primarily on the private Guidetti Ranch and extending south onto property of Pacific Gas and Electric Company. The substrate is sandstone (Chipping, pers. comm. 2016). We surveyed and censused this occurrence on 4 and 5 May 2016. We counted 5,720 stems (4,610 woody stems, 1,110 leafy sprouts; and 205 dead stems) on the Guidetti Ranch and adjacent property of Pacific Gas and Electric Company. This is a minimum number because there were many areas we did not search due to steepness of slopes or lack of paths through dense vegetation. The plants are primarily on the ridges and south-facing slopes. Previous reports regarding numbers of plants were 12 in 1979 (CDFG 1979), >100 in 1985 (McLeod 1985 in CDFW 2017), and 200 in 2015[2]. Our substantially higher number is likely the result of greater effort, using a systematic method, and the counting of every stem. The known occupied area comprises at least 32 ha, which is mostly on the Guidetti Ranch (30 ha) but also extending south and west onto private property owned by the Pacific Gas and Electric Company (3 ha). Wells (1962) described Indian Knob mountainbalm on Guidetti Ranch as a pioneer species in chaparral dominated by Santa Margarita manzanita *Arctostaphylos pilosula*, being aggressive along roads and confined to shallow sandy soils on the sandstone ridges. CDFW (2017) described the microhabitat as sandstone ridges in open disturbed areas in chaparral at 90 to 270 m elevation. In addition to the roadsides, old graded dirt/rock roads and ridges, we observed the species in the open areas on the steep slopes usually with a disturbed substrate, and also in the talus of graded dirt/rock roads, on cliff faces, in the fallen rock debris of collapsed cliff faces, on rock slides, and along trails. We searched several disturbed areas in the chaparral created by tree falls, which were characterized by a thin layer (15 cm) of fine organic debris over sandy soil, but found no Indian Knob mountainbalm there. On Guidetti Ranch it appears that Indian Knob mountainbalm is adapted for areas with disturbed soil and rock where, in the absence of recent fire, reproduction seems most likely by rhizomes. We suspect that reproduction by seeds may need fire, and there have been no wildfires on Guidetti Ranch since before the 1950's (Terry Guidetti, pers. comm. 2016).

Occurrence 7 before 2018. 35.209470, −120.677157 to 35.200040, −120.670969; and 35.203853, −120.670995 to 35.205170, −120.676575; 193 to 235 m elevation. The coordinates that we give are based on our field observations and using Google Earth aerial imagery. The known occupied area comprises ~28 ha, with the center at 35.203840, −120.674061. This occurrence is mostly on Baron Canyon Ranch Estates (277 ha), which is a private gated community in the mountains and hills 2.25 km south of the city of San Luis Obispo. The community comprises 29 parcels of land for houses (0.4 to 34.0 ha) and three common areas (172 ha). Most houses are on the ridges and hills, which are mostly undeveloped and with predominantly native vegetation. The section of the primary mountain ridge with Indian Knob mountainbalm is oriented mostly in a northwest to southeast direction, and Balm Ridge Way is the paved road that extends along it. This occurrence of Indian mountainbalm is on the primary mountain ridge and adjacent slopes, spanning a distance of 1.2 km. It is on the same primary mountain ridge as occurrence 5, which is mostly on Guidetti Ranch and immediately southeast of Baron Canyon Ranch Estates. Occurrence 7 extends for a

short distance S onto property owned by Pacific Gas and Electric Company and east onto Guidetti Ranch. The southern part of occurrence 7 adjoins occurrence 5. We observed Indian Knob mountainbalm primarily in a belt of Santa Margarita manzanita that appeared to stretch continuously across the several ridges and slopes. We counted 626 plants (598 woody stems, 28 leafy sprouts) on 27 July 2016, and there were likely many more plants that we did not observe because of the large occupied area, the steepness of some slopes, and the lack of access through the dense vegetation. We saw many tall individuals of Indian Knob mountainbalm growing within and rising above the dense mature chaparral, including one individual that was ~5.5 m tall. Similarly, Wells (1962) observed Indian Knob mountainbalm "often overtopping by five feet or more the even-statured young manzanitas dating from the last chaparral fire." LynneDee [Oyler] Althouse (1991 in CDFW 2017; Paso Robles, Calif., pers. comm. 2017) reported >500 plants (350 flowering, 150 vegetative) in 1991. Current threats include clearing of the native vegetation by private landowners. In 2016 we observed illegal clearing of at least 310 m^2 of native vegetation on one private property contrary to ordinance of San Luis Obispo County, and it included destruction of some Indian Knob mountainbalm, which was being investigated by CDFW.

Occurrence 6. 35.301508, −120.830263; 35.301639, −120.830129; 115 to 118 m elevation. This occurrence is in south Los Osos in Morro Dunes Ecological Reserve East on Baywood Fine Sand. It is 25 m northwest of the white water tank near Calle Cordoniz Road. The coordinates are from our GPS device next to the plants. We surveyed and censused this occurrence on 20 April 2016, and we counted 20 plants: 11 big individuals with woody stems, and nine small sprouts. The plants are in two colonies (20 m^2, 32 m^2) separated by 11 m, and with a total area of 63 m^2. Much of Los Osos is underlain by old, stabilized sand dunes (Wiegers 2009), and this occurrence is near the crest of a sand dune. The plants are along several well-established trails and at the edge of dense mature chaparral. Several of the taller individuals had collapsed and were growing with the primary stems horizontal across the ground. Previous records for this occurrence are 15 plants in 2012 (USFWS 2013b), 10 in 2010 (Butterworth 2010 in CDFW 2017), 20 to 25 in 2009 (USFWS 2013b), and 11 to 50 plants in 1985 (McLeod 1985 in CDFW 2017). We identify two primary threats to this occurrence: the dense vegetation immediately surrounding the plants, and the removal of Indian Knob mountainbalm by hikers and equestrians who trim the vegetation in an effort to keep the trails passable (pers. obs. 2017). Therefore, we recommend that CDFW (or their authorized agents) thin the vegetation in vicinity of the Indian Knob mountainbalm, and also place educational signs at strategic locations to inform hikers and equestrians about sensitive plants in the habitat.

Occurrence 8 (new). 35.190008, −120.650146; 124 m elevation. The coordinates that we give are from Google Earth aerial imagery. While working with vegetation contractors of the Pacific Gas and Electric Company on 1 December 2016, we encountered a disjunct colony of Indian Knob mountainbalm (78 woody stems, 2 leafy sprouts) that is 1.14 km southeast of the nearest colony of occurrence 5 below Indian Knob on Guidetti Ranch. The new occurrence is beside the dirt/rock road and in the south central part of Guidetti Ranch (Fig. 7), which is in the area protected by conservation easement to the City of San Luis Obispo. The soil/rock at occurrence 8 and occurrence 5 below Indian Knob appear similar using Google Earth aerial imagery. Although the landscape between the two occurrences is intact and mostly vegetated, there appears to be no similar soil/rock in this intervening area. The location below Indian Knob was previously surface mined, and the extracted soil/rock was used locally for road fill and road repair. T. Guidetti (pers. comm. 2018) stated that the stretch of road at occurrence 8 was covered with soil/rock from below Indian Knob. Thus, it seems likely the plants at occurrence 8 originated from individuals that were transported with soil/rock extracted from occurrence 5. Threats to this occurrence include low number of plants, vehicles running over the plants, and road maintenance.

Bull. Southern California Acad. Sci.
118(1), 2019, pp. 42–57

Optimizing a Municipal Wastewater-based *Chlorella vulgaris* Photobioreactor for Sequestering Atmospheric CO_2

Patrick Kim[1,2] and Ochan Otim[2,3]*

[1]*North Hollywood High School, 5231 Colfax Ave, North Hollywood, CA 9160*
[2]*TEAMS Research Institute, 4311 Wilshire Blvd., Los Angeles, CA 90010*
[3]*Environmental Monitoring Division, City of Los Angeles, 12000 Vista Del Mar, Playa Del Rey, CA. 90293*

Abstract.—Microalgae photobioreactors are among the most effective systems for capturing gaseous CO_2, the main contributor to global warming. Their capacity to generate massive amounts of biomass has been exploited serendipitously to sequester CO_2 and explicitly to remove nutrients from municipal wastewater. Unfortunately, research in this area has not included merging these dual capacities to address global warming. Instead, most are focused on thermolytic conversion of biomass into energy which in end returns CO_2 to the atmosphere. In this study, we investigated the potential of combining the two microalgal capacities (that of deriving nutrients from municipal wastewater and metabolic carbon from atmospheric or industrial CO_2 supplies), into an integrated means of reducing nutrients in ocean-bound wastewater and CO_2 in the atmosphere simultaneously. The test species used in this study was *Chlorella vulgaris* (*C. vulgaris*); the turbidity of *C. vulgaris* was used as a measure of yield in biomass. Our results show (i) that an open photobioreactor, and not a closed one, is the most productive, especially when augmented with industrial CO_2 (hence making a strong case for scrubbing CO_2 gas from industrial sources), (ii) that a mechanically agitated *C. vulgaris* culture is more productive than a static one, (iii) that without mechanical agitation, 32 ± 3 days of incubation are needed to reach the maximum yield of an open photobioreactor, (iv) that the optimal proportion of wastewater (%WW) required to support *C. vulgaris* growth is 80 ± 3%; at least 33% WW is required to observe growth above background, and (v) that without intervention, the upper pH limit of a WW-based *C. vulgaris* culture is 8.69 ± 0.09. Two mutually independent models are proposed to aide in scaling up an open WW-based *C. vulgaris* photobioreactor.

Global warming and eutrophication are two of the most pressing challenges confronting environmental scientists in recent times (Committee on Science for EPA's Future 2012). Global warming, the steady heating of the earth surface and of the atmosphere, is partly a consequence of atmospheric emission of greenhouse gases such as carbon dioxide (CO_2), methane (CH_4), nitrous oxide (N_2O), and some fluorinated compounds (Rey et al. 2018). These greenhouse gases do not only absorb and retain infra-red energy (Rey et al. 2018), they prevent the release of heat into the outer space from the earth surface (Akitt 2018). Of these gases, CO_2 is implicated the most in global warming (reviewed by Anderson et al. 2016). In 2015 alone, 82% of all greenhouse gases emitted was CO_2.[1] In modern times,

---

* Corresponding author: ochan.otim@lacity.org. ORCID: https://orcid.org/0000-0001-7272-4356

[1] Olivier J.G.J., G. Janssens-Maenhout, M. Muntean and J.A.H.W Peters. 2016. Trends in global CO_2 emissions. The Hague: PBL Netherlands Environmental Assessment Agency. Available

the main source of CO_2 is the combustion of fossil fuel to meet domestic and industrial energy needs (Fischer et al. 2018; Carotenuto et al. 2018). Efforts to curb global warming henceforth will, therefore, have to include controlling this anthropogenic CO_2 emission alongside reducing CO_2 levels already present in the atmosphere.

Eutrophication, the excessive plant growth in large water bodies, is due to increased availability of sunlight, carbon dioxide, and nutrients (Greeson 1969; Schindler 2006). This excessive plant growth in turn creates areas in aquatic environment where the amount of dissolved oxygen is not enough to support marine life. In current times, the discharge of large amounts of nitrogen and phosphorus into the aquatic ecosystems has increased the rate of eutrophication and the extent to which eutrophication is affecting inland waterways and coastal waters (Carpenter et al. 1998; Chislock et al. 2013). The affected areas (also referred to as dead zones) have been shown to occur frequently near where agricultural runoff and wastewater treatment effluent are released into large water bodies.[2] Efforts to remediate eutrophication resulting from these anthropogenic activities may have to include polishing agricultural runoffs and municipal wastewater before discharge.

Over the last few years, microalgae have emerged as promising vehicles for converting CO_2 into large quantity of biomass. Research in this area though is primarily focused on optimizing the biomass production for the biofuel industry with little considerations being given to the consequential release of the CO_2 back into the atmosphere (Xu et al. 2006; Sayre 2010; Mondal et al. 2017). In our opinion, the biomass so produced could be stored to control the amount of gaseous CO_2 in circulation. Storage could mean delaying or preventing the release of CO_2 into the atmosphere. Others have proposed chemical means (Obersteiner et al. 2001; Lackner et al. 2012; Wurzbacher et al. 2012) and the ocean (Shaffer 2010) as solutions towards reducing the amount of CO_2 in circulation. However, chemical means would require careful attention to the disposal of the chemical wastes so generated in the process, and both legal and environmental hurdles will have to be overcome before anthropogenic CO_2 is stored in the ocean.

In this study, we propose a natural way of sequestering CO_2 in biomass. We investigate whether a stable culture of microalgae with the following characteristics can be maintained in a mixotropic photobioreactor: (i) one that derives metabolic carbon from CO_2 (Sayre 2010; Mondal et al. 2017; Raven 2017) and (ii) one that would also utilize secondary-treated municipal wastewater as the only source of nutrients (Lau et al 1995; Wang et al. 2010; Craggs et al. 2011; Shi et al. 2016). We believe that a successful integration of these two microalgal natural capacities can play a role in scrubbing CO_2 gas not only from the atmosphere but from industrial sources as well while removing nutrients from ocean-bound municipal wastewater (WW) at the same time. This, metaphorically, is killing two birds with the same stone. The removal of nutrients in particular is of importance to watersheds and municipal wastewater treatment plants that discharge freshwater and treated wastewater effluents, respectively into large water bodies. Elevated level of anthropogenic nutrients in the ocean for example is known to promote toxic algal blooms (Anderson et al. 2002).

The key factors investigated in this study are those known to affect the productivity of microalgae photobioreactor. These factors include microalgae species to culture, the

---

from: http://edgar.jrc.ec.europa.eu/news_docs/jrc-2016-trends-in-global-co2-emissions-2016-report-103425.pdf. Accessed 05 July, 2018.

[2] Paine V. 2012. What Causes Ocean "Dead Zones"? Sci. Am., Available from: https://www.scientificamerican.com/article/ocean-dead-zones/. Accessed 15 January, 2019.

Table 1. Composition of secondary-treated wastewater used in this study. †

Test	Results
pH	7.3
Carbonaceous Biochemical Oxygen Demand	5 mg/L
Biological Oxygen Demand	12 mg/L
Settleable Solids	<0.1 mL/L
Turbidity	5.1 NTU
Mercury, Hg	0.00239 µg/L
Silver, Ag [a]	0.061 µg/L
Boron, B	0.541 mg/L
Antimony, Sb	2.75 µg/L
Beryllium, Be [a]	0.03 µg/L
Cadmium, Cd [a]	0.05 µg/L
Copper, Cu	13.4 µg/L
Nickel, Ni	6.52 µg/L
Thallium, Th [a]	0.02 µg/L
Zinc, Zn	14.8 µg/L
Arsenic, As	2.30 µg/L
Selenium, Se [a]	0.52 µg/L
Total Suspended Solids	9.7 mg/L
Total Dissolved Solids	768 mg/L
Total Organic Carbon	19.1 mg/L
Total Kjeldahl Nitrogen	47.8 mg/L
Organic Nitrogen	<1 mg/L
Total Phosphate	2.82 mg/L
Ammonia as Nitrogen	47.0 mg/L
Nitrate as Nitrogen	<0.1 mg/L
Nitrite as Nitrogen [a]	0.32 mg/L
Chloride	303 mg/L

† Available data at: http://ciwqs.waterboards.ca.gov/ciwqs/readOnly/PublicReportEsmrAtGlanceServlet?reportID = 2&isDrilldown = true&documentID = 1893752.

[a] Values lie between detection limit and regulatory reporting limit.

method of delivering CO_2 to the culture, the nutritional needs of microalgae, the pH changes occurring during incubation in the microalgae culture, and photobioreactor configuration (i.e., an open-air system versus a closed one; most researchers use the latter without provision for releasing metabolic O_2 known to be toxic to microalgae). Earlier studies in our lab (unpublished) suggests that *C. vulgaris* can flourish under the mixotropic cultivation setup adopted for this study. The potential of using *C. vulgaris* similarly has been demonstrated recently by Shi et al. (2016), and the kinetics of *C. vulgaris* growth in freshwater has also published by Adamczyk et al. (2016).

Materials and Methods

All containers used in this study were thoroughly washed with soapy water, rinsed with distilled water (DH_2O) and disinfected with 3% aqueous solution of hydrogen peroxide (PL Development, Clinton, SC, USA). Secondary-treated wastewater was acquired from the Hyperion Water Reclamation Plant (City of Los Angeles, CA, USA); its parameters, listed in Table 1, were determined as described elsewhere (Otim et al. 2018).

Chlorella vulgaris cultures (10 mL in Alga-Gro Freshwater growth medium) were purchased from Carolina Biological Supply (Burlington, NC, USA) and cultured using a

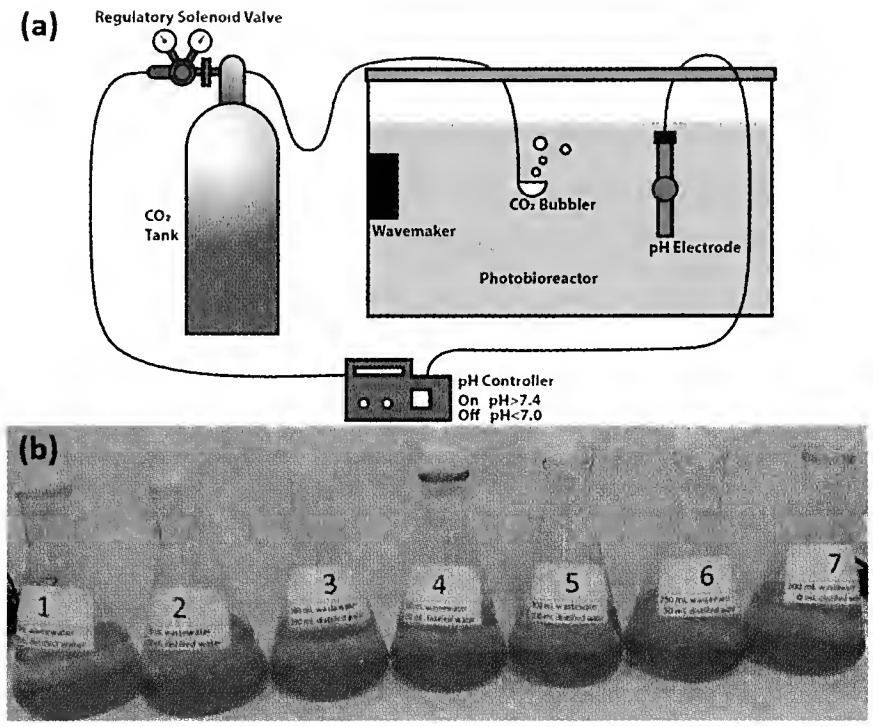

Fig. 1. (a) The setup used to maintain a viable stock of *Chlorella vulgaris* in distilled water. (b) Cultivating *Chlorella vulgaris* in secondary-treated wastewater (WW) collected from the City of Los Angeles Hyperion's 5-Mile Outfall system. The wastewater was serially mixed (in mL of WW) with distilled water to a final volume of 310 mL in each 500-mL flask (or 500-mL beaker, not shown) as follows: *Flask 1:* 0 (0% WW), *Flask 2:* 50 (16% WW), *Flask 3:* 100 (33% WW), *Flask 4:* 150 (50% WW), *Flask 5:* 200 (67% WW), *Flask 6:* 250 (83% WW), *and Flask 7:* 300 (100% WW). The 310 mL total volume includes 10 mL of laboratory stock of *Chlorella vulgaris* (see Materials and Methods section). Glass wool and perforated saran wraps were used to cover the open mouths of Erlenmeyer flasks and beakers, respectively.

modification of James (2012) protocol as follows. The *C. vulgaris* cultures were first stored as received at room temperature under an alternating cycle of artificial white light (16 h) and darkness (8 h) for seven days to allow acclimatization. Then before use, the cultures were diluted to 1 L with fresh Alga-Gro Freshwater growth medium and incubated for seven more days under alternating cycle of artificial white light as described above. To maintain a laboratory stock, *C. vulgaris* was cultured in an open photobioreactor (30-L DH_2O) fitted with the capacity to boost the level of CO_2 in microalgae culture automatically via a gas dispersion frit to bring down pH to 7.0 when necessary (Fig. 1a); the upper limit of pH was set to 7.4. Nutrients (20 mL of Guillard's (F/2) Marine Water Enrichment Solution; Carolina Biological Supply, Burlington, NC; Guillard and Ryther 1962; Guillard 1975) were supplied to the *C. vulgaris* laboratory stock every seven days.

To determine the ratio of wastewater-to-distilled water (WW/DH_2O) suitable for optimal growth, two separate trials of seven 310-mL photobioreactors were set up in 500-mL beakers (not shown) and in Erlenmeyer flasks shown in Fig. 1b (labeled 1 to 7) to assure reproducibility. This dual setup also served to gauge in a rudimentary way the effect of exposing different surface areas on photobioreactor performance. The WW/DH_2O ratios were formulated as follows (v/v): 0/300, 50/250, 100/200, 150/150, 200/100, 250/50, 300/0. Into each photobioreactor was added 10 mL of laboratory stock *C. vulgaris* (which brought the total volume to 310 mL) and, without stirring, the microalgae were allowed to grow as lawns. The endpoint for these experiments came when the green microalgae began to turn brown (beakers: 34 days; flasks: 29 days). Microalgal yield was measured as changes in turbidity (NTU) using a NUL-231 Turbidity Logger Sensor coupled to a USB-200 USB Module (Rochester, NY, USA). No external supplies of CO_2 or nutrients

were administered in these two sets of cultures beyond atmospherically or wastewater supplied (Table 1), respectively.

To measure and/or control the pH of microalgae cultures, an integrated pH monitoring system (Doctors Foster and Smith, Rhinelander, WI, USA) was used. The components of the system were (i) a Pintpoint pH electrode (measurement range: 1.00–14.00; resolution: 00.00 pH Unit; America Marine Inc., Ridgefield, CT, USA), (ii) a pair of CO_2 delivery regulators (Azoo, Taipei, Taiwan) controlled by a single solenoid valve (Jin Ben Sun Co., Ltd., Taoyuan City, Taiwan), and (iii) a Pinpoint pH Controller (America Marine Inc., Ridgefield, CT, USA) for ultimately powering, monitoring and controlling all the components of the system. Before using the automated pH monitoring system for acquiring experimental values, a two-point pH electrode calibration was carried out using a pH 7.00 certified reference buffer solution (to set the lower detection limits) and a pH 10.00 certified reference buffer solution (to set the slope). Both certified buffer solutions were supplied by Fisher Chemicals (Fair Lawn, NJ, USA). To monitor and regulate the pH of 30-L photobioreactors, the integrated system was configured as shown in Fig. 1a. The pH electrode was cleaned and recalibrated when necessary (usually once a week). To monitor the pH of the seven 310-mL photobioreactor flasks (Fig. 1b) and beakers (not shown), the pH electrode was used to gently stir the microalgae cultures for about 30s before taking measurements. The electrode was rinsed with distilled water between measurements. By design, the 310-mL photobioreactors required no additional CO_2 gas supplies.

To determine the empirical differences between an open microalgae photobioreactor system and a closed one by turbidity measurements, four separate 30-L tap water-based *C. vulgaris* photobioreactors similar to that shown in Fig. 1a were set up as follows. The first two were open to the atmosphere with one receiving additional supply of industrial CO_2 (Open, CO_2) and the other receiving no additional CO_2 supply beyond atmospherically supplied (Open, No CO_2). The third and the fourth photobioreactors were closed systems but similarly configured (i.e., Closed, CO_2 and Closed, No CO_2). Tap water (pH 7.27 ± 0.09, $n = 4$) was used here because it is the background matrix of the wastewater used in this study. To each photobioreactor was added a 1 L dilution of the stock *C. vulgaris* as described earlier in this section, and 20 mL of Guillard's (F/2) Marine Water Enrichment Solution (Carolina Biological Supply, Burlington, NC, USA) every seven days. Each photobioreactor was equipped with a circulation pump (wavemaker, Fig. 1a) to keep microalgae in suspension. These four pumps, discovered to increase the temperature of the microalgae cultures, were turned on and off automatically every 30 min to keep the temperature of the photobioreactors to within 23.1 ± 0.2°C. The light cycles and the pH of cultures were monitored and controlled as described earlier in this section. Turbidity was measured every seven days, and on the 10th day, over 21 days.

Non-linear modeling of turbidity and pH variation with time, and principal component analysis (PCA) were performed using the PAST software platform (PAleontological STatistics; Hammer et al. 2001). PCA, an unsupervised linear dimensionality reduction algorithm (reviewed by Jollife and Cadima 2016; see also Gewers et al. 2018) was used to find a more meaningful coordinate system to work with since our variables have different units (i.e., %WW, incubation days and pH). It was used similarly to study growth and biochemical composition of *C. vulgaris* in different growth media by Chia et al. (2013). Standardizing data for PCA was accomplished by subtracting the mean value from individual measurement and dividing the result by standard deviation.

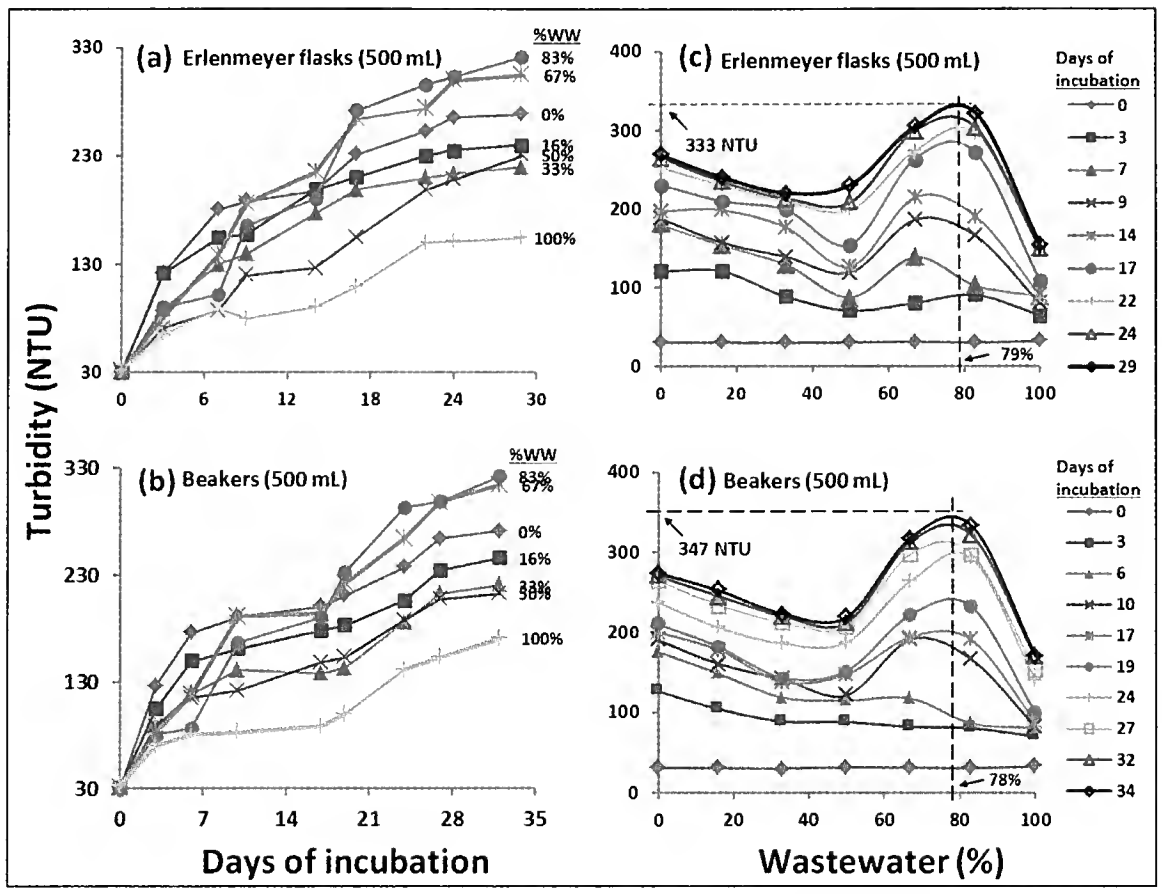

Fig. 2. The profiles of *Chlorella vulgaris* growth as measured by the turbidity of the seven wastewater/distilled water mixtures described in Fig. 1b. For cross authentication, duplicate test cultures were started on different dates with two different sets of container geometries to run for 29 days in 500-mL Erlenmeyer flasks (a) and 34 days in 500 m-L beakers (b). The end of incubation was determined by the browning of the microalgae in the cultures. Experimentally determined maximum turbidities are shown by the intersections of the horizontal dash lines and the ordinate in (c) and (d). Also shown at the intersection of each vertical dash line with the abscissa is the optimal %WW. The experimental coordinate for the maximum rabidity in the Erlenmeyer flasks (c) is (79%, 333 NTU) and in the beakers (d) is (78%, 347 NTU). Modelling (not shown) suggests that the coordinate for maximum turbidity should actually be (83%, 773 NTU).

Results

To determine the optimal WW/DH_2O ratio and incubation time required to maximize biomass yield, *C. vulgaris* was cultured in a pair of serially diluted wastewater photobioreactors for 29 and 34 days. Results show that yield, as measured by the turbidity of the cultures, is reproducibly related to time and exposed surface area (compare Erlenmeyer flasks results displayed in Fig. 2a with beakers results in Fig. 2b). The highest turbidity values were measured after 15 days of incubation in the 83% WW culture; the lowest being recorded in the 100% WW irrespective of the length of incubation time.

To acquire potentially useful information for scaling up a wastewater-based photobioreactor, a non-traditional interpretation of our data is provided in Figs. 2c-d. Four conclusions can be made from these two plots: (i) that 100% DH_2O or 100% WW is not the best medium for culturing *C. vulgaris* even though 100% DH_2O is more accommodating than 100% WW, (ii) that yield falls with increasing %WW during the first six days of incubation, (iii) that 80 ± 3% WW culture is the optimal range for realizing the most biomass in wastewater provided incubation is allowed to continue for at least 29 days (but not more than 34 days because the green microalgae turns brown thereafter under this condition), and (iv) that beyond 78-83% WW, wastewater severely limits *C. vulgaris* growth.

To understand the ability of *C. vulgaris* to absorb atmospheric CO_2, we monitored changes in pH in each of the WW/DH_2O cultures over time. The rationale was that pH is directly related to the availability of dissolved CO_2 in the cultures (Chi et al. 2011) which

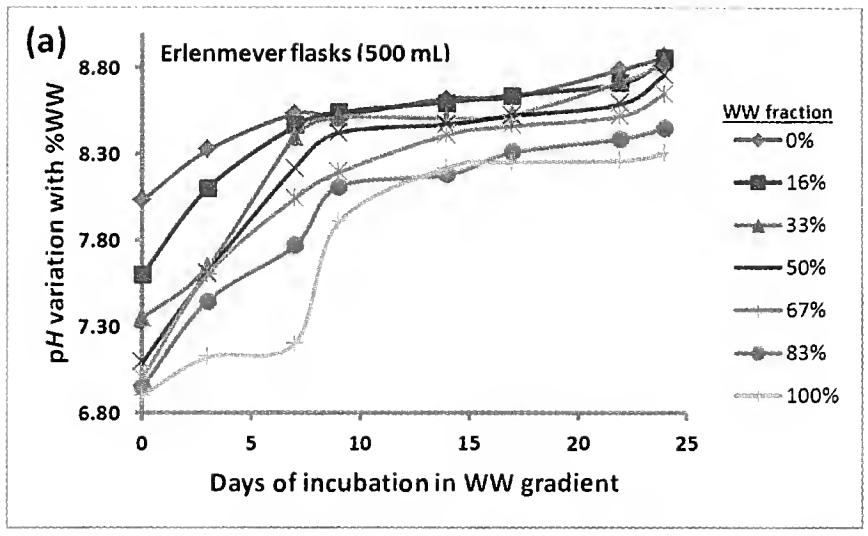

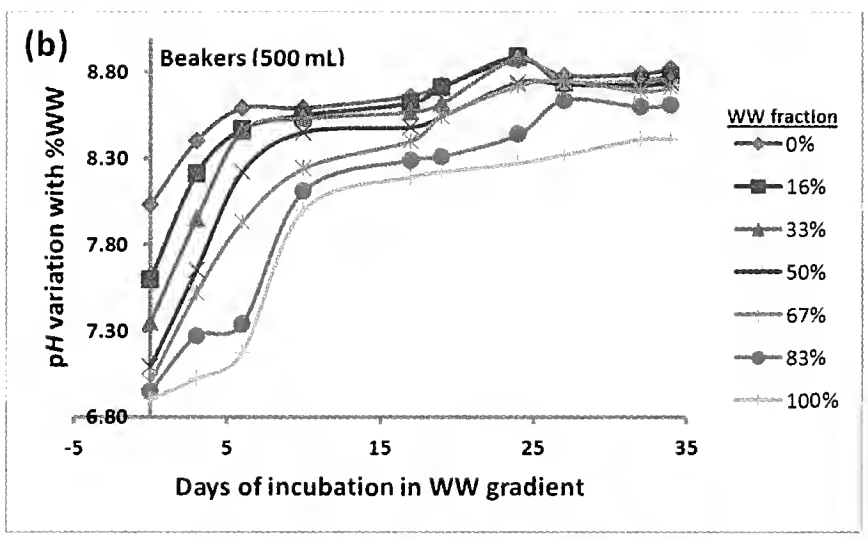

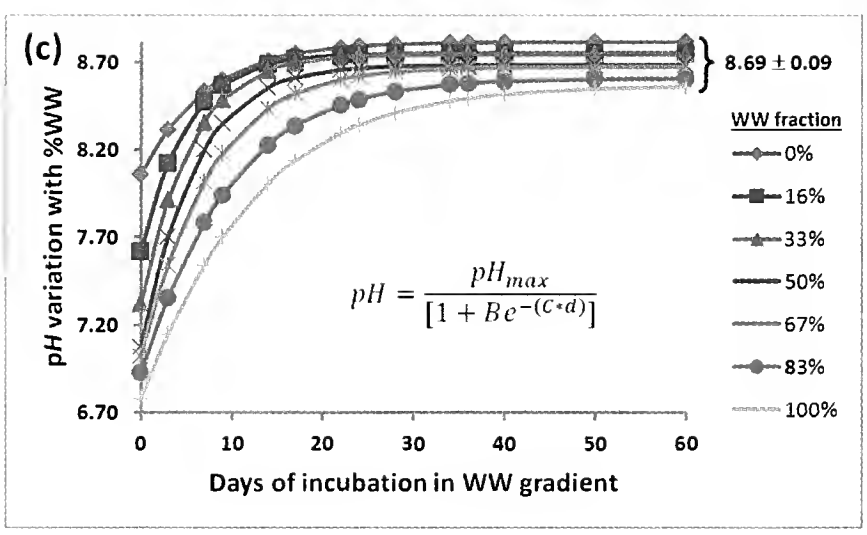

Fig. 3. The variation of pH with time in the WW-based photobioreactors at different %WW: (a) 500-mL Erlenmeyer flasks; (b) 500-mL beakers. The duplicate experiments (a) and (b) were started at different times for cross authentication. (c) Modeling the p*H* variation in (a) and (b) to determine the theoretical p*H* maximum (i.e., $pH_{max} = 8.69 \pm 0.09$). Note (i) that the $pH_{max} = 8.69 \pm 0.09$ is also the mean of pH_{max} values in Table 3, and (ii) that the inflection points in (c) are near constant in growth media containing 0% to 33% WW, but vary widely between 50% and 100% WW.

can in turn be directly linked to the capacity to capture atmospheric CO_2. Duplicate results from this pH study are presented in Fig 3a where eight pH measurements were taken on different days over a period of 29 days and in Fig. 3b where 10 measurements were taken similarly over a period of 34 days. In both duplicates, the lowest pH values were measured in 100% WW culture, and the highest in the 0% WW culture (DH_2O, pH 7.99 ± 0.06, n = 2). It can also be seen in both cases that an upper pH ceiling is reached in each %WW culture after 10 days of incubation. The average pH value at these ceilings is 8.7 ± 0.1 ($n = 14$). This average value reveals the enormous potential of a wastewater-based photobioreactor for absorbing CO_2.

Data from the open WW photobioreactor system (Fig. 1) show that the relationship between turbidity (τ) and the length of incubation in days (*d*) in any of our

Table 2. Values of constants τ_{max} and D in the Michaelis-Menten growth equation *Turbidity* = $[\tau_{max}{*}d]/[D + d]$ derived from regression analysis of turbidity data at each %WW (Fig. 2a-b). They are reported as mean±standard deviation.

	0%	16%	33%	50%	67%	83%	100%
τ_{max}	323 ± 17	296 ± 5	288 ± 18	379 ± 140	530 ± 15	764 ± 13	239 ± 25
D	7.3 ± 0.7	7.9 ± 0.8	10.8 ± 0.6	22.8 ± 15.1	22.5 ± 3.8	41.7 ± 5.5	17.6 ± 4.7

τ_{max} is the extrapolated maximum turbidity.
τ_{max} and D are strongly and positively correlated (Pearson $r = 0.90$).
Variable d is length of incubation in days.

310-mL wastewater-based *C. vulgaris* photobioreactors fits quantitatively into the following (Michaelis-Menten kinetics) equation:

$$\tau = \frac{(\tau_{max} * d)}{(D + d)} \tag{1}$$

where τ_{max}, the maximum turbidity, is obtained by extrapolating d in Eq. 1 beyond 250 days in this study, and D is the number of incubation days needed for τ to reach ½ τ_{max}. All τ_{max} and D values from this study are listed in Table 2.

To devise some means of predicting pH changes during *C. vulgaris* cultivation, given any %WW, a regression analysis (not shown) was performed for each of the plots presented in Fig. 3a-b. The results of the regression analysis suggest that pH variations can be model using the logistic expression below:

$$pH = \frac{pH_{max}}{[1 + Be^{-(C*d)}]} \tag{2}$$

where pH_{max} is the maximum pH to be expected when d is infinitely large. The distribution of pH_{max} values (Table 3) is found to mirror that of turbidity (Fig. 2). This apparent correlation seems to suggest that pH_{max} is a measure of the carbon requirement for *C. vulgaris* growth and, therefore, an indirect measure of capacity to absorb CO_2 gas. The meanings of B and C are unclear to us at this time. All values of pH_{max}, B, and C obtained here are listed in Table 3. Scatter plots based on this model are presented in Fig. 3c for comparison with experimental plots in Figs. 3a-b.

To determine the range of %WW values and incubation days within which photobioreactor setup such ours can perform above background, PCA was applied to a 7×10 correlation matrix derived from turbidity, or pH values in combination with corresponding %WW and number of incubation days. In Fig. 4a is presented a PCA biplot for the correlation matrix of turbidity changes with days of incubation in various %WW. The %WW markers

Table 3. Averages of Erlenmeyer flasks (Fig. 3a) and beakers (Fig. 3b) values for logistic constants pH_{max}, B and C in modeled growth equation $pH = pH_{max}/[1 + Be^{-(C*d)}]$. These values are obtained by regression analysis of pH as a function of incubation days at each %WW and are reported as mean±standard deviation.

	0%	16%	33%	50%	67%	83%	100%
pH_{max}	8.82 ± 0.05	8.75 ± 0.00	8.75 ± 0.02	8.68 ± 0.02	8.67 ± 0.09	8.61 ± 0.19	8.57 ± 0.08
B	0.09 ± 0.01	0.15 ± 0.00	0.19 ± 0.01	0.23 ± 0.00	0.24 ± 0.01	0.24 ± 0.04	0.26 ± 0.01
C	0.15 ± 0.06	0.22 ± 0.03	0.20 ± 0.04	0.19 ± 0.00	0.15 ± 0.02	0.12 ± 0.04	0.09 ± 0.00

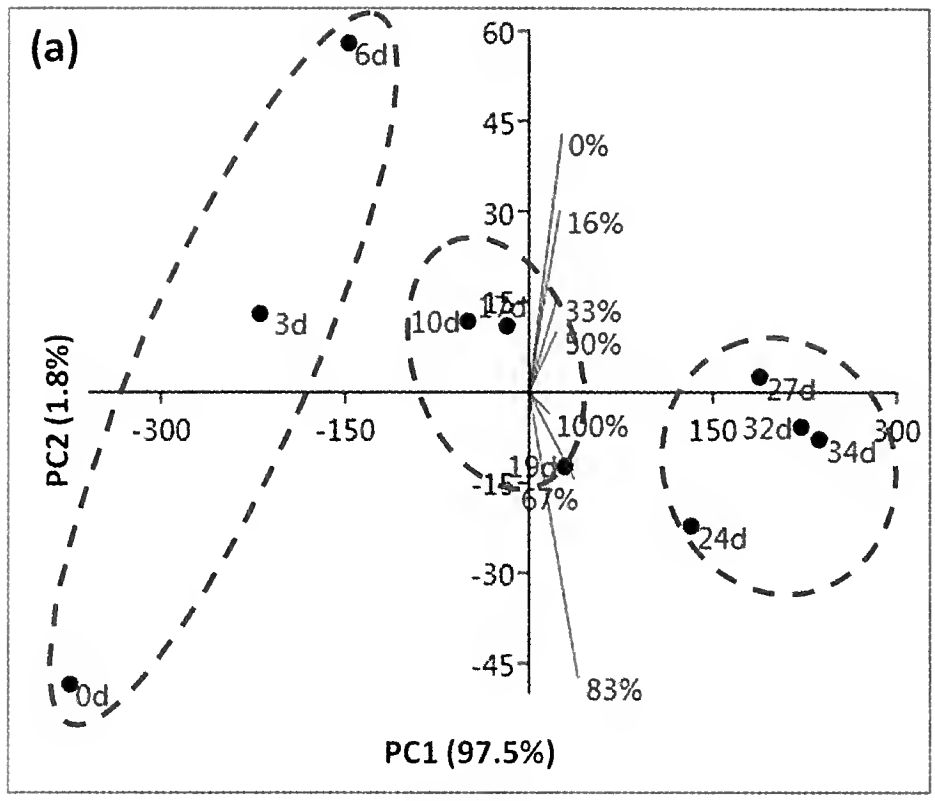

Fig. 4. Scatter plots of two key principal components (PC1 and PC2) from PCA to determine the best combination of %WW, cultivation time (in days, d), and p*H* values for optimal growth. (a) The loading of incubation days in an ordination space illustrating the influence of %WW as vectors (green lines) on incubation days. (b) The scores of %WW in the same space.

are shown as vectors (green lines), and the incubation days as numbers in'd' unit. There are two observations which can be made from Fig. 4a. First, that PC1 (which explains 97.5% of variance) strongly correlates with seven of ten incubation days: 0, 3, 6, 24, 27, 32, and 34 days. Of the seven days, PC1 increases with a set of four incubation days longer than 20 (24, 27, 32, and 34 days), and decreases with a set of three incubation days less than 10 (0, 3 and 6 days). The former suggests that turbidity and the set of days 24, 27, 32, and 34 (and days in-between) vary together. The latter implies that incubating *C. vulgaris* in wastewater for 0, 3 or 6 days (and days most likely in-between) will lead to a decrease in turbidity as shown here earlier. This axis (PC1, Fig. 4a) can, therefore, be viewed in similar PCA as a measure of the effect of incubation on algal growth; the larger the value along PC1, the larger the corresponding turbidity value will be. Days between 10 and 20, the 'Goldilocks' days, are not correlated with PC1. Notice also that all %WW vectors (green lines) are accounted

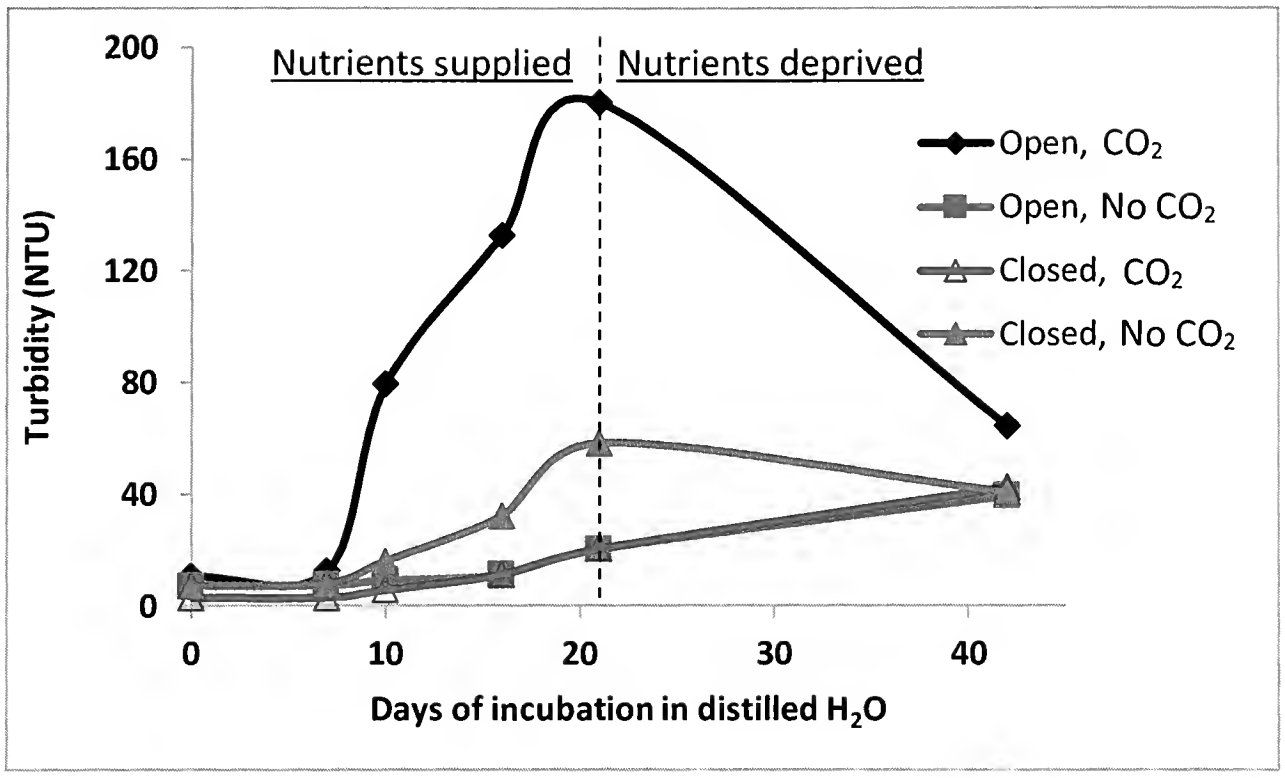

Fig. 5. Determining the level of gaseous CO_2 required for optimal *Chlorella vulgaris* growth rate in distilled H_2O (30 L, Fig. 1a). For the first 21 days (left of vertical dashed line), *Chlorella vulgaris* was supplied with nutrients as described in the text, but deprived of nutrients thereafter. Temperature was maintained at 23.1 ± 0.2°C over the 42-days of experiment.

for along PC1 with positive loadings. This simply restates the benefit derives from having wastewater in *C. vulgaris* cultures since the larger the values are along PC1, the better.

PC1, however, fails to offer the %WW range that would support optimal *C. vulgaris* growth. This information is provided in the loadings of WW vectors along the second principal component, PC2. It can be seen that PC2, which explains 1.8% of variation, correlates positively with the 0, 16, 33, and 50% WW vectors, but negatively, with the 67, 83, and 100% WW vectors. The 0, 16, 33, and 50% WW cultures were shown earlier in this section to lead to less than optimal turbidity values and hence do not support high *C. vulgaris* yield. The 83% WW culture on the other hand was shown to be the optimal WW level suitable for growth (followed by the 67% WW culture; Fig. 2). Based on these observations, values along PC2 can therefore be considered a measure of the capacity of wastewater to support *C. vulgaris* growth; the small the value, the large the turbidity will be. The 83% WW then stands out as the best growth medium for *C. vulgaris* since it has the lowest value along PC2.

Fig. 4b is a PCA scatter plot for pH. It can be seen that PC1 (which explains 92.3% of variance) is strongly and *positively* correlated with lower %WW (0 and 16% WW), but *negatively* correlated with higher %WW values (83 and 100%). Because evidence shows that lower %WW does not support growth optimally, but 83% is, this principal component can be used as a measure of the best condition for absorbing CO_2 (since the p*H* of an open photobioreactor is closely linked to the availability of CO_2 in the atmosphere). The smaller the values along PC1, the higher the capacity of the microalgae to absorb CO_2 gas. Note that the clustering of wastewater fractions in Fig. 4b mirrors the distribution of *B* values with %WW in Table 3 which may be suggesting the meaning of constant *B* in Eq. 2.

To understand the role of an open or a closed system against as far as CO_2 supply to a *C. vulgaris* culture is concerned, four separate 30-L tap water-based photobioreactors were set up. Fig. 5 is a summary of the results of these experiments. It can be seen that growth was generally exponential in each photobioreactor over the 21 days of experiment (left side of dashed line in Fig. 5). During this time, the open system registered the best performance

with additional CO_2. The worse performance was observed in the two photobioreactors configured to be open with no additional CO_2 supply or closed with additional supply of CO_2. To reaffirm the importance of non-maternal nutrients to *C. vulgaris*, the four photobioreactors above were incubated for 19 more days without added nutrients. The results, summarized on the right side of Fig. 5 (days between 21 and 40) show that biomass production declined significantly during the period, even in the best photobioreactor configuration (i.e., open with additional CO_2 supply).

Discussion

We have shown that the temporal growth profile of *C. vulgaris* in a wastewater-based photobioreactor follows a nonlinear kinetics (Figs. 2a-b). This is consistent with what others have observed (Ammar 2016). However, that *C. vulgaris* exhibits clearly segmented growth response to wastewater as shown in Figs. 2c-d is a novelty. In this newly discovered profile, the accumulation of *C. vulgaris* biomass declines progressively in low levels of wastewater (0-50% WW), recovers rapid in the 50-83% WW range and then falls precipitously in the 83% to100% WW range. To explain this profile, it is useful to think of the decline in low levels of wastewater as a reflection of *C. vulgaris* adapting to wastewater-induced shock (Wang et al. 2009). This is justifiable because the burden of adjustment logically increases with the proportion of wastewater in cultures. The rapid biomass increase in the 50-83% WW range then can be thought of as the benefits microalgae derive from wastewater, however miniscule they may be in low %WW cultures is enough to overcome the wastewater-related shock in this %WW range. Beyond this %WW range, the precipitous drop in biomass production may be explained hypothetically as a breach of microalgae cellular biochemistry by high levels of wastewater components. More studies are required to test these hypotheses.

The role that 'maternal' nutrients play in growth, which is clearly exhibited in Fig. 2 (0% WW cultures), is worth mentioning here. The fact that *C. vulgaris* grows at all and more so in 100% DH_2O means that maternally stored nutrients (in the cytoplasm and in the inter-thylakoid regions of *C. vulgaris* chloroplast; Safi et al. 2014) are used, we believe, for autonomous growth. This continues until the maternal nutrients are exhausted (in about the sixth day of incubation; Fig. 2d) whereupon wastewater becomes the source of nutrients.

This study finds that the optimal conditions for culturing *C. vulgaris* in an open wastewater-based photobioreactor is 80 ± 3% WW over a 29-34 incubation days window. It also finds that additional metabolic carbon source beyond atmospheric CO_2 is required to maximize the biomass production in a photobioreactor (i.e., Open, CO_2 system, Fig. 5). The importance of an open photobioreactor system also needs to be emphasized here for two reasons. First, studies show that, without additional source of carbon (industrial CO_2 for example), the capacity of *C. vulgaris* cells to photosynthesize falls which in turn causes a drop in biomass production (Lundquist et al. 2009; Gebreslassie 2013; Raven 2017). Indeed, most photobioreactors fail because of inadequate supplies of metabolic carbon and yet one cheap source of CO_2, the flue gas from power plants, is always available (Gebreslassie, 2013; Kumar et al. 2011). Secondly, O_2 gas, the byproduct of photosynthesis, is toxic to algae (Molina-Grima et al. 2001). It has been shown that microalgae can only tolerate up to 400% of O_2 above the level in O_2 saturated air (Chisti 2007). Having an open wastewater photobioreactor would therefore reduce toxicity by allowing O_2 produced during

photosynthesis to escape (while still leaving enough for microbes to use in the breaking down of organic matter in wastewater; Azov et al. 1982; Abdel-Raouf et al. 2012).

This study identified five elements of a wastewater-based *C. vulgaris* photobioreactor (τ_{max}, pH_{max}, D, B, C) which could be useful for forecasting productivity even though the meanings of B and C is still to be determined. For any chosen %WW, we have introduced (i) the concept of the minimum days (D) a static photobioreactor would need to produce biomass above background, (ii) the concept of pH_{max}, the upper ceiling of pH which can be used to predict the capacity of a wastewater-based *C. vulgaris* photobioreactor to absorb CO_2 in an open photobioreactor system, and (iii) the concept of τ_{max}, the upper ceiling of biomass production when incubation is continued indefinitely beyond the minimum days, D (i.e., $d >> D$; Eq. 1). One property of τ_{max} needs elaboration. Unlike pH_{max} and D, the values of τ_{max} cannot be obtained directly by *C. vulgaris* cultivation because of the limits imposed on production by the carrying capacity of photobioreactors and the long incubation time required to achieve it. For example, the average carrying capacity of our 310-mL system was 340 NTU (the mean of 333 NTU and 347 NTU; Fig. 2a and Fig. 2b, respectively) and yet τ_{max} was determined to be 773 NTU in a 83% WW culture (after 550 years of incubation).

A number of factors were confirmed in this study to have significant consequence on the effectiveness of using microalgae to polish municipal wastewater. For example, we find that efficient removal of nutrients from wastewater as measured by increase in turbidity depends on constant agitation of the *C. vulgaris* cultures. This is of consequence in municipalities where microalgae have been adopted to polish wastewater, but agitation has not been incorporated into their photobioreactor designs (Craggs et al. 2003). Exacerbating this problem is the fact that the C:N ratio in a typical municipal wastewater is low when compared to the carbon requirements of microalgal biomass. This low C:N ratio limits the capacity of microalgae to produce biomass in wastewater (Benemann 2003). This imbalance is usually manifested as elevated pH levels during incubation (resulting from the use of bicarbonate ions as a CO_2 source for algal photosynthesis, releasing hydroxide ions; Craggs et al. 2011) which in turn prevents growth of both microalgae and bacteria which degrade the organic compounds in wastewater (Azov et al. 1982). This scenario was observed in photobioreactors which were not supplied with additional CO_2 (Figs. 3, 5). Boosting carbon supply to a wastewater-based culture would not only enhance microalgal yield as has been shown here, it would also fulfill a goal to scrub CO_2 gas from sources beyond the atmosphere. Note that the main function of microalgae for polishing municipal wastewater is to remove N, and not P (Choi and Lee 2015). This is because the large N:P ratio requirement for biomass production in microalgae means no additional microalgal biomass production is needed above that required to assimilate N to remove P from municipal wastewater (Lau et al. 1995; Benemann 2003; Craggs et al. 2011).

The environmental remediation approach proposed in this study will results in massive amounts of algal biomass, the fate of which must be addressed appropriately. Fortunately, some means for doing so already exist even though they were not designed with addressing environmental issues in mind. For example, microalgae biomass has been turned into chemical feedstock for biodegradable plastics (Lambert and Wagner 2017), lubricants (Ruiz et al 2016), fertilizers (Uysal et al. 2015), and pharmaceutical/nutraceutical products (Jha et al. 2017). In the skin-care natural product industry, the capacity of microalgae to developed sun blocking agents to protect and heal themselves from the damaging impacts of exposure to solar radiation and other environmental hazards has been harnessed to protect human skin (Stolz and Obermayer 2005). In some parts of the world, microalgae have

been used sustainably as sources of animal feed because of their ability to concentrate carbohydrates, proteins and vegetable oils, micronutrients, vitamins, and valuable pigments (Lambert and Wagner 2017). In an application incompatible with our goal, microalgae biomass has also been used as human dietary supplements (Yaakob et al. 2014). And of recent, a technology has emerged that has potential to convert microalgal biomass into a host of products. Currently, this proprietary technology employs high energy electron beams to convert cellulose in corn cobs to edible sugar, alcohol, biodegradable plastics and several other products on industrial scale[3]. Microalgal biomass could be treated similarly.

Capturing and storing CO_2 emission is one feasibly way of mitigating climate change. How the captured CO_2 is stored however will have an impact on the effectiveness of long-term sequestration. For example, the ocean's capacity to absorb and store huge quantities of CO_2 could be used to sequester CO_2. This though comes with environmental cost and legal problems. First, several studies have shown that sequestering CO_2 in the ocean leads to global warming which ultimately leads to excessive plant growth. As pointed out in the Introduction section, this excessive plant growth creates dead zones in the ocean (Shaffer 2010). Secondly, the Clean Water Act makes it impossible to sequester CO_2 into the ocean.[4,5] The Act prohibits point source discharges into navigable waters in the USA without a permit; it also ensures that marine environments will not suffer unreasonable degradation or irreparable harm from anthropogenic activities. One alternative to the ocean is geological sequestration (Shaffer 2010). This alternative involves injecting captured CO_2 into geologic environments (Aarnes et al., 2010; Plasynski et al., 2011). However, the alternative also comes with one major environmental concern, that of leaks from storage sites.

Conclusions

We have demonstrated that a microalgae-based photobioreactor can offer a potential solution to lowering the level of atmospheric CO_2 while cleaning nutrients-laden municipal wastewater at the same time. By culturing *C. vulgaris* in various photobioreactor systems containing wastewater, we have shown that wastewater plays two competing roles during *C. vulgaris* growth: a mostly detrimental and dominant role at low levels where we believe wastewater interferes with the metabolic mobilization of the maternal nutrients required for the initial growth, and a mostly supportive role that is very evident in the 50-83% WW range cultures. As such, the optimal conditions for *C. vulgaris* to absorb atmospheric CO_2 are found to be 78-83% dilution of wastewater (the baseline is 33% WW) and 24 days of incubation in open air. We have also shown that principal components analysis can be applied to rudimentarily acquired data such as ours to aid in determining the optimal wastewater requirement of a photobioreactor. The size of the chosen photobioreactor would be limited by the carrying capacity of photobioreactor.

---

[3] Stahl, L. 2019. The unlikely, eccentric inventor turning inedible plant life into fuel. CBS 60 Minutes. Available from: https://www.cbsnews.com/news/marshall-medoff-the-unlikely-eccentric-inventor-turning-inedible-plant-life-into-fuel-60-minutes/. Accessed 15 January, 2019.

[4] Cleanwat.001. 2002. Federal Water Pollution Control Act. Available from https://www.epa.gov/sites/production/files/2017-08/documents/federal-water-pollution-control-act-508full.pdf. Accessed 15 January, 2019.

[5] Heinrich J. 2002. Legal implications of CO_2 ocean storage. Available from: https://sequestration.mit.edu/pdf/Legal_Implications_Ocean_Storage.pdf. Accessed 15 January, 2019.

Acknowledgements

The authors would like to acknowledge TEAMS Research Institute members, especially Brendon Cho, Brandon Chon, and Sue Byun for their meticulous preliminary background studies and institutional support. This study was funded by a grant from the Southern California Academy of Sciences, and by the City of Los Angeles. PK is a high school student.

Literature Cited

Abdel-Raouf, N., A.A. Al-Homaidan and I.B.M Ibraheem. 2012. Microalgae and wastewater treatment. Saudi J. Biol. Sci., 19:257–275.

Adamczyk, M., J. Lasek and A. Skawińska. 2016. CO_2 Biofixation and Growth Kinetics of *Chlorella vulgaris* and *Nannochloropsis gaditana*. Appl. Biochem. Biotechnol., 179:1248–1261.

Ammar, S.H. 2016. Cultivation of Microalgae *Chlorella vulgaris* in Airlift photobioreactor for Biomass Production using commercial NPK Nutrients. Al-Khwarizmi Engineering Journal, 12(1):90–99.

Anderson, D.M., P.M. Glibert and J. Burkholder. 2002. Harmful algal blooms and eutrophication: Nutrient sources, composition, and consequences. Estuaries, 25(4):704–726.

Anderson, T.R., E. Hawkins and P.D. Jones. 2016. CO_2, the greenhouse effect and global warming: from the pioneering work of Arrhenius and Callendar to today's Earth System Models. Endeavour, 40: 178–187.

Akitt, J.W. 2018. Some observations on the greenhouse effect at the earth's surface. Spectrochim. Acta A, 188:127–134.

Azov, Y., G. Shelef and R. Moraine. 1982. Carbon limitation of biomass production in high-rate oxidation ponds. Biotechnol. Bioeng., 24:579–594.

Benemann, J.R. 2003. Biofixation of CO_2 and greenhouse gas abatement with microalgae - technology roadmap. Report No. 7010000926. U.S. Department of Energy National Energy Technology Laboratory, 30 pp.

Carotenuto, F., G. Gualtieri, F. Miglietta, A. Riccio, P. Toscano, G. Wohlfahrt and B. Gioli. 2018. Industrial point source CO_2 emission strength estimation with aircraft measurements and dispersion modelling. Environ. Monit. Assess., 190(3):165.

Carpenter, S.R., N.F. Caraco, D.L. Correll, R.W. Howarth, A.N. Sharpley and V.H. Smith. 1998. Nonpoint pollution of surface waters with phosphorus and nitrogen. Ecol. Appl., 8:559–568.

Chi, Z., J.V. O'Fallon and S. Chen. 2011. Bicarbonate produced from carbon capture for microalgae culture. Trends Biotechnol., 29:537–541.

Chia, M.A., A.T. Lombardi, G. Melão Mda. 2013. Growth and biochemical composition of *Chlorella vulgaris* in different growth media. An. Acad. Bras. Ciênc., 85(4):1427–1438.

Chislock, M.F., E. Doster, R.A. Zitomer and A.E. Wilson. 2013. Eutrophication: Causes, Consequences, and Controls in Aquatic Ecosystems. Nature Education Knowledge 4(4):10. Accessed 15 January 2019.

Chisti, Y. 2007. Biodiesel from microalgae. Biotech. Adv., 25:294–306.

Choi, H.J. and S.M. Lee. 2015. Effect of the N/P ratio on biomass productivity and nutrient removal from municipal wastewater. Bioprocess Biosyst. Eng., 38:761.

Committee on Science for EPA's Future. 2012. Challenges of the 21st Century. Pp. 27–53 inScience for Environmental Protection: The Road Ahead. National Academies Press, xvi+234 pp.

Craggs, R.J., R.J. Davies-Colley, C.C. Tanner and J.P.S. Sukias. 2003. Advanced ponds systems: performance with high rate ponds of different depths and areas. Water Sci. Technol., 48(2):259–267.

Craggs, R.J., S. Heubeck, T.J. Lundquist and J.R. Benemann. 2011. Algal biofuels from wastewater treatment high rate algal ponds. Water Sci. Technol., 63:660–665.

Fischer, M.L., W.R. Chan, W. Delp, S. Jeong, V.H. Rapp and Z. Zhu. 2018. An estimate of natural gas methane emissions from California homes. California Energy Commission. Publication Number: CEC-500-2018-021.

Gebreslassie, B.H., R. Waymire and F. You. 2013. Sustainable design and synthesis of algae-based biorefinery for simultaneous hydrocarbon biofuel production and carbon sequestration. Aiche J., 59: 1599–1621.

Gewers, F.L., G.R. Ferreira, H.F. Arruda, F.N. Silva, C.H. Comin, D.R. Amancio and L.D. Costa. 2018. Principal Component Analysis: A natural approach to data exploration. CoRR, arXiv:1804.02502.

Greeson E.G. 1969. Lake eutrophication – a natural process. J. Am. Water Resour. Assoc., 5(4):16–30.

Guillard, R.R.L. 1975. Culture of Phytoplankton for Feeding Marine Invertebrates. Pp. 29–60 in Culture of Marine Invertebrate Animals. (W.L. Smith and M.H. Chanley, eds.) Plenum Press, viii+338 pp.

Guillard, R.R.L. and J.H. Ryther. 1962. Studies on Marine Planktonic Diatoms I. *Cyclotella nana* Hustedt and *Detonula confervacea* (Cleve) Gran. Can. J. Microbiol., 8:229–239.

Hammer, Ø., D.A.T. Harper and P.D. Ryan. 2001. PAST: Paleontological statistics software package for education and data analysis. Palaeontologia Electronica 4(1): 9pp. https://folk.uio.no/ohammer/past/. Accessed 30 January, 2018.

James, D.E. 2012. Culturing Algae. 2nd ed. Carolina Biological Supply Company, Burlington, North Carolina, USA, 28 pp.

Jha, D., V. Jain, B. Sharma, A. Kant and V. K. Garlapati. 2017. Microalgae-based pharmaceuticals and nutraceuticals: an emerging field with immense market potential. ChemBioEng Reviews, 4(4): 257–272.

Jolliffe, I.T. and J. Cadima. 2016. Principal component analysis: a review and recent developments. Phil. Trans. R. Soc. A, 374:20150202.

Kumar, K., C.N. Dasgupta, B. Nayak, P. Lindblad and D. Das. 2011. Development of suitable photobioreactors for CO_2 sequestration addressing global warming using green microalgae and cyanobacteria. Bioresour. Technol., 102:4945–4953.

Lackner K.S, S. Brennan, J.M. Matter, A.-H.A. Park, A. Wright and B. van der Zwaan. 2012. The urgency of the development of CO_2 capture from ambient air. PNAS, 109(33):13156–13162.

Lambert, S. and M. Wagner. 2017. Environmental performance of bio-based and biodegradable plastics: the road ahead. Chem. Soc. Rev., 46(22):6855–6871.

Lau, P.S., N.F.Y. Tam and Y.S. Wong. 1995. Effect of algal density on nutrient removal from primary settled wastewater. Environ. Pollut., 89:59–66.

Molina-Grima, E., J. Fernández, G. Acién Fernández and Y. Chisti. 2001. Tubular photobioreactor design for microalgae cultures. J. Biotechnol., 92:113–131.

Mondal, M., S. Goswami, A. Ghosh, G. Oinam, O.N. Tiwari, P. Das and G. N. Halder. 2017. Production of biodiesel from microalgae through biological carbon capture: a review. 3 Biotech., 7:99.

Obersteiner, M., Ch. Azar, P. Kauppi, K. Möllersten, J. Moreira, S. Nilsson, P. Read, K. Riahi, B. Schlamadinger, Y. Yamagata, J. Yan and J.-P. van Ypersele. 2001. Managing climate risk. Science, 294 (5543):786–787.

Otim, O., T. Juma and R. Savinelli. 2018. The effect of a massive wastewater discharge on nearshore ocean chemistry. Environ. Monit. Assess., 190:180.

Raven, J.A. 2017. The possible roles of microalgae in restricting the increase in atmospheric CO_2 and global temperature. Eur. J. Phycol., 52:506–522.

Rey, M., I.S. Chizhmakova, A.V. Nikitin and V.G. Tyuterev. 2018. Understanding global infrared opacity and hot bands of greenhouse molecules with low vibrational modes from first-principles calculations: the case of CF_4. Phys. Chem. Chem. Phys., 20:21008–21033.

Ruiz, J., G. Olivieri, J.H. de Vree, R. Bosma, P. Willems, J.H. Reith, M.H.M. Eppink, D.M.M. Kleinegris, R.H. Wijffels and M.J. Barbosa. 2016. Towards industrial products from microalgae. Energy Environ. Sci., 9(10):3036–3043.

Safi, C., B. Zebib, O. Merah, P.Y. Pontalier and C. Vaca-Garcia. 2014. Morphology, composition, production, processing and applications of *Chlorella vulgaris*: A review. Renew. Sust. Energ. Rev., 35: 265–278.

Sayre, R. 2010. Microalgae: the potential for carbon capture. BioScience, 60:722–727.

Shaffer, G. 2010. Long-term effectiveness and consequences of carbon dioxide sequestration. Nat. Geosci., 3: 464–467. https://doi.org/10.1038/NGEO896.

Schindler, D.W. 2006. Recent advances in the understanding and management of eutrophication. Limnol. Oceanogr., 51:356–363.

Shi, J., P.K. Pandey, A.K. Franz, H. Deng, and R. Jeannotte. 2016. *Chlorella vulgaris* production enhancement with supplementation of synthetic medium in dairy manure wastewater. AMB Express, 6:15.

Stolz, P. and B. Obermayer. 2005. Manufacturing microalgae for skin care. Cosmetics Toiletries, 120: 99–106.

Uysal, O., F.O. Uysal and K. Ekinci. 2015. Evaluation of microalgae as microbial fertilizer. Eur. J. Sustain. Dev., 4:77–82.

Wang, L., M. Min, Y. Li, P. Chen, Y. Chen, Y. Liu, Y. Wang and R. Ruan. 2010. Cultivation of green microalgae *Chlorella* sp. in different wastewaters from municipal wastewater treatment plant. Appl. Biochem. Biotechnol., 162:1174–1186.

Wurzbacher, J.A., C. Gebald, N. Piatkowski and A. Steinfeld. 2012. Concurrent separation of CO_2 and H_2O from air by a temperature-vacuum swing adsorption/desorption cycle. Environ. Sci. Technol., 46:9191–9198.

Xu, H., X. Miao and Q. Wu. 2006. High quality biodiesel production from a microalga *Chlorella protothecoides* by heterotrophic growth in fermenters. J. Biotechnol., 126:499–507.

Yaakob, Z., E. Ali, A. Zainal, M. Mohamad and M. S. Takriff. 2014. An overview: biomolecules from microalgae for animal feed and aquaculture. J. Biol. Res. (Thessalon), 21(1):6.

Bull. Southern California Acad. Sci.
118(1), 2019, pp. 58–70

An Ecological Niche Model to Predict Range Expansion of the Eastern Gray Squirrel in California

Carly M. Creley,[1]* Fraser M. Shilling,[2] and Alan E. Muchlinski[3]

[1] *Department of Geosciences and Environment, California State University, Los Angeles, Los Angeles, CA 90032*
[2] *Department of Environmental Science and Policy, University of California, Davis, Davis, CA 95616*
[3] *Department of Biological Sciences, California State University, Los Angeles, Los Angeles, CA 90032*

Abstract.—The eastern gray squirrel, *Sciurus carolinensis* (EGS) has been introduced to California and has expanded its geographic range since initial introductions. In this study we projected the potential future geographic range of the EGS in California using Maxent to create an ecological niche model. Location data were obtained over the time period of 2004–2015 from museum specimens, wildlife rehabilitation centers, the California Department of Public Health, the California Roadkill Observation System, and non-iNaturalist citizen science observations. Research grade data from iNaturalist was obtained over the time period of 2004–2018. Range and habitat suitability maps were developed by mapping in ArcGIS. Three threshold selection methods were used to create different estimates of the potential future range of the EGS in California. The first method used the 10th percentile logistic threshold, the second used the minimum training presence logistic threshold, and the third used Jenks Natural Breaks. We propose that Jenks Natural Breaks has distinct advantages over the other two methods for estimating the potential future range of the introduced EGS in California, because it provides information on the habitat suitability ranking throughout California, whereas the other methods only provide a binary suitable/unsuitable map.

The objective of this study was to develop an ecological niche model (ENM) with an appropriate threshold value that could best identify potential range expansion of the invasive eastern gray squirrel, *Sciurus carolinensis* (EGS) within California and in the future, project potential areas of overlap with congeners. The EGS is native to the deciduous forests of the eastern United States (Koprowski 1994). The species was introduced to California in 1939 at Stanford University and in 1943 at Golden Gate Park in San Francisco, but it may have been introduced earlier by settlers who frequently introduced species from their homes in the eastern United States (Byrne 1979). Populations of the EGS currently exist in developed and forested areas of California. They are currently widespread throughout central California, with concentrations around Sacramento, both peninsulas of San Francisco Bay, and San Jose, and smaller populations in the Central Valley. Additionally, populations are spreading from Santa Cruz into the Santa Cruz Mountains and Monterey Peninsula (Creley and Muchlinski 2017).

Sciurus carolinensis carolinensis is most likely the major subspecies present in California, as determined by the coat color and physical characteristics of observed squirrels.

---

* Corresponding Author: carlycreley@gmail.com

S. c. carolinensis has a gray dorsum with a cinnamon wash sometimes present on the dorsum and hips. The tail is the same shade of gray, with a light white frosting on the tips of the hairs. A white eye ring is usually visible (Thorington et al. 2012). Some EGSs in California are melanistic, a common trait in the northern portion of the native range (Thorington et al. 2012). The EGS has a broad diet (Bertolino 2008), can establish a population from a small number of founders (Wood et al. 2007), can survive and reproduce in urban, suburban, or natural habitats, and has a favorable public perception (Bertolino and Genovesi 2003), which all contribute to its invasive success. The species has been introduced to the western United States, Europe, Africa, and Australia (Bertolino 2008; Benson 2013; Bertolino and Lurz 2013; Bertolino et al. 2014). Populations have been associated with negative ecosystem effects, the decline of native species, and damage to forests in the United Kingdom, Ireland, Italy, and parts of western North America (Gurnell et al. 2004; Bertolino 2008; Benson 2013; Bertolino and Lurz 2013).

The original native range of the EGS consists of mature, continuous woodlands over 40 ha in size, with diverse woody understories and tree species such as oak (*Quercus*), hickory (*Carya*), and walnut (*Juglans*) (Koprowski 1994). However, EGSs can also live in urban and suburban environments, even with relatively few mature trees (Thorington et al. 2012). EGSs move primarily along river corridors, secondarily on roads/right-of-ways, and thirdly on tracks/paths (Stevenson et al., 2013). Their ability to live in developed environments may significantly increase their dispersal capability.

In order to understand the future potential distribution of the EGS, it is critical to model their potential landscape and ecological niche occupancy. Creley and Muchlinski (2017) mapped the species distribution within California as of 2015, but ENMs had not been made. The methodologies for creating ENMs for invasive species are not well established (Aguierre-Gutierrez et al. 2013; Uden et al. 2015). It was important to map a range of suitable habitat estimates in order to prevent drawing conclusions from one arbitrary threshold, as cautioned against by Merow et al. (2013). Standard thresholds that have been used in previous studies to produce ENMs include the 10^{th} percentile logistic threshold (Belarmain Fandohan et al. 2015; Chalghaf et al. 2016; Sage et al. 2017), which could produce a very conservative estimate of potential future range for an invasive species, and the minimum training presence logistic threshold (Beane et al. 2013; Coudrat and Nekaris 2013; Botero-Delgadillo et al. 2015), which could produce an overestimate of potential future range. We used these two standard thresholds in the present study, as well as a third method - selecting a threshold value based on Jenks Natural Breaks (Jenks 1967). Previously, Colnar and Landis (2007) developed a regional risk assessment for the European green crab, *Carcinus maenas*, at Cherry Point, Washington, USA using Jenks Natural Breaks, and Schleier III and Sing (2008) used it to partition an overall risk score for the introduction of *Gabusia affinis* (western mosquitofish) into Montana watersheds. Beyond invasive species modeling, Jenks Natural Breaks have been used to classify groundwater into zones of vulnerability for nitrogen contamination in Florida's aquifers (Cui et al. 2016), to rank the susceptibility of locations to terrorist actions (Patterson and Apostolakis 2007), and to assess the risk of flooding in the Bengawan Solo River basin in Indonesia (Rahadianto et al. 2015).

The model used location and environmental data from the invaded range in California and the native range for *S. carolinensis* in the eastern United States, which encompasses a wider range of environmental conditions than those found within the current range in California, to estimate habitat suitability. Our methods may be applicable to further studies on invasive species modeling, for which methods of estimating the potential range, as

opposed to the current range, are limited and have not been consistently evaluated (Aguierre-Gutierrez et al. 2013; Uden et al. 2015).

Materials and Methods

We obtained presence only location data for 2004 to 2018. The model included 3,725 spatial location points of the EGS in California, as well as 8,988 points from across the native range in the eastern United States. We obtained presence points in California from iDigBio, the Global Biodiversity Information Facility (GBIF), Vertnet, wildlife rehabilitation centers, the California Department of Public Health's West Nile Virus Surveillance Program, the California Roadkill Observation System operated by the University of California, Davis (Waetjen and Shilling 2017), iNaturalist, and the authors. Location data from the native range of the EGS across the United States are from iNaturalist. We filtered the data to include only the native range of *S. carolinensis*, according to Koprowski (1994). We excluded regions from which the EGS is nonnative, and areas outside of the United States.

VertNet, a National Science Foundation funded project, makes museum-curated biodiversity-data free and available on the web, while the Global Biodiversity Information Facility provides open international data. The iNaturalist sightings were filtered to include only those that were open access and research grade, which include an observation date, photo, coordinates, and in which the species identification has been verified by at least one other user. Records in biodiversity databases are constantly changed and updated, so all data from iDigBio, GBIF, and Vertnet were obtained on 31 August 2015. Records from iNaturalist were obtained on 12 October 2018. Some redundancy may exist between the databases, but Maxent automatically removes replicates, so these duplicate observations did not change the projections.

Since all sources are likely to include some misidentifications of related species identified as EGS, reports from outside of the previously published range were scrutinized for accuracy. Field surveys were conducted in regions that had not been included in prior range maps but that had numerous reports, including the Santa Cruz Mountains, the Central Valley, and southern California. Records that could not be corroborated were expunged. In the case of the California Roadkill Observation System data, 82% of EGS with images were correctly identified. The remainders were misidentified as California ground squirrel, Douglas squirrel, or western gray squirrel (WGS).

Data used in this manuscript are available for use by others under a Creative Commons By Attribution Non-Commercial 4.0 International License. Observations obtained through iNaturalist are utilized under a Creative Commons By Attribution Non-Commercial License or from observations that are in the Public Domain. The names of GBIF and iNaturalist contributors can be obtained through a search of the California location data using the data posted at doi: 10.13140/RG.2.2.24275.84004 and the native range of the United States data at doi: 10.13140/RG.2.2.17564.95360.

We converted location data into geographic coordinates with Google Maps. We spatially rarefied the data to one point per 51.8 ha (0.25 mi^2) using the Spatially Rarefy tool in the SDM toolbox (Brown 2014) in order to eliminate spatial clusters that could cause the model to be overfit to the environmental biases of those points (Boria et al. 2014). The rarefied presence data were reduced from 12,713 to 5,627 points. Since the predictive accuracy of the maps and the ability of the models to project presence data was more important than identifying the tolerance ranges of the species, we did not remove highly correlated variables (Merow et al. 2013).

For the environmental background we used the bio 1 through bio 19 variables from BIOCLIM1 remote sensing data (Hijmans et al. 2005), which include quarterly and annual temperature and precipitation trends, with other annual environmental trends. Additionally, we used monthly precipitation, monthly maximum temperature, monthly minimum temperature, altitude, impervious surface, land cover, and tree canopy from the United States Geological Survey (USGS 2016). The full list of biotic and abiotic factors used in our model is available at doi: 10.13140/RG.2.2.15802.70085. We paired the location presence data with environmental background data throughout the contiguous United States. The model can predict habitat suitability for areas that the species is equally likely to reach (Merow et al. 2013). The environmental background data covers all reasonable possible distributions (Saupe et al. 2012).

We selected Maxent to create the ENM because of its high performance at estimating local occurrences with small to medium sample sizes (Elith et al. 2006; Aguierre-Gutiérrez et al. 2013; Ng and Jorda, 2001). In order to allow the model to reach the default 0.00001 convergence level, we allowed a maximum of 5,000 iterations (Young et al. 2011), set the regularization parameter to the default value of one in order to reduce overfitting (Merow et al. 2013), and created 15 replicates for the model using subsampling (Young et al. 2011). We set aside 25% of the data for testing, and used 75% for training the model. We used the random seed option in order to increase the randomness of the runs (Jobe and Zank 2006; Young et al. 2011). We adjusted the sample radius to -100, and did not extrapolate. The logistic output using the default τ value of 0.5 was selected because the actual probability of the EGS being present in suitable habitat is unknown.

We produced habitat suitability maps by importing the rasters for the average of the fifteen replicates for each model into ESRI's ArcMap 10.3.1 (ArcGIS® 10.3.1; Esri software) using the NAD 1983 California (Teale) Albers (Meters) projected coordinate system and the GCS North American 1983 (NAD1983) datum. When coordinates were provided without a datum, they were assumed to be in NAD83. Each pixel encompasses approximately 720 square meters. We clipped the output rasters to the shape of California, using the United States Census Bureau's Tiger/Line 2010 (United States Census Bureau 2010). We used topographic and political basemap layers from ESRI.

We used three thresholds to create potential range estimates. The first estimate of the potential range was established by using the 10th percentile training presence logistic threshold, which set the threshold at the level where 90 percent of the presence points were in raster squares with at least the threshold score. We created a second estimate of the potential range using the minimum training presence logistic threshold, which is set at the level of the lowest scoring occupied square. We manually classified the resulting raster of California for the first two thresholds by setting the upper bound of the unsuitable habitat class at the threshold level for each map, as indicated in the Results table created by Maxent.

Third, we used Jenks Natural Breaks to group the resulting raster into five classes based on natural breaks in the data. The approach grouped the relative habitat suitability ranking of each raster square (Rahadianto et al. 2015) by similar values and maximized the difference between the classes (ESRI 2016). We created 5 habitat categories (HC) from the groupings of data. HC1 represents where the species is now found and adjacent highly suitable habitat, HC2, HC3, and HC4 represent decreasingly suitable, but still suitable habitat, while HC5 represents unsuitable habitat. Therefore, the threshold for suitable habitat was set at the lowest relative habitat suitability ranking score of HC4.

Results

The high value of the Test Area Under the Curve (AUC) of the Receiver Operating Characteristic (ROC) Plot (0.8272 on a scale of 0.5 = random association of data to model, to 1.0 = perfect association of data to the model) and Training AUC (0.828) indicate an excellent fit of the data to the model produced by Maxent. The plot is available at doi: 10.13140/RG.2.2.12531.78883. However, since the ROC Plot is constructed from all possible threshold values and the plot does not yield information about any specific threshold value, the selection of a biologically meaningful threshold value for graphing results of the model is critical for obtaining the most accurate map of potential future range.

Three different threshold values were used for the range of suitable to unsuitable habitat found using the ENM for the EGS in California. Use of the 10^{th} percentile logistic threshold (Fig. 1) produced the most limited estimate of potential future range. In the binary map, suitable habitat scored above the threshold value of 0.3051 (Table 1). The potential range produced using this threshold value is very similar to the current range of the species in northern and central California as of 2018. Therefore, the time frame of projected range expansion is very limited. EGSs currently exist outside of habitat that is predicted suitable through use of this threshold, as the method excludes the 10 percent of observation locations with the lowest relative scores in order to produce the threshold value. EGSs are currently found outside of projected suitable habitat near Salinas, Tracy, Modesto, and east and south of Sacramento along the Sierra Nevada foothills from north of the American River to Columbia.

Use of the minimum training presence logistic threshold (Fig. 2) also produced a binary output map, but in this case the logistic threshold value was reduced to 0.0299 (Table 1). A very large increase in projected suitable habitat for the EGS in California results from the reduction in threshold value. The potential range using this threshold value includes most of the state, with the exception of the Mojave Desert, the very north-central and northeast portion of the state, the higher elevations of the Sierra Nevada Mountain Range, and a southern portion of the San Joaquin Valley.

The Jenks Natural Breaks method produced a binary map with suitable habitat above the threshold of 0.0530, but the specificity of information within the suitable habitat category was much greater than in either of the previous two methods (Tables 1, 2). In the map classified using Jenks Natural Breaks (Fig. 3), the two highest relative habitat category rankings (HC1 and HC2) are centered on the San Francisco Bay area, south through the Santa Cruz Mountains to habitats on the Monterey Bay Peninsula, east through Sacramento into the foothills of the Sierra Nevada Mountains, and along the southern California coasts. Concentric areas of decreasingly suitable habitat (HC3 and HC4) surround the most suitable areas and continue south along most of coastal California and the coastal/inland mountain ranges to the border with Mexico. HC3 and HC4 are also found along river corridors exiting the Sierra Nevada Mountains. Unsuitable habitats (HC5) are in and east of the Sierra Nevada Mountains, the northern Cascade Range, a major portion of the San Joaquin Valley south of Sacramento, and the deserts of southern California.

Discussion

Our results indicate that the method for selecting a threshold value to establish a break between suitable and unsuitable habitat with Maxent is an especially critical issue for an introduced species which is expanding its geographic range. We have shown that a high AUC value by itself is not sufficient to support the predictive accuracy of a single map based

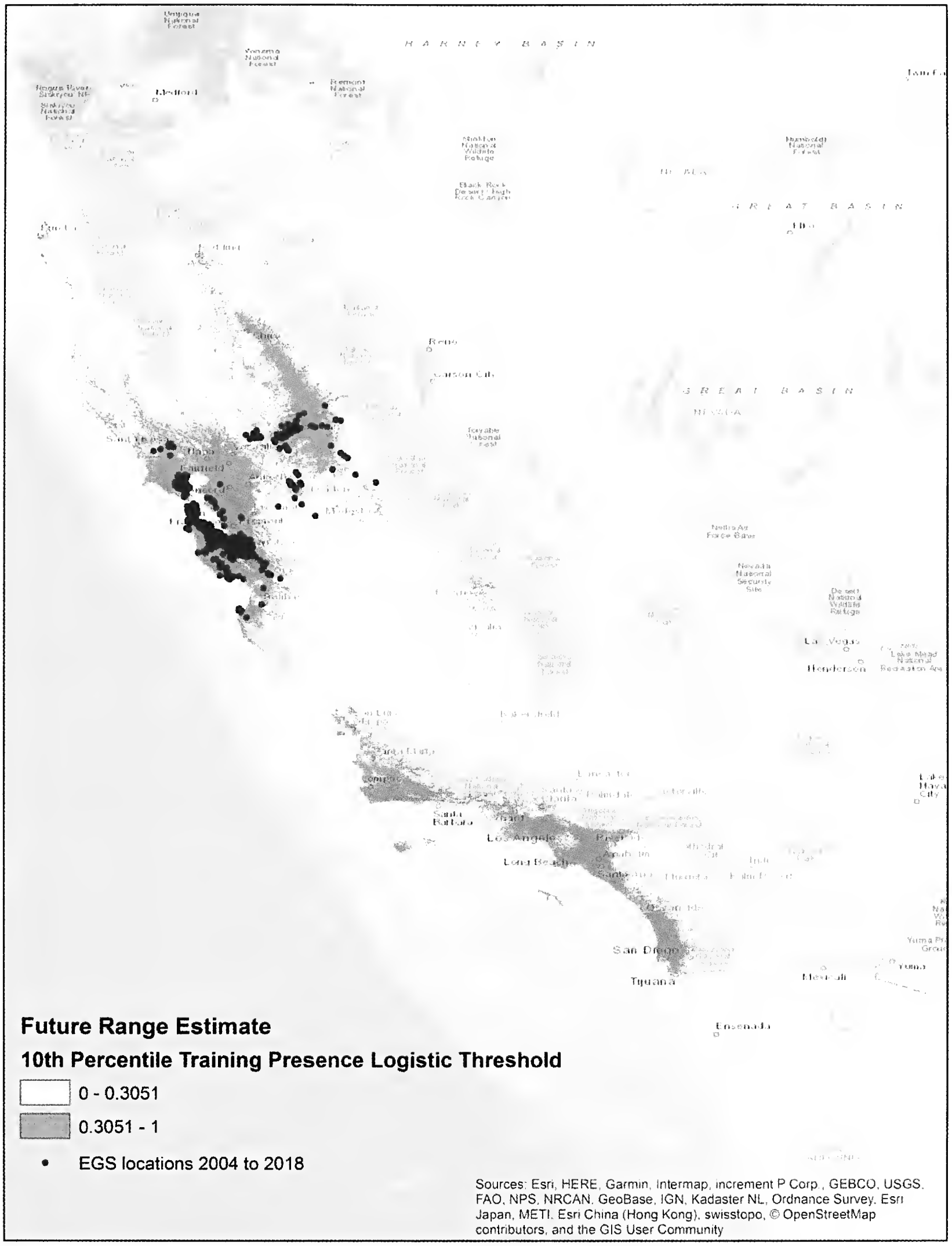

Fig. 1. Estimate of suitable habitat predicted by the model using the 10th percentile training presence logistic threshold based upon eastern gray squirrel locations from 2004 to 2018.

upon a single arbitrarily selected threshold value. AUC is not a perfect, objective measure of the predictive power of the model, but few alternatives are available for presence only data (Merow et al. 2013). The commonly used 10th percentile training presence logistic threshold as well as the minimum training presence logistic threshold are clearly arbitrary values with little biological basis for selection. And, as shown by the maps presented in this

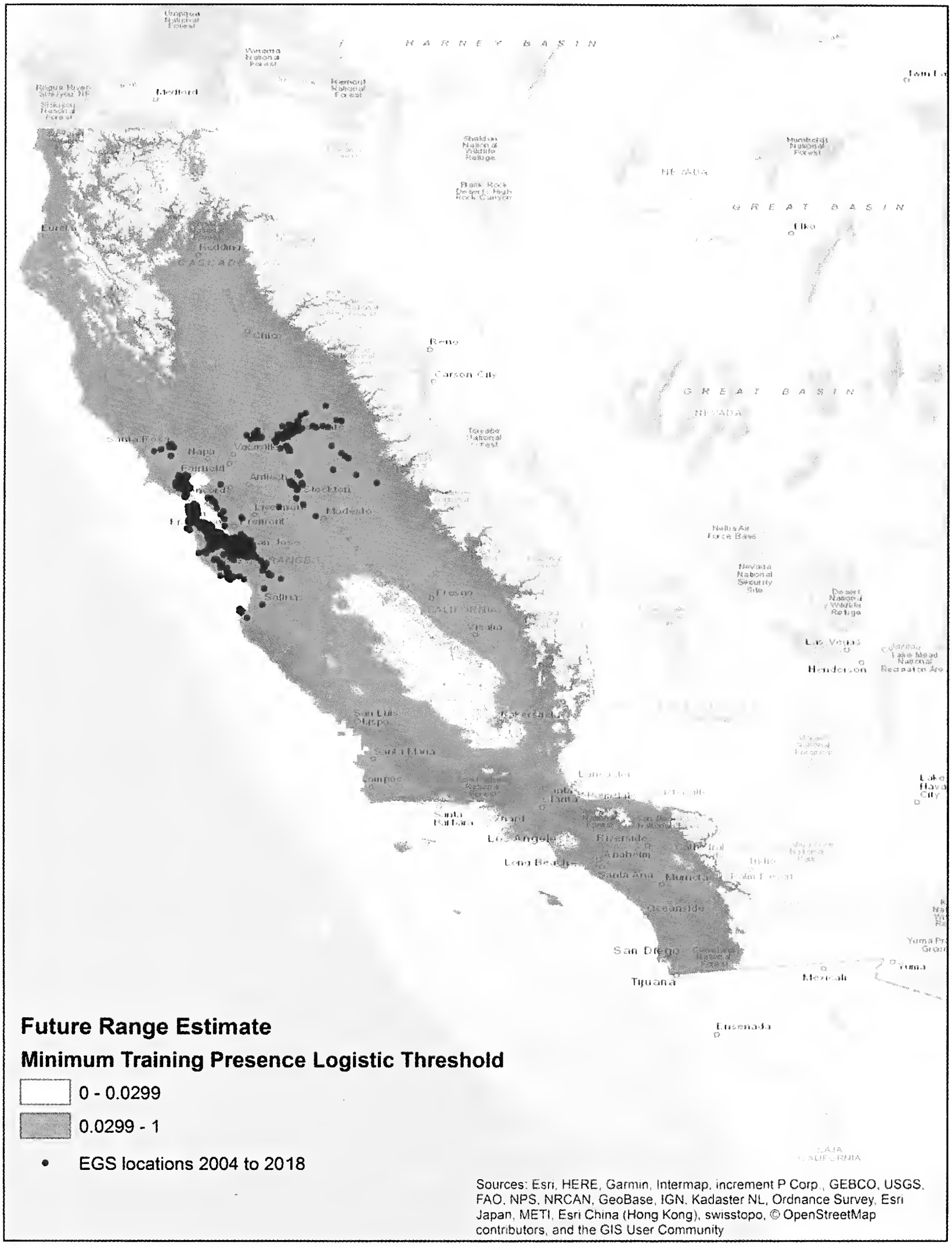

Fig. 2. Estimate of suitable habitat predicted by the model using the minimum training presence logistic threshold based upon eastern gray squirrel locations from 2004 to 2018.

paper, these thresholds produce vastly different projections of suitable habitat. The use of Jenks Breaks to establish a threshold value is based upon the natural clustering of values in the logistic output of the model and hence should be less arbitrary, and more meaningful, in terms of the biology of the species being studied. This method also provides graded

Table 1. Threshold breakpoints.

Class	10th percentile training presence logistic threshold	Minimum training presence logistic threshold	Jenks Natural Breaks
Suitable	0.3051 - 1	.0299-1	0.0530 - 1
Unsuitable	0 - 0.3051	0-0.0299	0 - 0.0530

"likelihoods" of predicted occupancy, which may be more easily tested in the future with new occupancy records.

The 10th percentile training presence logistic threshold provided the most conservative estimate of the potential range by assuming that some of the presence data may be misidentified, improperly reported, or outside of the area in which the EGS can persist, and then removing those points (Young et al. 2011; Uden et al. 2015). The map is inherently skewed toward the realized niche of the EGS in California, as the species has only been introduced to a few locations within the state. It is closely aligned with the original data set and may be biased toward human accessible areas. The threshold may be too conservative, as the EGS is still spreading, and is likely to tolerate habitat with conditions at least as extreme as those in the current range in California. The EGS already inhabits areas outside of the region projected as suitable in this map.

The map created with the minimum training presence logistic threshold reflects a much broader range of conditions throughout California and is our least conservative estimate of the future range. However, use of this threshold value most likely over-predicts the potential range because the inclusion of a single erroneous location point within the data could greatly affect the map. The map using this lower threshold provides an accurate estimate of potential range only if it is absolutely certain that all location data have been correctly identified as EGSs, and all individuals and populations currently exist in suitable habitat. While it is highly likely that the EGS will expand its range to include some of the areas mapped by this method, it is highly unlikely that the species will inhabit all of the area. If the EGS is introduced to or expands it range to new areas and survives, the distribution is likely to more closely resemble the maximum estimate map than the minimum estimate using the 10th percentile logistic threshold.

The map created with Jenks Natural Breaks provides the most useful, detailed classification of the relative habitat suitability rankings, and therefore the risk of invasion to various parts of California. We assume that the lowest ranking habitat, HC5, is unsuitable based upon the lowest grouping of values (0.000 to 0.0530), whereas each higher rank represents increasingly suitable habitat. As the EGS continues to spread, the habitat suitability ranking may increase in areas with habitat similar to newly invaded areas and therefore we cannot say that this map is a permanent ranking of habitat suitability. For example, areas

Table 2. Habitat classes created with Jenks Natural Breaks.

Habitat class	Relative habitat suitability ranking
1	0.4627 - 0.7515
2	0.2917 - 0.4627
3	0.1562 - 0.2917
4	0.0530 - 0.1562
5	0 - 0.0530

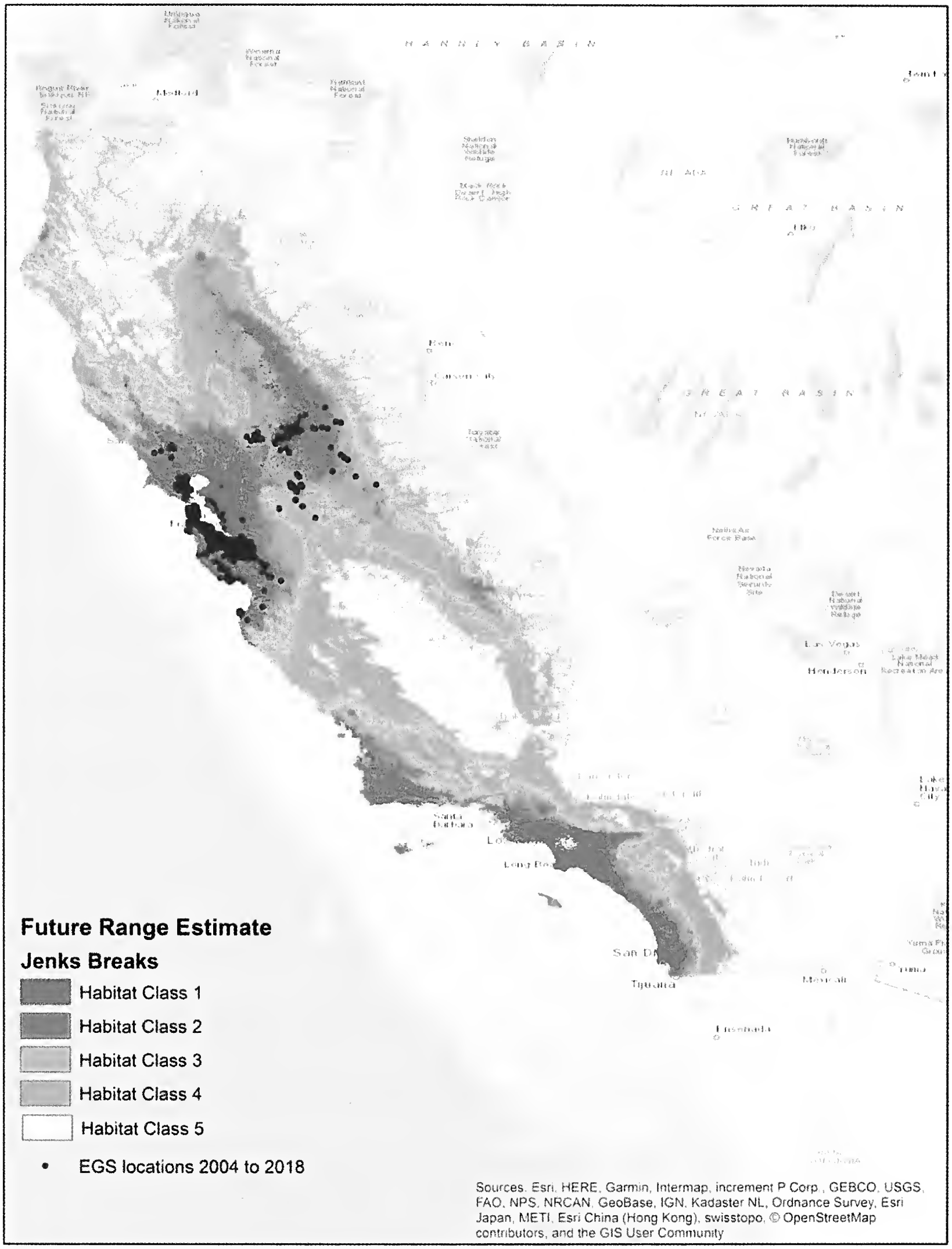

Fig. 3. Estimate of suitable habitat predited by the model using Jenks Natural Breaks, with five habitat classes (HC), based upon eastern gray squirrel locations from 2004 to 2018. HC1 represents the most suitable habitat. HC2-HC4 represent decreasingly suitable habitat, and HC5 is considered unsuitable habitat.

now ranked as HC3 could in the future be ranked as HC2 if many populations of EGSs become established within HC3. We believe that setting the threshold for suitable habitat above HC5 created the most reasonable estimate of the potential future range by including a broader range of habitat than the minimum estimate, but excluding the most extreme

desert, mountain, and Central Valley habitats of the maximum estimate. The Jenks Natural Breaks map is, at this time, our most reasonable estimate of the future range of the EGS in California.

We selected Maxent to create the ENM because of its high performance at estimating local occurrences. Absence data were not available or informative, so a presence-absence experiment could not be done (Yackulic et al. 2012). Additionally, presence only data may be better than presence-absence data for estimating fundamental niches because invasive species have not yet inhabited their full potential range (Jiménez-Valverde et al. 2008). For presence only data, machine learning methods such as Maxent consistently outperformed earlier methods, such as Bioclim or regression models in predictive success (Elith et al. 2006). It is especially good for small and medium data sets because the generative learning method uses an algorithm to build a model, as opposed to a discriminative model that estimates the value of one categorical variable based on the other (Ng and Jordan 2001; Aguierre-Gutiérrez et al. 2013).

Location data were limited to 2004–2018 because habitat loss has been extensive in California over the past century, to ensure the use of current species distributions, and because satellite collection for BIOCLIM only started in 1972 (United States Geologic Survey [USGS] 2015). Overall, 2,825 of the 3,725 EGS records in California, 75.84%, were obtained from wildlife rehabilitation records. Records indicated the location that the person submitting the squirrel reported finding it. Rehabilitation facilities are very likely to accurately identify the species, but may cause geographic bias toward the residential areas surrounding each center. Citizen science data offers the benefit of having broad sources, but may be skewed toward urbanized areas, roads, or other easily studied sites (Baldwin 2009). The data are not random, but rarefaction has been used to equalize the sampling effort among areas, which allowed us to make a reasonable inference of the species distribution (Yackulic et al. 2012). The assumption that detection probability is constant across sites need not be met because citizen science and historic records simulate repeat-visits to each site (Yackulic et al. 2012).

The higher elevations of the Sierra Nevada were classified as unsuitable using all thresholds, but elevation may have been the only factor causing the unsuitable classification, as the highest point in the native range of *S. carolinensis* is at 6,643 feet, at Clingman's Dome in Tennessee, which is the highest point in the state and the Smoky Mountains. Elevation alone may not actually exclude the EGS. The species' invasive ability worldwide, especially into areas with Mediterranean climates, such as South Africa and Italy (Gurnell et al. 2004; Bertolino 2008; Benson 2013; Bertolino and Lurz 2013) suggests that it could acclimate to conditions in much of California.

Finally, with future studies the potential invasion by the EGS into occupied and unoccupied eastern fox squirrel (EFS) or WGS habitat is an excellent test case for several hypotheses regarding invasion ecology. These hypotheses include, 1) "biotic resistance", which suggests that high-biodiversity ecosystems are more resistant to invasion than low-diversity ecosystems; 2) "enemy release", which posits that the absence of enemies (i.e., competitors and predators) increases the likelihood of invasion; and 3) "propagule pressure/introduction effort", which proposes that the introduced population size and the frequency of introduction can contribute to successful invasion (Jeschke 2014). The first hypothesis could be tested with the EFS by comparing the rate and success of invasion from neighboring areas of low and high-biodiversity systems (e.g., oak woodlands in the Sierra Nevada mountain foothills). The second hypothesis could be tested by comparing EGS invasion and persistence success with the presence of competitors (e.g., EFS or WGS)

and predators, such as hawks and owls. Because the EGS tolerates urban and suburban areas, predators may be less prevalent in areas where they have succeeded. The third hypothesis could be tested using a combination of estimates (e.g., from historical accounts) or measurements (e.g., for newly-discovered populations) of founder population size and continued introduction (e.g., from connected populations) and reproductive rate to predict expansion and persistence. There is already some evidence that the EGS may be replacing the EFS on the western side of the San Francisco Bay (Creley and Muchlinski 2017) so assessing potential causal factors for replacement is important. Finally, the model uses current environmental conditions, and could be adapted to include estimates for changes in climate, which may reduce the amount of suitable habit, shift it to higher elevations, or render hotter and more extreme areas of currently suitable habitat unsuitable in the future.

Literature Cited

Aguirre-Gutiérrez, J., L.G. Carvalherio, C. Polce, E.E. van Loon, N. Raes, M. Reemer and J.C. Biesmeijer. 2013. Fit-for-purpose: Species distribution model performance depends on evaluation criteria – Dutch hoverflies as a case study. PLOS One, 8(5):1–11.

Baldwin, R.A. 2009. Use of maximum entropy modeling in wildlife research. Entropy, 11:854–866.

Beane, N.R., J.S. Rentch and T.M. Schuler. 2013. Using maximum entropy modeling to identify and prioritize red spruce forest habitat in West Virginia. U.S.F.S., Newtown Square, PA.

Belarmain Fandohan, A., A.M.O. Oduor, A. Idelphonse Sode, L. Wu, A. Cuni Sanchez, E. Assede and G.N. Gouwakinnou. 2015. Modeling vulnerability of protected areas to invasion by *Chromolaena odorata* under current and future climates. Ecosystem Health and Sustainability, 1(6):1–12.

Benson, E. 2013. The urbanization of the eastern gray squirrel in the United States. J. Am. Hist., 100(3):691–710.

Bertolino, S. and P.W.W. Lurz. 2013. Callosciurus squirrels: Worldwide introductions, ecological impacts and recommendations to prevent the establishment of new invasive populations. Mammal Rev., 43(1):22–23.

Bertolino, S., N.C. di Montezemolo, D.G. Preatoni, L.A. Wauters and A. Marinoli. 2014. A grey future for Europe: *Sciurus carolinensis* is replacing native red squirrels in Italy. Biol. Invasions, 16(1):53–62.

Bertolino, S. 2008. Introduction of the American grey squirrel (*Sciurus carolinensis*) in Europe: A case study in biological invasion. Curr. Sci., 95(7):903–906.

Bertolino, S. and P. Genovesi. 2003. Spread and attempted eradication of the grey squirrel (*Sciurus carolinensis*) in Italy, and consequences for the red squirrel (*Sciurus vulgaris*) in Eurasia. Biol. Cons., 109(3):351–358.

Boria, R., L. Olson, S. Goodman and R. Anderson. 2014. Spatial filtering to reduce sampling bias can improve the performance of ecological niche models. Ecol. Model., 275:73–77.

Bortero-Delgadillo, E., N.J. Bayly, S. Escudero-Paez and M.I. Moreno. 2015.

Understanding the distribution of a threatened bird at multiple levels: A hierarchical analysis of the ecological niche of the Santa Marta Bush-tyrant (*Myiotheretes pernix*). Condor, 117(4):629–643 DOI 10.1650/CONDOR-15-26.1.

Brown, J.L. 2014. SDMtoolbox: A python-based GIS toolkit for landscape genetic, biogeographic and species distribution model analyses. Methods Ecol. Evol., 5:694–700.

Byrne, S. 1979. The distribution and ecology of the non-native tree squirrels *Sciurus carolinensis* and *Sciurus niger* in Northern California. Ph.D. Dissertation, University of California, Berkeley.

Chalghaf, B., S. Chlif, B. Mayala, W. Ghawar, J. Bettaieb, M. Harrabi, G.B. Bertin, E. Michael and A.B. Salah. 2016. Ecological niche modeling for the prediction of the geographic distribution of *Cutaneous leishmaniasis* in Tunisia. Am. J. Trop. Med. Hyg., 94(4):844–851.

Colnar, A.M. and W.G. Landis. 2007. Conceptual model development for invasive species and a regional risk assessment case study: The European green crab, Carcinus maenas, at Cherry Point, Washington, USA. Hum. Ecol. Risk Assess., 13(1):120–155.

Coudrat, C.N.Z. and A.I. Nekaris. 2013. Modeling niche differentiation of coexisting, elusive and morphologically similar species: A case study of four macaque species in Nakai-Nam Theun national protected area, Laos. Animals, 3(1):45–62.

Creley, C.M. and A.E. Muchlinski. 2017. Distribution of the eastern gray squirrel (*Sciurus carolinensis*) within California as of 2015. Bull. South. Calif. Acad. Sci., 116(3):204–213.

Cui C, W. Zhou and M. Geza. 2016. GIS-based nitrogen removal model for Assessing Florida's surficial aquifer vulnerability. Environ. Earth Sci., 75:1–15.

Elith, J., C. Graham, R. Anderson, M. Dudik, S. Ferrier, A. Guisan, R. Hijmans, F. Huettmann, J. Leathwick, A. Lehmann, J. Li, L. Lohmann, B. Loiselle, G. Manion, C. Moritz, M. Nakamura, Y. Nakazawa, J. Overton, A.T. Peterson, S. Phillips, K. Richardson, R. Scachetti-Pereira, R. Schapire, J. Soberon, S. Williams, M. Wisz and N. Zimmermann. 2006. Novel methods improve prediction of species' distributions from occurrence data. Ecography, 29(2):129–151.

[ESRI] Environmental Systems Research Institute. 2016. Classifying numerical fields for graduated symbology. ESRI, Redlands, California.

Gurnell, J., L.A. Wauters, P.W.W. Lurz and G. Tosi. 2004. Alien species and interspecific competition: Effects of introduced eastern grey squirrels on red squirrel population dynamics. J. Anim. Ecol., 73(1):26–35.

Hijmans, R.J., S.E. Cameron, J.L. Parra, P.G. Jones and A. Jarvis. 2005. Very high resolution interpolated climate surfaces for global land areas. In. J. Climatol., 25(15):1965–1978.

Jeschke, J. 2014. General hypotheses in invasion ecology. Divers. Distrib. 20:1229–1364.

Jenks, G.F. 1967. The data model concept in statistical mapping. International Yearbook of Cartography, 7:186–190.

Jiménez-Valverde, A., J.M. Lobo and J. Hortal. 2008. Not as good as they seem: The importance of concepts in species distribution modeling. Divers. Distrib., 14(6):885–890.

Jobe, R.T. and B. Zank. Modeling species distributions for the Great Smoky Mountains National Park using maxent. Department of the Interior, Draft Document – August 27, 2008. https://s3-us-west-2.amazonaws.com/oww-files-public/7/74/Jobe_2008_MaxEnt.pdf.

Koprowski J. 1994. *Sciurus carolinensis*. Mamm. Species, 480:1–9.

Merow, C., M.J. Smith and J.A.J. Silander. 2013. A practical guide to MaxEnt for modeling species' distributions: What it does, and why inputs and settings matter. Ecography, 36:1058–1069.

Ng, A.Y. and M.I. Jordan. 2001. On discriminative vs. generative classifiers: A comparison of logistic regression and naive bayes. NeurIPS, 14.

Patterson S.A. and G.E. Apostolakis. 2007. Identification of critical locations across multiple infrastructures for terrorist actions. Reliab. Eng. Syst. Safe., 92(2):1183–1203.

Rahadianto H., A. Fariza and J. Akhmad Nur Hasim. 2015. Risk-level assessment system on Bengawan Solo river basin flood prone areas using analytic hierarchy process and natural breaks: Study case: East Java, Yogyakarta, Indonesia. ICoDSE, 2015, Red Hood, New York.

Sage K.M., T.L. Johnson, M.B. Teglas, N.C. Nieto and T.G. Schwan. 2017. Ecological niche modeling and distribution of *Ornithodoros hermsi* associated with tick-borne relapsing fever in western North America. PLOS Negl. Trop. Dis., 11(10):e0006047.

Saupe, E.E., V. Barve, C.E. Myers, L. Soberón, N. Barve, C.M. Hensz, A.T. Peterson, H.L. Owens and A. Lira-Noriega. 2012. Variation in niche and distribution model performance: The need for a priori assessment of key causal factors. Ecol. Model., 237-238:11–22.

Schleier III, J.J. and S.E. Sing. 2008. Regional ecological risk assessment for the introduction of *Gambusia affinis* (western mosquitofish) into Montana watersheds. Biol. Invasions, 10(8):1277–1287.

Stevenson, C., M. Ferryman, O. Nevin, A. Ramsey, S. Bailey and K. Watts. 2013. Using GPS telemetry to validate least-cost modeling of gray squirrel (*Sciurus carolinensis*) movement within a fragmented landscape. Ecol. Evol., 3(7):2350–2361.

Thorington, R., J. Koprowski, M. Steele and J. Whatton. 2012. Squirrels of the World. Baltimore, Maryland: Johns Hopkins University Press.

Uden, D.R., C.R. Allen, D.G. Angeler, L. Corral and K.A. Fricke. 2015. Adaptive invasive species distribution models: A framework for modeling incipient invasions. Biol. Invasions, 17(10):2831–2850.

United States Census Bureau. 2010. Tiger/Line 2010 shapefile: State of California counties [USGS] United States Geological Survey. 2016. USGS products Landsat data, http://glovis.usgs.gov/.

[USGS] United States Geological Survey. 2015. Landsat—Earth observation satellites: U.S. geological survey fact sheet 2015–3081.

Waetjen, D.P. and F.M. Shilling. 2017. Large extent roadkill and wildlife observation systems as sources of reliable data. Front. Ecol. Evol., 5:89. doi: 10.3389/fevo.2017.00089.

Wood, D.J., J.L. Koprowski and P.W.W. Lurz. 2007. Tree squirrel introduction: A theoretical approach with population viability analysis. J. Mammal, 88(5):1271–1279.

Yackulic, C., R. Chandler, E. Zipkin, J.A. Royle, J. Nichols, E. Campbell Grant and S. Veran. 2012. Presence-only modeling using MAXENT: When can we trust the inferences?. Methods in Ecol. Evol., 4(3):236–243.

Young, N. and L. Carter, P. Evangelista. 2011. A MaxEnt model v3.3.3e tutorial (ArcGIS v10).

Bull. Southern California Acad. Sci.
118(1), 2019, pp. 71–75

The San Quintín Kangaroo Rat is Not Extinct

Scott Tremor,[1]* Sula Vanderplank,[1,2] and Eric Mellink[2]

[1]*San Diego Natural History Museum. P.O. Box 121390. San Diego, CA 92112*
[2]*Departamento de Biología de la Conservación, Centro de Investigación Científica y de Educación Superior de Ensenada, B.C., Carretera Ensenada-Tijuana # 3918, 22860 Ensenada, B.C., México*

The range of the San Quintín kangaroo rat (*Dipodomys gravipes*) is restricted, so far as known historically, to a stretch of coastal habitat less than 150 km in length and a few kilometers in width (Best and Lackey 1985) at the southern end of the California Floristic Province—a global biodiversity hotspot and one of the most critically endangered ecosystems on earth (Myers et al. 2000). This rodent was described in 1925 by Laurence M. Huey, who reported it from the coastal plains from San Telmo south to El Socorro and on the floodplain of the Arroyo El Rosario along the Pacific coast of northern Baja California, Mexico. The area between El Socorro and El Rosario is largely unsuitable.

Huey asserted that the "mother lode of this species is found near Mesa Agua Chiquita, with 1,000 individuals in 10 acres" (field notes archived at the San Diego Natural History Museum). He described the habitat in this area as hard [clay] soils covered with grasses. Little is known about the broader habitat requirements for *D. gravipes*, but it appears similar in its niche requirements to Stephen's Kangaroo rat *D. stephensi* which occupies areas with high disturbance, open conditions and weedy forbs (Tremor et al. 2017). Burrow entrances were closed but connected by visible runways up to 75 m long (Fig. 1). Previously, Nelson (1922) had written that in this area "the vegetation is so low and insignificant that the plain has the appearance of an open prairie". Both descriptions could refer to areas recovering from wheat cultivation years earlier, and the grasses could be non-native annual species (e.g., *Bromus* spp.).

Agriculture in the San Quintín area began in 1891 when British farmers converted parts of the landscape to wheat cultivation, built a dam for irrigation, and installed a flour mill (Taylor 1996). The settlement was abandoned in 1917 (Phelts-Ramos 2004). Subsequently, only four ranches persisted in the San Quintin Valley, until 1947, when Title 3050 (which granted agricultural lands to families from other regions of Mexico as a cession by the government) led to a massive expansion of agriculture in the valley (Ramírez-Velarde 2004). However, full expansion of agriculture in the area was restricted by the lack of roads allowing for export of produce from the area, until 1973 when the road connecting it with Ensenada was paved.

In 1972, before the building of the transpeninsular highway, "the broad open areas 8.5 miles N of San Quintín were dotted with *D. gravipes* burrows" (Best 1983). Eight years later this area was converted to cropland. In 1980, the population had shrunk, and Best trapped only two individuals in >1000 trap nights. Likewise, the area 9.6 km east of El Rosario, where he had collected 35 specimens in 1972, was in 1980 covered by the paved transpeninsular highway (Best 1983). The Arroyo del Rosario area still produced 7 specimens in 1989 (Troy L. Best *in litt.* to EM, 20 July 1989).

*Corresponding author: stremor@sdnhm.org

Fig. 1. *Dipodomys gravipes* habitat at Mesa Agua Chiquita. Note the long and visible runways. Photo by S. Vanderplank.

Dipodomys gravipes has a high affinity for flat terrain and is intolerant of cultivation. Between April 1989 and September 1990, Mellink surveyed all habitats where the species had been previously found, including coastal scrub, fallow fields, and river wash. Yet this effort totaling more than 800 trap-nights, spread over 12 cycles of trapping events within the historical range, failed to yield any kangaroo rats other than *D. simulans*. As a result of extensive and profound habitat alteration by agriculture, *D. gravipes* has been listed as endangered by the Mexican government since the publication of its first list of species at risk (Instituto Nacional de Ecología 1994). Since then, and given the lack of further captures, biologists and conservationists have feared the species could be extinct (Ceballos and Navarro, 1991; Mellink 1992[1], 1996[2]; Mellink and Luévano 2005).

---

[1] Mellink, E. 1992. Status de los heterómidos y cricétidos endémicos del estado de Baja California. Comunicaciones Académicas. CICESE. Ensenada, B. C. 10pp.

[2] Mellink, E. 1996. Problemas de conservación de la fauna silvestre en el estado de Baja California. Conferencia magistral. XIV Simposio sobre Fauna Silvestre. Facultad de Medicina Veterinaria y Zootécnia. Universidad Nacional Autónoma de México. México, D. F.

Fig. 2. *Dipodomys gravipes* from Mesa Agua Chiquita. Note the rear foot measurement of 46 mm and thin white lateral tail stripe. Photo by S. Vanderplank.

On 4 July 2017, Tremor and Vanderplank during routine trapping and general inventory, placed traps in the vicinity of San Telmo and the vicinity of San Quintin. Sherman traps (30.5 cm) were set from sundown (approximately 20:00 PM) to dawn (approximately 05:30 AM) and baited with rolled oats. They set 13 traps along runways and burrow entrances on a disturbed embankment adjacent to a fallow agricultural field 5.6 km east of San Quintín, on Mesa Agua Chiquita (near the "mother lode" described by Huey). Runs were visible in the non-native vegetation, which included *Mesembryanthemum crystallinum*, *Brassica tournefortii*, *Salsola tragus*, and *Hirschfeldia incana,* with individuals of the native species *Ambrosia chenopodiifolia* and *Malosma laurina* nearby. Three female and one male *D. gravipes,* all adults, were trapped. Other species trapped were three individuals of the pocket mouse *Chaetodipus fallax* and one woodrat (*Neotoma bryanti*). The pocket mice appeared to be sharing the burrows of *D. gravipes*. Traps were set at three additional nearby locations and at San Telmo, but no *D. gravipes* were caught there.

Identification of *D. gravipes* was based, among other characters, on measurements of females, greater than the range of values of *D. simulans* (Table 1). Five toes on its hind feet distinguish *Dipodomys gravipes* from sympatric *D. merriami*, which have four toes. Also, diagnostic was the width and pattern of the tail which in *D. gravipes* is thicker than in *D. simulans*, with the white lateral tail stripe narrow and indistinct where it merges with black dorsal and ventral tail stripes (Best and Lackey 1985). The feet were also thick, as described by Huey (1925). The adults captured were unusually feisty for the genus *Dipodomys*

Table 1. Body measurements (mm) of *D. gravipes* females captured (2017) and females only specimen data from the San Diego Natural History Museum (SDNHM) from the same species and its closest congeneric species, *D. simulans*. All measurements in millimeters. Ear length excluded as historic methods of taking these measurements differs from current methods.

	Dipodomys gravipes						*D. simulans*
	Three captures 2017				SDNHM specimens from San Quintin region (n = 35)	Best 1983 Mean	SDNHM specimens from San Quintin region (n = 51)
	1	2	3	Mean			
Total length	295	290	300	295	280-320	300	247-292
Tail	175	185	188	183	161-187	173	145-175
Hind foot	46	42	40	43	41-45	44.1	38-42

and difficult to handle; the adult male escaped before being measured, though it appeared significantly larger than the females.

Data from the live captures were tabulated and later compared to specimens housed at the San Diego Natural History Museum (SDNHM), which houses extensive collections of this species. Museum collections of *D. simulans* from the local region were compared to *D. gravipes* in order to provide a more accurate comparison, since *D. simulans* has a wide range and can be highly variable. Ear measurements were not included because they have historically been recorded using differing techniques and therefore cannot be used for accurate comparison.

The presence of this species adjacent to fallow agricultural land suggests that the recent drought and subsequent fallowing may have increased available habitat and favored the recovery of *D. gravipes*. If this is true, concern should be elevated for this species in the event of increased intensity of agriculture in future, if and when the drought abates. It is not clear whether this discovery represents a rebound of this species or a last remnant population. Surveys have begun throughout the broader region in an attempt to guide future efforts to recover the species.

This discovery is a note of hope for the species and of great importance to regional conservation. Nevertheless, the primary threats of habitat destruction and agricultural expansion (Álvarez-Castañeda et al 2008)[3], which cause fragmentation and reduced genetic vigor, in addition to direct habitat loss, leave this species highly threatened. The human population in the range of *D. gravipes* also continues to increase, presumably increasing pressures such as artificial lighting, application of rodenticides, predation by domestic pets and overgrazing by livestock. Additional data on range and abundance are needed, and genetic studies in areas previously occupied are recommended in the absence of voucher specimens. Our finding is undeniably good news, but no conservation strategy can be proposed until the current status and distribution of *D. gravipes* is better understood.

[3] Álvarez-Castañeda, S.T., Castro-Arellano, I. & Lacher, T. 2008. *Dipodomys gravipes*. The IUCN Red List of Threatened Species 2008: e.T6676A12794061. Downloaded on 02 October 2017.http://dx.doi.org/10.2305/IUCN.UK.2008.RLTS.T6676A12794061.en.

Acknowledgements

We are most grateful to Exequiel Ezcurra for allowing our surveys to be conducted under permit SGPA/DVGS/09514/16. Terra Peninsular facilitated fieldwork in the region, and the San Diego Natural History Museum provided equipment and resources. We thank them all.

Literature Cited

Best, T.L. 1983. Morphologic variation in the San Quintin kangaroo rat (*Dipodomys gravipes* Huey 1925). Am. Midl. Nat., 109:409–413.

Best, T.L. and Lackey, J.A., 1985. Dipodomys gravipes. Mamm. Species, (236), pp. 1–4.

Ceballos, G. and D. Navarro. 1991. Diversity and conservation of Mexican mammals. Pp. 167–198 in Latin American mammalogy: history, biodiversity, and conservation. (M.A. Mares and D.J. Schmidly, eds.). University of Oklahoma Press.

Huey, L.M. 1925. Two new kangaroo rats of the genus *Dipodomys* from Lower California. Proc. Biol. Soc. Wash., 38:83–84.

Instituto Nacional de Ecología. 1994. NORMA Oficial Mexicana NOM-059-ECOL-1994, que determina las especies y subespecies de flora y fauna silvestres terrestres y acuáticas en peligro de extinción, amenazadas, raras y las sujetas a protección especial, y que establece especificaciones para su protección. Diario Oficial de la Federación 16 May 1994.

Mellink, E. and J. Luévano. 2005. *Dipodomys gravipes*. Pp. 613–615 in G. Ceballos and G. Oliva (coord). Los mamíferos silvestres de México. Fondo de Cultura Económica – CONABIO. México, D.F.

Myers, N., Mittermeier, R.A., Mittermeier, C.G., Da Fonseca, G.A. and Kent, J. 2000. Biodiversity hotspots for conservation priorities. Nature, 403(6772): 853.

Nelson, E.W. 1922. Lower California and its natural resources. Mem. Natl. Acad. Sci., 16:1–194.

Phelts-Ramos, S. 2004. El antiguo molino de trigo de San Quintín y su gradual desmantelamiento: voces de la Península: San Quintín, entre la tierra y el mar: una historia compartida. Revista de Geografía e Historia de Baja California 2:8–12.

Ramírez-Velarde, D. 2004. Ranchos de San Quintín: Voces de la península: San Quintín, entre la tierra y el mar: una historia compartida. Revista de Geografía e Historia de Baja California, 2:16–19.

Taylor, L.D. 1996. Gunboat diplomacy's last fling in the new world: the British seizure of San Quintín, April 1911. The Americas, 52:521–543.

Tremor, S., D. Stokes, W. Spencer, J. Diffendorfer, H. Thomas, S. Chivers, and P. Unitt (eds) 2017. San Diego County Mammal Atlas. Proceedings of the San Diego Society of Natural History 46. 438p.

Bull. Southern California Acad. Sci.
118(1), 2019, pp. 76–78

Additional Information on a Nonnative Whiptail Population (*Aspidoscelis flagellicauda/sonorae* complex) in Suburban Orange County, California

Richard A. Erickson[1]* and Weston G. Burt[2]

[1] *San Diego Natural History Museum, P. O. Box 121390, San Diego, CA 92112*
[2] *32232 Avenida los Amigos, San Juan Capistrano, CA 92675*

The lowlands of cismontane southern California have proven to be hospitable not only to humans but to many exotic plant and animal species (Cox 1999). In addition to 14 nonnative reptile species established in the area[1] is a localized population of confusing whiptails in Orange County that was first reported by Winkleman and Backlin (2016). That report was based on observations in south Irvine in May 2014 and April-June 2015 and at least one similar whiptail seen in adjacent Lake Forest in July 2015. Four specimens collected in Irvine at that time were identified as belonging to the *Aspidoscelis flagellicauda/sonorae* complex. The Gila Spotted Whiptail (*A. flagellicauda*) and Sonoran Spotted Whiptail (*A. sonorae*) are morphologically similar all-female species native to Arizona, New Mexico, Sonora, and Chihuahua and previously not known to occur away from their native ranges.

Gary Nafis[2] provided an update on the status of these lizards, noting that they are not extirpated in Irvine, as suspected by Winkleman and Backlin (2016), and "as of 7/17, they have been found only in Orange County in Irvine, Lake Forest, and Aliso Viejo, but they appear to be spreading quickly." The reference to Aliso Viejo was presumably based on the observations detailed here. Information displayed on iNaturalist[3] under the name of Sonoran Spotted Whiptail includes the Irvine observations and others beginning in 2015, but the precise locality data is "obscured" according to the wishes of reporting individuals or institutions. All of the iNaturalist locations, obscured or otherwise, are within the general geographic boundaries described above (G.B. Pauly pers. comm.).

Our observations come primarily from a church campus in suburban central Laguna Woods (33.609882 N, -117.733124 W; adjacent to the vast retirement community formerly known as Leisure World), approximately 4.8 km south-southwest of the locations reported by Winkleman and Backlin (2016). The manicured landscape with scattered ornamental shrubs provides suitable habitat for the whiptails, not unlike the situation described by Winkleman and Backlin (2016). Sandy substrates are especially favored by these lizards. Like Winkleman and Backlin, we initially struggled with their identification, generally trying to force the label of Orange-throated Whiptail (*A. hyperythra*) upon them.

Our first observation was of a single individual on 13 June 2010. Infrequent observations continued through 2016, but in 2017 we increased our effort to document them. Spotted

---

* Corresponding author: richard.erickson@lsa.net

[1] http://www.californiaherps.com (accessed May 2018).

[2] *Aspidoscelis flagellicauda* x *Aspidoscelis sonorae* complex, http://www.californiaherps.com (accessed May 2018).

[3] https://www.inaturalist.org/observations?place_id=2738&taxon_id=73691 (accessed May 2018).

Fig. 1. Spotted Whiptail (*Aspidoscelis flagellicauda/sonorae* complex) in residential Aliso Viejo, Orange County, 1 June 2018. Photo by Richard A. Erickson.

whiptails were seen from 16 April 2017 to 22 July 2017 but were not seen on 30 July 2017 or thereafter. We collected individuals on 1 and 4 July 2017 (LACM 189582 & 189583; collected under California Department of Fish and Wildlife Scientific Collecting Permit #000777) and saw at least three more after that. Our first observation of 2018 was on 22 April 2018.

On three occasions in May and June 2017, and three more in May and June 2018 (Fig. 1), we observed spotted whiptails amongst ornamental landscaping at two locations in nearby portions of Aliso Viejo, along Canyon Wren Lane and Calle Corta to the intersection of Chickadee Lane. These observations extended the known range another 1.2 km south-southwest of the church site.

In summary, all of our observations of spotted whiptails were in suburban landscaping >0.6 km removed from native coastal sage scrub and up to 6 km south-southwest of the original Irvine location. Our observations of activity extend from 16 April 2017 to 22 July 2017 with the exception of one fall sighting on 4 September 2016 (iNaturalist records extend to 31 October 2017). In light of the apparent displacement of Western Fence Lizards (*Sceloporus occidentalis*) by nonnative Italian Wall Lizards (*Podarcis siculus*) elsewhere in in the Los Angeles Basin (G.B. Pauly pers. comm.) and the related warning of Deichsel et al. (2010), we note that as of May 2018 fence lizards were still present at all locations where we have seen whiptails. The spotted whiptail population in Orange County is known to have been present since at least 2010, with the first observations in the city of Laguna Woods. It has since been found in the neighboring cities of Irvine, Lake Forest, and Aliso Viejo. This area has received industrial-scale residential landscaping since the 1960s. The widespread movement of plants, soil, and materials involved in such endeavors has been

implicated in the establishment in southern California of species such as the Brown Anole (*Anolis sagrei*; Mahrdt et al. 2014), Common Coqui (*Eleutherodactylus coqui*[4]; SDSNH 76135 and 76138), and others (G.B. Pauly pers. comm.). While we hope that these species will remain restricted to the highly altered urban environment, the spotted whiptail has already been found at the edge of protected open space in Irvine, where it is feared that it may threaten or outcompete native species in natural habitats (R.S. Winkleman pers. comm.).

Acknowledgements

We thank Gregory B. Pauly, Ryan S. Winkleman, William E. Haas, Eric R. Lichtwardt, Kimball L. Garrett, Adelle F. Burt, and two anonymous reviewers for their assistance in our study and/or the preparation of this note.

Literature Cited

Cox, G.W. 1999. Alien Species in North America and Hawaii: Impacts on Natural Ecosystems. Island Press.

Deichsel, G., G. Nafis and J. Hakim. 2010. Geographic distribution: *Podarcis siculus* (Italian Wall Lizard). Herpetol. Rev., 41:513–514.

Mahrdt, C.R., E.L. Ervin and G. Nafis. 2014. Geographic distribution: *Anolis sagrei* (Cuban Brown Anole). Herpetol. Rev., 45: 658–659.

Winkleman, R.S. and A.R. Backlin. 2016. Geographic distribution: *Asidoscelis flagellicauda/sonorae* complex (Spotted Whiptail). Herpetol. Rev., 47: 256–257.

[4] *Eleutherodactylus coqui*, http://www.californiaherps.com (accessed May 2018).

CONTENTS

Cover: Flowers of the federally/State endangered Indian Knob mountainbalm Eriodictyon altissimum, southwest Guidetti Ranch, San Luis Obispo County, California. 4 May 2016. Photo with permission by Connie Rutherford.